

Polymeric Hydrogel Systems as Emerging Biomaterial Platforms to Enable Hemostasis and Wound Healing

Sara Pourshahrestani,* Ehsan Zeimaran, Nahrizul Adib Kadri, Nurshen Mutlu, and Aldo R. Boccaccini*

Broad interest in developing new hemostatic technologies arises from unmet needs in mitigating uncontrolled hemorrhage in emergency, surgical, and battlefield settings. Although a variety of hemostats, sealants, and adhesives are available, development of ideal hemostatic compositions that offer a range of remarkable properties including capability to effectively and immediately manage bleeding, excellent mechanical properties, biocompatibility, biodegradability, antibacterial effect, and strong tissue adhesion properties, under wet and dynamic conditions, still remains a challenge. Benefiting from tunable mechanical properties, high porosity, biocompatibility, injectability and ease of handling, polymeric hydrogels with outstanding hemostatic properties have been receiving increasing attention over the past several years. In this review, after shedding light on hemostasis and wound healing processes, the most recent progresses in hydrogel systems engineered from natural and synthetic polymers for hemostatic applications are discussed based on a comprehensive literature review. Most studies described used in vivo models with accessible and compressible wounds to assess the hemostatic performance of hydrogels. The challenges that need to be tackled to accelerate the translation of these novel hemostatic hydrogel systems to clinical practice are emphasized and future directions for research in the field are presented.


to death results from uncontrollable bleeding or its consequences.^[2] Uncontrollable bleeding is a major contributor to death in emergency, battlefield, and hospital settings. Hemorrhage represents a leading cause of one-third of prehospital deaths in emergency civilian settings.^[3] More than half of the potentially preventable battlefield deaths were also due to exsanguination from extremity wounds.^[4] It has been reported that considerable blood loss from junctional, truncal, and internal noncompressible injuries in both civilian and battlefield settings can lead to significant prehospital mortalities arising from hemorrhagic shock coagulopathy, multiple organ failure, life-threatening sepsis, and acidosis.^[3] Furthermore, in a medical setting, surgeries including spinal, hepatic, cardiovascular and orthopedic procedures, are associated with severe bleeding.^[5] If not managed properly, surgical hemorrhage can lead to multiple adverse side effects including increasing the need for blood transfusion, hypovolemic shock and hypothermic coagulopathy^[6] and, in major surgery, excessive blood loss is correlated with increased mortality rates.^[7] Hemostasis (stopping bleeding) is therefore of preponderant importance in battlefield and emergency civilian conditions, as well as during trauma surgery or long surgical procedures.

1. Introduction

Severe trauma, a main cause of mortality that is increasing on a global scale, contributes to the worldwide death of more than 5.8 million people each year,^[1] and about 40% of trauma leading

Dr. S. Pourshahrestani, Dr. E. Zeimaran, N. A. Kadri
Department of Biomedical Engineering
Faculty of Engineering
University of Malaya
Kuala Lumpur 50603, Malaysia
E-mail: sara.pourshahrestani@um.edu.my;
sara.pourshahrestani@gmail.com

N. Mutlu
FunGlass – Centre for Functional and Surface Functionalized Glass
Alexander Dubcek University of Trencin
Trencin 911 50, Slovakia
Prof. A. R. Boccaccini
Institute of Biomaterials
Department of Materials Science and Engineering
University of Erlangen-Nuremberg
Erlangen 91058, Germany
E-mail: aldo.boccaccini@ww.uni-erlangen.de

 The ORCID identification number(s) for the author(s) of this article can be found under <https://doi.org/10.1002/adhm.202000905>

© 2020 The Authors. Published by Wiley-VCH GmbH. This is an open access article under the terms of the Creative Commons Attribution-NonCommercial-NoDerivs License, which permits use and distribution in any medium, provided the original work is properly cited, the use is non-commercial and no modifications or adaptations are made.

DOI: 10.1002/adhm.202000905

Hemostasis, derived from the Greek roots *háima* (blood) and *stasis* (halting), is a physiological process and the first stage of wound healing which leads to stoppage of bleeding from damaged blood vessels via clot formation.^[8] However, in cases of uncontrolled massive bleeding caused by major trauma or surgery, the body's natural hemostasis process is not able to efficiently control bleeding, thereby leading to severe blood loss and delayed wound healing.^[3]

The utilization of hemostatic technologies including dressings, bandages, powders, glues, and tourniquets is therefore an efficient way to cease the bleeding from externally accessible injuries (often compressible) including surgical lacerations, puncture wounds, heterogeneous blunt trauma, etc. However, for massive exsanguination scenarios of noncompressible torso hemorrhage (e.g., major car accidents, blast injury, poly trauma, etc.), transfusion of blood products, use of coagulation factors and antifibrinolytic drugs are the clinical gold standard. For a comprehensive discussion on the numerous approved hemostatic technologies for external, intracavitary, and intravenous applications, the interested reader should refer to a detailed review by Hickman et al.^[9] In brief, some of topical and externally administered hemostatic technologies to stanch accessible bleeding scenarios include zeolite and kaolin-based materials (e.g., QuikClot powder, Advanced Clotting Sponge, Combat Gauze), oxidized regenerated cellulose (e.g., Surgicel), collagen-based hemostats (e.g., Avitene, Helistat, Instat), gelatin-based materials (e.g., GelFoam, FloSeal, GRF Glue), alginate-based technologies (e.g., Algosteril), chitosan-based materials (e.g., Hem-Con, ChitoFlex, Celox), and composite fibrin glues and adhesives (Vitagel, Tissel, Evicel, etc.).^[9–10] There are also topical hemostatic patches which are approved for surgical procedures including fibrinogen and thrombin-coated collagen patch (TachoSil), polyethylene glycol-coated collagen patch (Hemopatch), and a patch (Veriset) composed of oxidized cellulose (layer 1)–trilysine (layer 2)–polyethylene glycol (layer 3).^[11] Additionally, XSTAT, a self-expanding sponge with volume-filling capability, is a recent technology approved for use in military and civilian prehospital settings, which has been shown to have potential to manage noncompressible intracavitary and junctional hemorrhage. The technology consists of an applicator containing expandable compressed cellulose sponge coated with chitosan that is able to stop the bleeding within seconds when it expands axially upon contact with blood.^[9,12] ResQFoam is another recent technology made of an injectable self-expandable polyurethane foam and is designed to stop noncompressible abdominal hemorrhage in both civilian and military situations. This technology works through injecting two liquid polymers (an isocyanate phase and a polyol phase) into the abdominal cavity that create a foam upon combining and can expand rapidly to compress the injury, thereby temporarily stanching the bleeding before being removed by the surgeon. This product, to the authors' knowledge, is currently being investigated in clinical trials.^[13]

As previously emphasized, severe bleeding is also a major complication in surgical settings. Therefore, management of surgical hemorrhage is of paramount importance. In the past decades, various topical hemostats, adhesives and sealants have been developed and reported to possess potential capability to establish hemostasis during surgical procedures.^[14] While hemostats are known to halt bleeding either mechanically or

through augmenting the blood clotting cascade,^[15] adhesives are capable to bind various tissues together and have also the ability to bind blood vessels together. Tissue sealants are also able to prevent blood leakage from blood vessels.^[16] However, there are some shortcomings that may limit universal applicability of some of these products, as described in the literature for collagen-based products,^[17] gelatin-based hemostatic agents,^[18] and oxidized cellulose-based hemostatic products.^[17,18b,19] Moreover, it has been reported that fibrinogen and thrombin-based injectable solutions (fibrin sealants) may be washed away by blood flow, therefore preventing hemostasis if used in severe or brisk arterial bleeding. Additionally, they may contribute to infection or reduced wound healing if thick layers of these products are used.^[14a,20] Even though cyanoacrylates are strong synthetic adhesives, they may cause allergic reactions and their rapid curing process was found to be exothermic. Additionally, owing to concerns about potential toxicity of the degradation products, internal use of such products remains limited.^[14a,20a,21] Hence, treatment of bleeding complications is a crucial focus in the clinical arena and thereby designing an ideal hemostatic technology to effectively halt bleeding in difficult clinical situations continues to be an active area of research.

Hydrogels, 3D crosslinked hydrophilic polymers with similar physical structure to the natural extracellular matrix (ECM),^[22] have attracted worldwide attention for use in a variety of pharmaceutical and biomedical applications (e.g., delivery of therapeutic agents^[23] and tissue engineering^[24]) owing to their remarkable properties such as porous structure, flexibility in fabrication, capability to hold huge amounts of water or biological fluids, ability to mimic natural tissue physical properties, biocompatibility, and ability to storing therapeutic nanoparticles and biomolecules within their networks.^[25] More recently, hydrogels possessing additional outstanding characteristics, including injectability, which allows them to be easily administered at the target site via minimally invasive procedures,^[26] have emerged as promising matrices that can effectively stop bleeding and promote wound healing. Injectable hydrogels offer outstanding features such as the capability to completely fill irregularly shaped wounds as well as the ability to reach deep bleeding wounds resulting in less pain and scarring.^[27]

An ideal polymeric hydrogel for hemostatic applications is expected to offer the following advantages: i) the hydrogel should be able to halt bleeding instantaneously and stimulate efficient wound healing,^[28] ii) hemostatic hydrogels should possess adequate adhesiveness and excellent mechanical properties even under wet and dynamic conditions to allow them to adhere quickly and seal injuries completely, avoiding the hemostatic hydrogels migrating away from the bleeding site, and therefore instantly stopping bleeding, and ^[29] iii) as an hemostat, hydrogels must exhibit quick gelation to immediately control bleeding and to prevent liquid hydrogel precursors being diffused away from the bleeding site by the blood flow.^[29b,30] On the other hand, swift gelation may result in formation of weaker hydrogels with minimal adhesive strength as the raw materials do not have enough time to be homogeneously mixed to form a strong network or to react with the tissue. Hence, a balance between short gelation time and suitable adhesive and mechanical properties is vital to allow hemostatic hydrogels to adhere to the tissue in a wet environment and to retain their integrity even when

Table 1. Criteria of an ideal hydrogel for hemostatic applications.^[29a,b,31]

- i. Stops hemorrhage within few seconds of application and promotes wound healing process
- ii. Possesses sufficient adhesion to wet tissues and mechanical strength to maintain blood pressure (adhesion strength of commercially available tissue adhesives is typically ≈ 10 kPa)
- iii. Provides preferable gelation time of < 5 s to immediately cease the bleeding (typical gelation time of thrombin and fibrinogen-based glue is 5 s)
- iv. Exhibits adequate burst pressure to withstand biological pressures (systolic blood pressure: ≈ 16 kPa (≈ 120 mmHg) and diastolic blood pressure: 10.6 kPa (≈ 80 Hg))
- v. Should be biocompatible and hemocompatible (hemolysis rate should be $\leq 5\%$)
- vi. Fully degradable after a certain period of time, e.g., a suitable degradation time frame consistent with the natural wound healing process

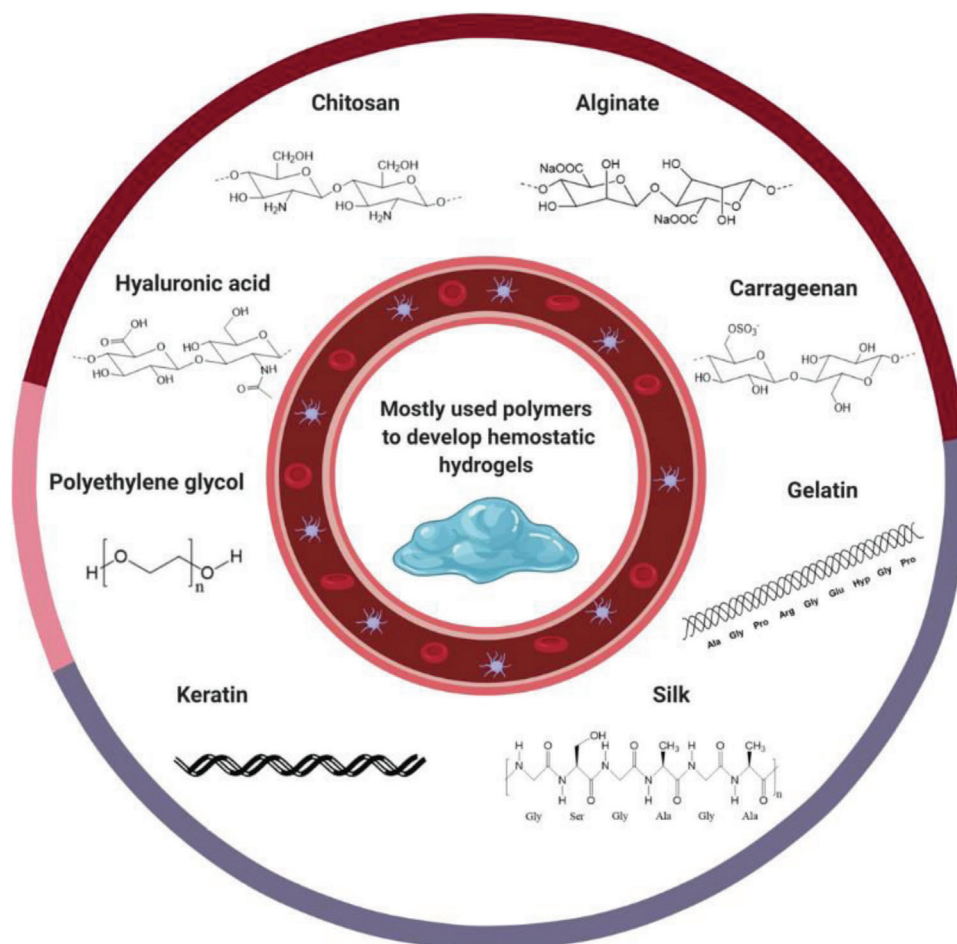


Figure 1. A variety of natural and synthetic polymers utilized to engineer hemostatic hydrogels. Figure created with BioRender.com.

gelation occurs rapidly.^[29b,30] iv) Depending on the structure and density of crosslinking, hydrogels can swell upon contact with blood via absorbing water, thereby concentrating the blood components. Although this is a desirable property when developing hydrogel systems for hemostatic applications, the swelling properties should be controlled because, with over swelling, hydrogels may lose their mechanical strength leading to their disintegration before completing the wound healing process. Furthermore, highly swollen hydrogels may result in surrounding tissue compression.^[29b,31] Beside these characteristics, an ideal candidate needs to be also antibacterial, biodegradable, hemocompatible and biocompatible without releasing toxic products as it di-

rectly contacts physiological fluids.^[32] **Table 1** summarizes the criteria of an ideal hydrogel-based hemostatic system.

Thus far, several natural and/or synthetic polymers have been employed to engineer hydrogels as hemostat, adhesive or sealant, and some of them have also displayed efficient wound healing properties (**Figure 1**). The developed hemostatic hydrogels have been prepared by chemical interactions including Michael-type addition, enzyme-mediated, Schiff base reaction, photopolymerizations (using photoinitiators and ultraviolet (UV)/visible light), 1-ethyl-3-(3-dimethylaminopropyl) carbodiimide/*N*-hydroxysuccinimide (EDC/NHS) chemistry and physical interactions such as ionic/electrostatic interaction,

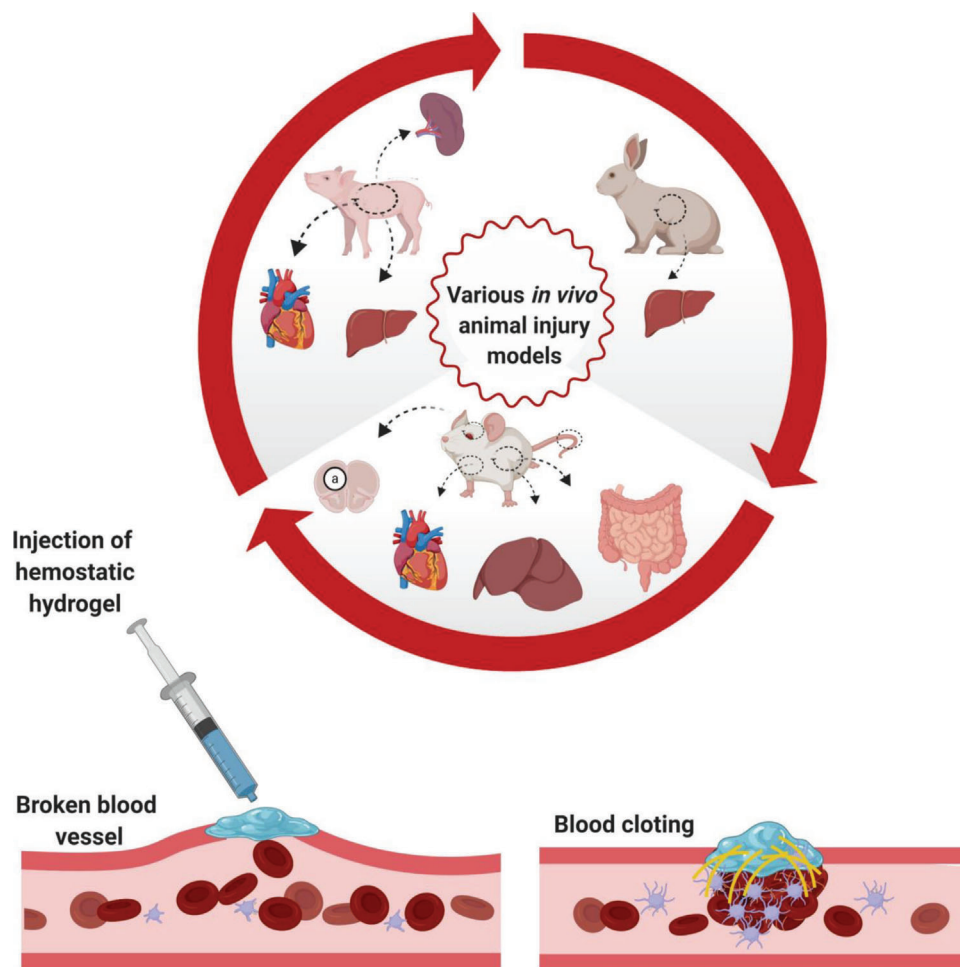


Figure 2. The various in vivo animal injury models which have been utilized to evaluate the hemostatic functions of polymeric hydrogel systems and schematic illustration of the injection of hydrogels in a bleeding site leading to stemming bleeding. Figure created with BioRender.com.

metal–ligand interaction and hydrogen bonds. For further details on crosslinking methods to engineer injectable hydrogels, readers are referred to several excellent review articles.^[26b,33]

In this review, after describing the basic principles of hemostasis and the wound healing process, we summarize recent advances in the different categories of the polymers that are being utilized in the developments of hemostatic hydrogels as hemostats, adhesives or sealants. Most hydrogel systems described here are for localized accessible injuries and have shown potential to treat surgical hemorrhage. There are also some systems that have shown potential to treat incompressible wounds in critical situations. Reported in vitro and in vivo preclinical animal studies will be particularly highlighted (**Figure 2**). The hemostatic polymeric systems are discussed in detail under several subgroups including gelatin, keratin, silk, chitosan, hyaluronic acid, alginate, carrageenan, polyethylene glycol-based hydrogels as well as several other less common polymeric hydrogels. The mechanisms of polymeric hydrogel systems contributing to stimulation and promotion of hemostasis and wound healing are additionally summarized for each subgroup.

2. Biology of Wound Healing

Wound healing consists of four overlapping phases including hemostasis, inflammation, proliferation, and remodeling phases (**Figure 3**). Hemostasis, the first phase of wound healing, occurs very quickly and begins at the onset of injury and closes with the hemostatic plug formation, leading to bleeding suppression. This phase of wound healing comprises 3 steps including i) vasoconstriction, ii) platelet plug formation, and iii) blood coagulation. The vasoconstriction, a brief reflexive contraction, is the first step that leads to narrowing of the blood vessels, thereby diminishing blood loss during injury. Following vasoconstriction, platelet plug formation occurs which is the second critical step in hemostasis and involves adhesion, activation, and aggregation of the platelets into a plug. During an injury, platelets adhere to the exposed subendothelial collagen directly via two receptors (glycoprotein VI (GP VI) and integrin $\alpha 2\beta 1$) and via binding to von Willebrand factor (VWF) by their GP1b receptor.^[34] This adherence triggers the platelet activation process characterized by shape change and secretion of the granules that are rich in certain chemicals (e.g., serotonin, thromboxane A2 (TXA2) and

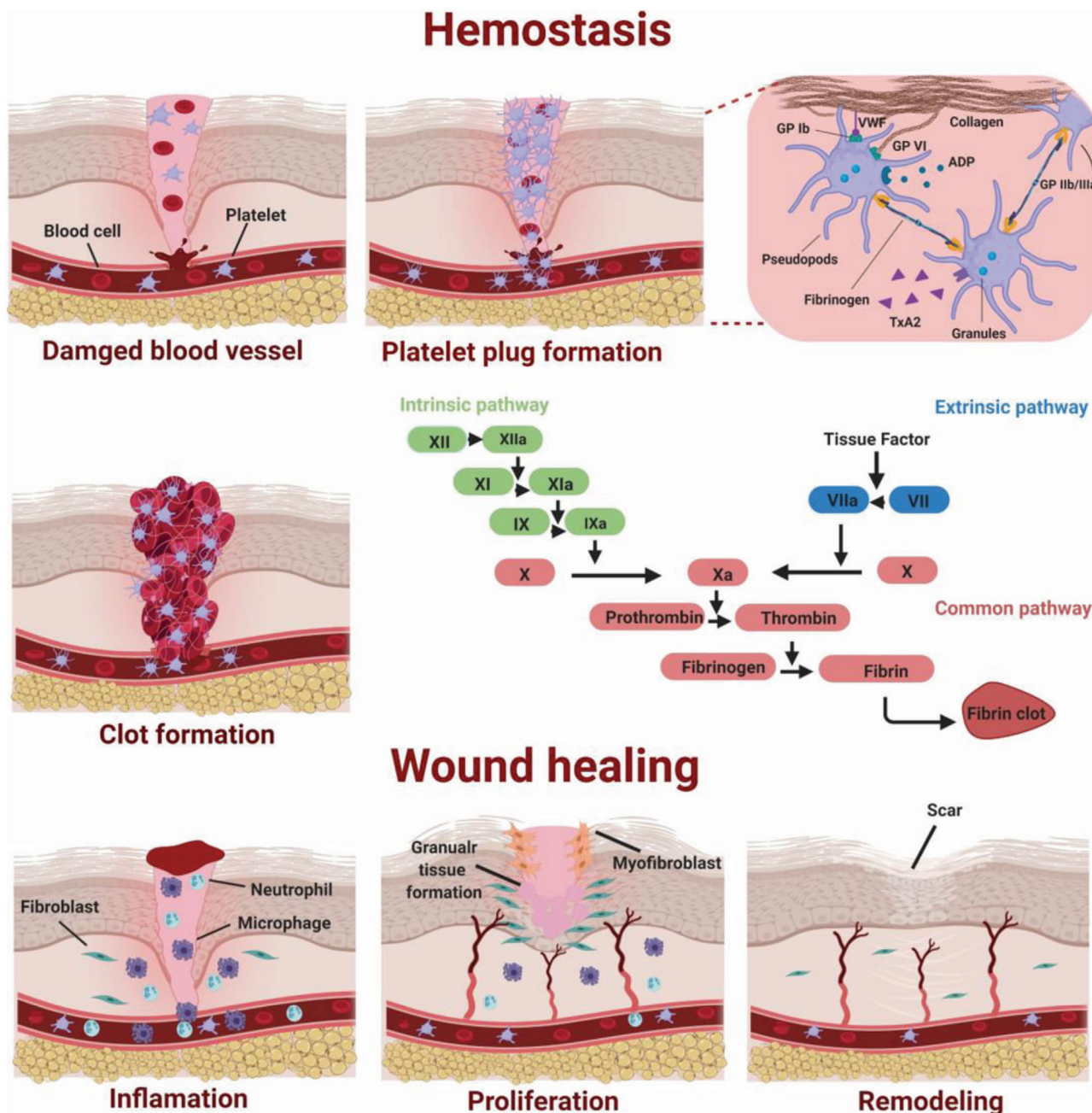


Figure 3. Schematic representation of hemostasis and other 3 stages of the wound healing process. Figure created with BioRender.com.

adenosine diphosphate (ADP)). These substances play important roles in platelet function as they lead to a conformational change in GPIIb/IIIa, a receptor on platelet surface that allows platelets to bind to fibrinogen, thereby leading to aggregation of platelets into a temporary platelet plug over the injured vessel wall.^[35] This phase of hemostasis, defined as primary hemostasis, is short-term and eventually causes formation of an initial plug. Traditionally, the secondary hemostasis phase (known as coagulation cascade) is a process that occurs via two distinct pathways including the extrinsic and intrinsic pathways and leads to generation of a meshwork of insoluble fibrin. Once a blood vessel is injured,

the extrinsic pathway begins, which involves the interaction of tissue factor (TF) exposed to the blood with coagulation factor VII (FVII), resulting in its activation. When Factor XII encounters foreign materials with negatively charged surfaces, the intrinsic pathway is initiated. Ultimately, these two pathways lead to Factor X activation, an enzyme that helps the conversion of prothrombin into thrombin, which in turn rapidly converts fibrinogen to fibrin monomer (common pathway). Finally, fibrin monomers self-polymerize to form protofibrils, which then aggregate laterally to make fibers and branch resulting in the formation of a 3D network or gel. The fibrin gel is then stabilized by

intra- and interfiber crosslinking induced by Factor XIIIa, leading to increasing clot stiffness.^[36] It is noteworthy to highlight that according to the cell-based model of hemostasis,^[37] activated platelets also play a central role in amplifying the coagulation process. The model proposes that the coagulation process occurs via three overlapping phases including: i) initiation, ii) amplification, and iii) propagation. The initiation phase which takes place on the TF-bearing cell initiates when the TF-bearing cells are exposed to the flowing blood upon vascular injury and leads to generation of activated factor IX and X and small amounts of thrombin. In the amplification phase, the thrombin formed during the previous stage has several key functions. Not only it activates platelets but also it leads to activation of cofactor V and VIII to Va and VIIa on the activated platelet surface. The factor XI is also activated on the platelet surface by the thrombin during this phase. In the last stage of this cell-model, propagation, which occurs on the surface of activated platelets, a burst of thrombin is ultimately generated, which is sufficient for formation of a fibrin meshwork.^[38] Inflammatory phase is the second stage of wound healing that begins immediately after hemostasis and lasts up to about 4 days. This phase of wound healing is characterized by host of key cells including neutrophils which are engaged in infection control, and macrophages that are capable to remove damaged cells and tissue debris from the wound area and activating fibroblasts with the ultimate goal of tissue repair by releasing various kinds of growth factors and cytokines in the wound.^[39] The proliferative phase is the rebuilding phase of the wound healing process, which is characterized by few major processes including angiogenesis, granulation tissue formation, wound contraction and epithelialization.^[40] Angiogenesis involves new blood vessel formation. In granulation tissue formation, once fibroblast cells migrate into the wound site, they start proliferation and secrete various ECM proteins such as fibronectin, fibrin, collagen and other components to form a provisional ECM.^[39b] When the wound site is covered with granulation tissue, wound edges begin to be contacted by myofibroblasts, thereby decreasing the size of the wound. Next, during the epithelialization phase, epithelial cells start to migrate from the wound margins across the wound bed to seal the wound.^[41] The remodeling phase, in which the maturation of granulation tissue into scar involves reorganization and rearranging of collagen fibers to maximize tensile strength, is the last phase of the wound healing process.^[41–42] However, it is found that the ultimate resulting scar would have only 80% of the tensile strength of the normal dermis.^[43] Depending on the wound type, this phase of wound healing process can last for a year or longer.

3. Natural Protein-based Hemostatic Hydrogels

3.1. Gelatin

Gelatin, a form of denatured collagen, is a natural protein that has a similar chemical composition to that of collagen. Gelatin has been known to have outstanding properties, including biodegradability, biocompatibility, nontoxicity, efficient absorption capacity, and cost effectiveness, enabling it to be a promising biopolymer for biological glues, drug delivery systems and both hard and soft-tissue engineering applications.^[44] One of the most promising applications of gelatin is its use to stanch bleeding and the

first clues about this efficiency dates back to the late nineteenth century.^[45] The working principle behind the hemostatic effect of gelatin is that it can not only activate and aggregate platelets causing the acceleration of blood coagulation, but also it can swell upon contact with blood, thereby providing a tamponade effect.^[9,46] However, gelatin suffers from low shape stability, rapid degradation profile, and poor mechanical properties at physiological temperature (37 °C), which limit its biomedical applications and hence strategies are required to improve its properties.^[47]

One of the promising approaches to enhance the mechanical properties and therapeutic potential of gelatin-based hemostatic hydrogels is integrating gelatin with functional nanoparticles that can endow the hydrogel with desired integrity for hemostatic application while maintaining its intrinsic properties intact. Synthetic silicate nanoplatelets, a recent class of ultrathin inorganic materials, are highly charged nanoparticles with disc-shaped morphology, thickness of ≈ 1 nm and diameter of 20–30 nm, which have shown great promise as hemostatic product.^[48] These 2D nanosilicates (nSi, e.g., Laponite) possess unique bioactive features, shear-thinning property and dual charged surface (the top and bottom surfaces are negatively charged while the edge is positively charged), which enable them to physically interact with polymers and create shear-thinning injectable hydrogels in aqueous solutions.^[49] Shear-thinning behavior enables hydrogels to be easily injected through syringes and they can be rapidly self-healed after release of the stress, therefore preventing material flow into adjacent areas.^[25e] These nanoparticles are also found to be cytocompatible and they have been shown to dissociate into nontoxic components (Si (OH)₄, Mg²⁺, Na⁺, Li⁺) in physiological conditions.^[49a,50]

Taking advantage of these outstanding properties of nSi, in a noteworthy example, Gaharwar and co-workers engineered a series of shear-thinning and mechanically strong injectable nanocomposite (NC) hydrogels composed of these nanoplatelets and gelatin through physical crosslinking.^[51] According to the results, addition of the nanoplatelets to the gelatin, which was a viscous liquid at 37 °C, resulted in formation of a gel within a minute. The nanoplatelets could effectively improve the thermal and physiological stabilities of the nanocomposite hydrogels, which was attributed to the intense electrostatic interactions between nanoplatelets and gelatin. While gelatin samples rapidly dissolved in PBS at 37 °C, no weight loss was observed for the nanocomposite hydrogels over 24 h. The rheological analysis also confirmed the shear-thinning characteristic and rapid self-healing ability of the resulting hydrogels, therefore preventing the nanocomposite hydrogels from being washed away from the bleeding site. The results from the *in vitro* blood coagulation evaluation demonstrated that the blood clotting time of the nanocomposite hydrogels was reduced as more nanoplatelets were loaded within the hydrogel matrix compared to the control. The authors pointed out that the enhanced hemostatic capacity of nanocomposite hydrogels, which also resulted in strongest blood clots in comparison to those of pure gelatin, stemmed from the nanoplatelet's negative surface charge that can accelerate concentration of blood components near the nanocomposite surface. *In vitro* cell viability experiments also revealed that the nanocomposites induced negligible cytotoxic effect toward RAW macrophages. As compared to 9NC100 gels (9 and 100 represent the concentrations of total solid and nanosilicate,

respectively), gelatin-containing nanocomposite hydrogels showed higher cell viability and lower inflammation. In vivo biocompatibility of 9NC75 gel was tested when it was subcutaneously injected in rats. The 9NC75 gel underwent degradation predominantly in vivo within 28 days after implantation, and it induced low chronic inflammation. A standardized liver bleeding model (a circular liver laceration) was used to assess the capability of the hydrogels to stop otherwise lethal bleeding. It was found that both 9NC75 gel and a commercial zeolite-based hemostat showed strong clotting effects and stopped bleeding successfully within seconds after application on the site of lesion. Importantly, the amount of total blood loss was significantly diminished by the application of the hydrogel with respect to untreated bleeding and no rebleeding occurred after removal of the superficial part of the hydrogel.^[51] This type of injectable nanocomposite gel represents thus an attractive alternative hemostat to treat incompressible injuries in out-of-hospital and emergency settings.

Gelatin is well known to present poor mechanical properties owing to possessing highly hygroscopic nature under wet conditions. Depending on the temperature, gelatin can undergo structural changes.^[52] An available gelatin-based tissue adhesive, for instance, has been found to suffer from low adhesive strength in wet condition.^[53] Therefore, it is appealing to develop a new class of gelatin-based tissue adhesives that not only are mechanically stable but also exhibit strong tissue adhesion ability. An emerging approach to overcome this existing challenge of tissue adhesives is to develop mussel-inspired hydrogels that have been shown to possess impressive ability to adhere to wet surfaces.^[54] Marine mussels are known to strongly attach to various substrates in wet conditions and the great adhesion ability of mussels stems from 3,4-dihydroxyphenyl-L-alanine (DOPA), a catechol-containing amino acid which is found in the structure of foot proteins secreted by marine mussels.^[55] Therefore, mussel-inspired bioadhesives draw a great deal of attention by utilizing catechol group containing compounds such as DOPA and dopamine. Catechol groups are key component which can adhere to a variety of surfaces in wet environments through covalent crosslinking, hydrogen bonding and coupling with metals, thereby conferring adhesive properties to the hydrogels.^[56]

To endow gelatin-based hydrogels with high adhesion ability and improved mechanical properties, Choi et al. recently generated a novel mussel-inspired tissue adhesive hydrogel (DOPA-Fe³⁺ gelatin) and investigated its adhesive properties and hemostatic functions in vivo using a rat model of hemorrhaging liver (Figure 4).^[57] First, gelatin was isolated from ECM extraction of human adipose tissue, and its tyrosine residues were oxidized to DOPA (or DOPA-quinone) via an enzymatic reaction with tyrosinase. A hemostatic, elastic and sticky tissue adhesive hydrogel was then formed within seconds at 37 °C upon mixing of DOPA-modified gelatin with FeCl₃ solution, which was found to be stable at body temperature, even in an aqueous environment. Comparison between rheological properties of DOPA-Fe³⁺ gelatin hydrogel, DOPA-modified gelatin and pure gelatin revealed that DOPA-Fe³⁺ gelatin hydrogel exhibited higher elastic and loss moduli compared to other gelatin hydrogels. Interestingly, the improved mechanical properties were correlated with the rapid crosslinking between Fe³⁺ ions and catechol groups of DOPA. In vitro cell studies using human adipose derived stem

cells (HASCs) revealed that the DOPA-Fe³⁺ gelatin hydrogel exhibited comparable biocompatibility to DOPA-modified gelatin and pure gelatin and did not cause significant cytotoxicity. Fluorescence micrographs demonstrated that most cells were spread on all the surfaces after culturing for 5 days. In vivo injection of this hydrogel to the hemorrhaging site in rat liver demonstrated higher hemostatic efficacy in comparison to that of other gelatin hydrogels by immediately producing an adhesive barrier to flow of blood from the injured site. The total blood loss was significantly reduced from 307.5 ± 145.7 mg in the control, 336.7 ± 293.0 mg in pure gelatin and 340.0 ± 179.7 mg in DOPA-gelatin treated livers to 27 ± 13 mg. Furthermore, histological analysis of the bleeding liver at 1 h after treatment with the hydrogel indicated its good adhesion to liver tissue and showed the migration of host cells into the hydrogel shortly after its injection. No obvious fibrosis or inflammation was observed around the injection site, confirming the biocompatibility of the hydrogel in vivo. The authors attributed the excellent adhesive behavior of the hydrogel to the gelatin remnant catechol groups, which after oxidation and following reaction with tissue amine groups serve as adhesive moieties on the surface of the tissue.^[57] It was suggested that the developed adhesive hydrogel could be applicable in a variety of surgical operations. However, the authors did not investigate the degradability of the hydrogels. Further studies are also required to evaluate the biocompatibility of the engineered DOPA-Fe³⁺ gelatin hydrogel as FeCl₃ is generally considered to lead to endothelial damage by oxidative injury.^[58]

A series of adhesive hemostatic hydrogels were fabricated via incorporation of various concentrations of polydopamine functionalized Laponite (PD-LAP, 0, 0.5, 1, 2 wt%) into mixtures of preprepared gelatin methacrylate (GelMA) and thiolated gelatin (Gel-SH).^[59] GelMA is a photopolymerizable hydrogel that has shown promising characteristics for biomedical applications.^[60] The study revealed that not only gelling time was reduced by increasing the PD-LAP concentration, but also the viscosity was decreased, indicating the shear-thinning properties of the resulting hydrogel. The incorporation of more PD-LAP in the hydrogel network also enhanced the swelling ratio and degradation of the hydrogel (61 ± 1% over 14 days of incubation). While the highest concentration of PD-LAP (2 wt%) negatively affected the mechanical properties of Gel-PD-LAP due to nanoplates agglomeration and uneven distribution, the 1 wt% of PD-LAP with homogeneous distribution markedly improved the mechanical properties of Gel-PD-LAP. This effect was attributed to photocrosslinking of GelMA upon exposure to visible light, Michael reaction between methacrylate groups and thiol groups of GelMA and Gel-SH, respectively, and physical interaction of PD-LAP with the hydrogel network. Maximum adhesive strength was also reported for Gel-2%PD-LAP which was found to be substantially higher than that of commercial sealants. The authors speculated that this improvement in adhesion strength was caused by Michael addition and catechol groups' strong binding affinity to amines and thiol groups in the hydrogel network. Additionally, covalent crosslinking reaction between quinone, oxidized form of catechol presented in the PD structure, and functional groups found on biological substrates (e.g., NH₂) could lead to strong interfacial binding and therefore increasing the adhesive ability of Gel-PD-LAP. More notably, the hemostatic capability of the hydrogels were assessed in vitro and interestingly Gel-2%PD-LAP showed

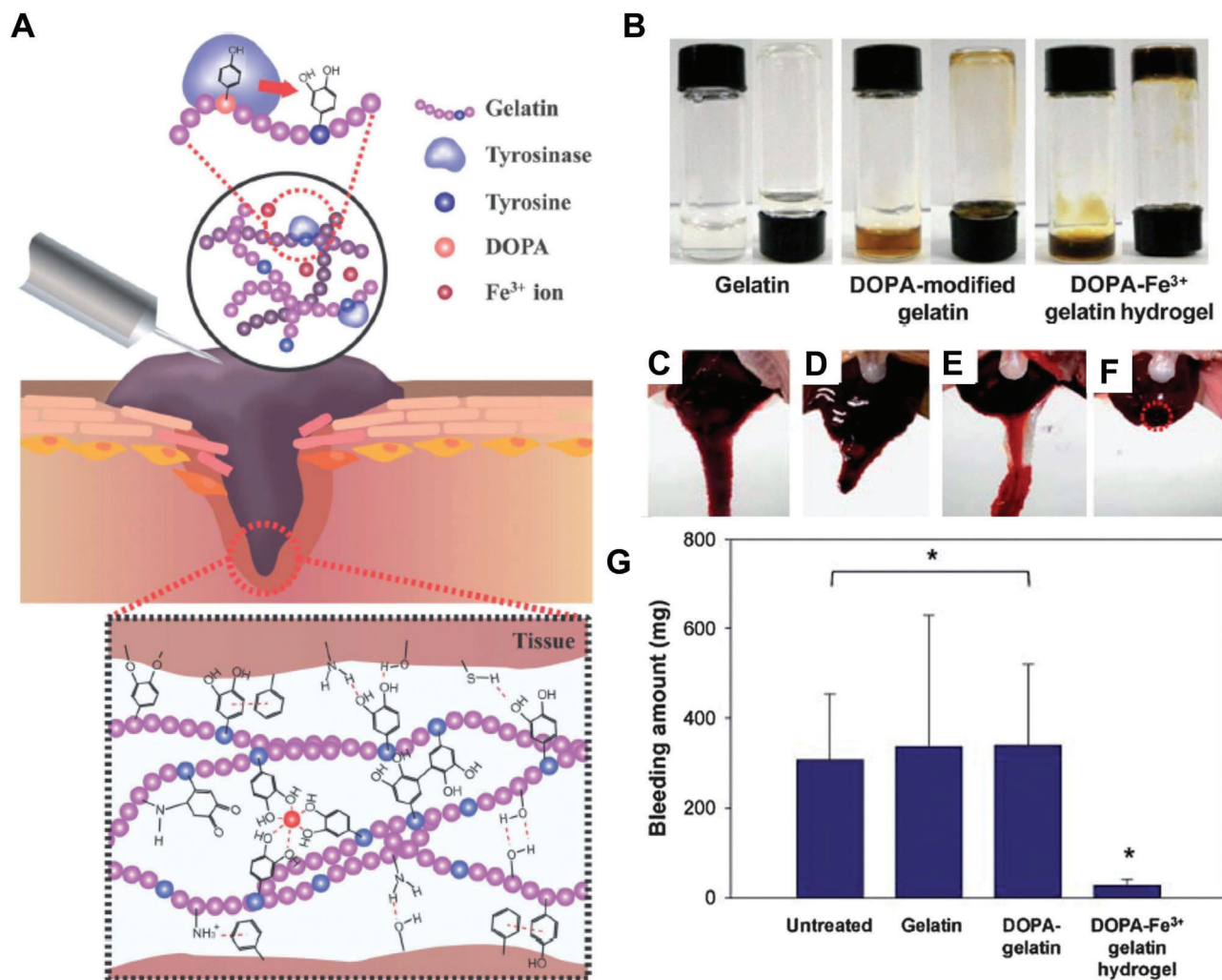


Figure 4. A) Schematic illustration of DOPA-modified human origin gelatin hydrogel crosslinked by Fe³⁺. B) Photographic images of the gelatin alone, gelatin hydrogel modified with DOPA and the hydrogel crosslinked by Fe³⁺. Photographs of bleeding livers C) without treatment and treated with D) gelatin, E) DOPA-gelatin and F) DOPA-Fe³⁺ gelatin hydrogel after 1 min. The red circle in (F) shows the sealing of the injured site. G) The bleeding amounts (mg) from injured sites under different treatment groups. Reproduced with permission.^[57] Copyright 2014, The Royal Society of Chemistry.

shorter blood-clotting time and lower blood clotting index (BCI) than Gel-0%PD-LAP, indicating the beneficial effects of PD-LAP in the enhancement of the blood-clotting ability of the resulting hydrogel. It was hypothesized that while tamponade ability of gelatin and negative charge of Gel-SH can contribute to the hemostatic capability of Gel-PD-LAP, the negative surface charge of the LAP, which was considerably increased after functionalizing with PD, had more pronounced effects on hemostatic efficacy of Gel-PD-LAP, leading to acceleration of platelet aggregation and activation of the clotting cascade. Besides reducing hemolysis ratio and increasing blood compatibility of the nanocomposite hydrogel, the incorporation of PD-LAP nanoplates into the GelMA/Gel-SH network also enhanced cytocompatibility and promoted fibroblast cell attachment and proliferation.^[59] However, further investigations are required, in particular new studies to validate these findings *in vivo*.

Despite significant progress in the development of efficient hemostatic materials to stop uncontrollable bleeding in surgery

and emergency situations, there is still an unmet challenge in controlling bleeding from tissues and organs in wet and dynamic biological environments. Therefore, development of an efficient hemostatic material which can excellently seal bleeding within seconds from wet and mobile tissues may fulfil these challenges.

Hong et al. engineered a novel photo-triggered imine-crosslinked adhesive hydrogel using GelMA, *N*-(2-aminoethyl)-4-(4-(hydroxymethyl)-2-methoxy-5-nitrosophenoxy) butanamide-modified HA (HA-NB) and lithium phenyl-2,4,6-trimethylbenzoylphosphinate (LAP, polymerization initiator) and investigated the hemostatic potential of the hydrogel in various *in vivo* models including rabbit arteries and livers as well as pig hearts and carotid arteries (Figure 5).^[61] Results of this study demonstrated that when GelMA alone or with HA-NB was exposed to UV in the presence of LAP, a rapid formation of a gel resulted. The GelMA/HA-NB/LAP hydrogel exhibited strong adhesion as well as higher mechanical properties compared to other samples. Results of burst pressure tests on wet

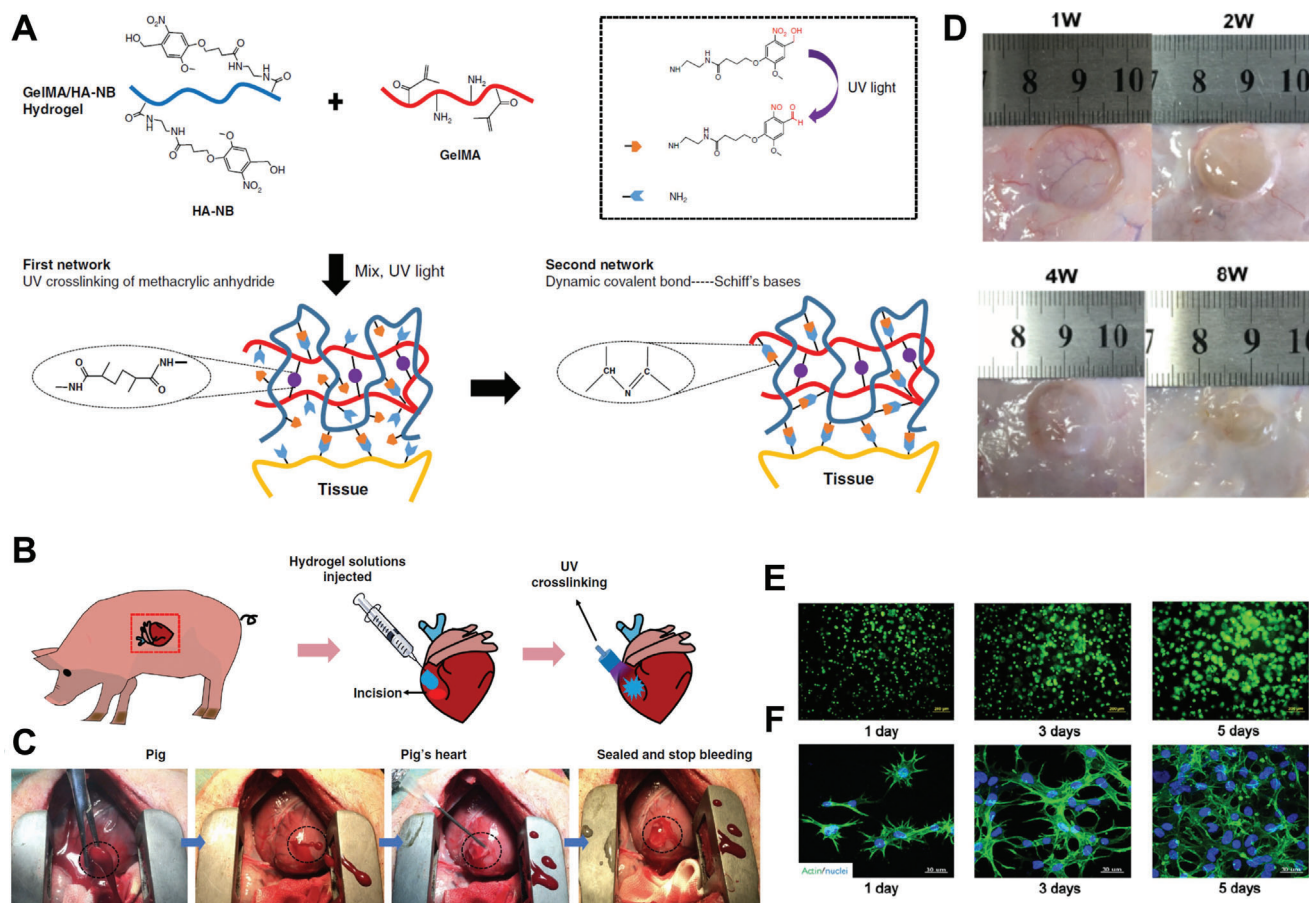


Figure 5. Schematic diagrams representing A) the preparation of GelMA/HA-NB/LAP hydrogel and B) the surgical procedure. C) Pictures displaying quick hemostasis in a pig cardiac puncture injury model after injection of matrix gel and UV crosslinking. D) Macroscopic images of excised GelMA/HA-NB/LAP over 56 days of implantation. E) Fluorescence images of live/dead staining of L929 fibroblasts encapsulated in GelMA/HA-NB/LAP and F) confocal images of DAPI/F-actin staining of C3H cells seeded on the GelMA/HA-NB/LAP at days 1, 3, and 5. Reproduced with permission.^[61] Copyright 2019, Springer Nature.

porcine sausage skins manifested that the GelMA/HA-NB/LAP resulted in higher burst pressure compared to other hydrogels, commercial surgical glues, and normal systolic blood pressure. The authors claimed that the double-network structure of the hydrogel and Schiff bases (UV-crosslinking of GelMA, Schiff bases interaction between HA-NB's photogenerated aldehyde groups and tissue amino groups, and Schiff bases interaction between HA-NB and GelMA) increase internal crosslinking, thereby enhancing the tissue adhesion and internal strength of the hydrogel. Furthermore, the hydrogel was shown to be cytocompatible in both in vitro (toward L929 fibroblastic cells and C3H cells) and postoperative recovery conditions and it additionally showed good biodegradability in vivo, as only about 20.0% of subcutaneously injected hydrogel remained over the course of 56 days.^[61] Subsequently, the engineered GelMA/HA-NB/LAP hydrogel demonstrated in vitro and in vivo instant hemostatic capacity when compared to available products. While thrombin and fibrinogen-based glue was flushed away by blood flow and prevented hemostasis in vitro in a fresh pig liver, the novel hydrogel effectively secured bleeding. The in vivo findings also indicated that application of hydrogel in rabbit's liver and

femoral artery injuries led to immediate wound sealing and hemostasis and the hydrogel was found to be superior to the glue. The authors further demonstrated the great potential of the hydrogel to stop bleeding following pig's carotid artery damage and cardiac penetration injuries.^[61] For the carotid artery damage, the hydrogel with superior wet adhesion capability exhibited rapid sealing of the severely bleeding artery in comparison to the commercial products and it even presented wound healing effect after surgery. For a pig heart bleeding model, the hydrogel could also quickly stop the blood loss within 30 s with respect to the commercial products which failed to stanch bleeding (Figure 5C). According to postoperative analysis, no abnormalities were observed 2 weeks after surgery and staining images of cardiac tissue showed no necrosis and negligible inflammation at the wound site, indicating the hydrogel biocompatibility.^[61] Overall, the authors found that this promising hydrogel can be used for sutureless sealing of wounds, making it applicable for surgery and emergency hemostasis.

In another interesting work, Krishnadoss et al. used choline-based bioionic liquid (BIL) to functionalize GelMA and polyethylene glycol diacrylate (PEGDA). The hydrogels were crosslinked

by visible light photopolymerization (60 s for GelMA and 120 s for PEGDA) utilizing LAP, leading to engineer two novel products (BioGel and Bio-PEG) with excellent adhesion and hemostatic performance under wet conditions.^[32c] The choline, an essential component of the phospholipid bilayer of the cellular membrane, can lead to enhancement of interactions with cell membranes by electrostatic bonding.^[62] The results demonstrated that both GelMA- and PEGDA-based polymers followed the same trend of degradation and with increasing BIL concentration the degradation was increased. However, PEGDA led to lower degradation owing to lower water uptake which is attributed to its lower hydrophilic affinity compared to GelMA. The choline based BIL conjugation to GelMA and PEGDA backbones led to an improvement in their adhesive properties and mechanical properties, which were shown to be strongly dependent on the concentrations of BIL (0–20%). The driving mechanism behind the good adhesion properties of the BioGel sample was reported to be related to electrostatic interactions between cholinium ion from the BioGel pendant (which is positively charged) and phosphatidyl group (which is negatively charged) and also to the interaction between the BioGel polymer's carboxyl anion pendants and the cholinium head of the phosphatidyl choline. Electrostatic interactions between phosphatidyl heads of the cell bilayer and pendant cholinium groups also led to high levels of adhesion in the BioPEG structure. Bioadhesive properties of the hydrogels were also confirmed in vivo by the burst pressure measurement on porcine heart and lung, and it was found that BioGel (100.00 ± 2.89 kPa) and Bio-PEG (61.66 ± 6.01 kPa) had higher burst pressure values than those of GelMA (9.33 ± 1.20 kPa) and PEGDA (7.33 ± 1.45 kPa).^[32c] Cytotoxicity experiments have also demonstrated the good biocompatibility of the hydrogels. Most importantly, the bioadhesive hydrogels were shown to be capable of increasing blood clot formation and accelerating in vitro clotting time depending on BIL concentration. The in vivo study in rat tail cut and liver wedge resection bleeding models further confirmed the reliability of the hydrogels as hemostatic adhesives. While total blood volume (TBV) loss with applications of GelMA in tail cut and liver injury models were $8.27 \pm 2.77\%$ and $34.5 \pm 2.9\%$, respectively, BioGel was found to efficiently stop bleeding and it reduced TBV loss to $6.64 \pm 2.62\%$ and $16.2 \pm 4.6\%$, respectively. Application of PEGDA and BioPEG also showed losses of TBV of $12.06 \pm 0.98\%$ and $9.282 \pm 1.522\%$, respectively, indicating that functionalization of polymers with BIL can improve the hemostatic functions of the hydrogels.^[32c] The adhesives could be applicable for surgical and in-field settings.

To further improve the mechanical properties and stability of gelatin-based hydrogels, in a study by Luo et al., an in situ injectable hemostatic hydrogel was generated by intermolecular crosslinking between sodium hyaluronate and gelatin (HA/G) via EDC/NHS chemistry, which led to amide bond linkages between primary amino groups of gelatin and activated carboxyl groups of HA.^[63] The results revealed that chemical crosslinking and addition of HA can significantly enhance the rheological and mechanical properties as well as stability of gelatin. In comparison to self-crosslinking gelatin (sc-G), which demonstrated gelation time of 90 s and storage modulus of 50 Pa, HA/G was found to be gelled faster (50 s) and could reach higher storage modulus (400 Pa).^[63] While gelatin alone displayed insufficient stability and fast enzymatic degradation after incubation for 4h,

HA/G showed lower proteolytic degradation rate, highlighting its higher stability. The remaining weight ratio of HA/G was found to be $48.20 \pm 13.35\%$ compared to $2.37 \pm 3.36\%$ for gelatin. When both sc-G and HA/G were seeded with mice embryonic preosteoblast cells (3T3-E1), the cells showed well-spread adhesion, proliferation and a fusiform morphology and no significant cytotoxicity was observed. To evaluate the capacity of sc-G and HA/G hydrogels to withstand blood pressure and to assess their sealing ability, the burst pressure test was carried out and the results demonstrated that both hydrogels achieved higher burst pressures when compared to normal arterial blood pressure and commercial thrombin and fibrinogen-based glue, implying their good sealing efficacy to treat a severe bleed. Further, based on in vivo observations, implantation of HA/G hydrogel on the wound of rat bleeding liver significantly reduced the amount of blood loss from 233.8 ± 181.4 mg in the untreated control to 120.4 ± 149.5 mg, which was lower than that in the sc-G treated rat (194.7 ± 140.5 mg). It was found that HA/G hydrogel can cease the bleeding via providing a mechanical barrier. Finally, all results confirmed the potential advantage of HA/G as an injectable hydrogel for hemorrhage control in the clinic.^[63]

3.2. Keratin

Keratin, a family of fibrous structural proteins containing the sulfur-rich cysteine amino acid, is an insoluble protein which is known to be the key structural component of hair, nails, wool, feather, and horns.^[64] Keratin biomaterials have been shown to serve as a biocompatible matrix for regeneration of damaged tissue owing to their intrinsic capabilities to promote cellular adhesion, proliferation, and tissue regeneration.^[65] Bioactivity, structural integrity, and controllable degradability are other unique properties of keratin, allowing this naturally occurring protein to be used for various biomedical applications including dental implants, drug delivery, bone regeneration, and wound dressings.^[66] Recently, keratin proteins were found to have another promising characteristic, namely hemostatic effects, that enable them to remarkably reduce blood clotting time and blood loss via decreasing the plasma clotting lag times.^[67] Keratin proteins are believed to simulate an ECM-like structure when they are in the form of a crosslinked hydrogel network, and therefore they provide a site for receptor-mediated platelet adhesion that produces a catalytic surface for the clotting cascade. Keratin was also shown to contribute to hemostasis via causing polymerization of fibrinogen into fibrin.^[67a]

Aboushwareb et al. performed a study to elucidate the hemostatic performance of keratin hydrogel derived from human hair as compared to two commercial products including a zeolite-based hemostat and a chitosan-based bandage using rabbit models of lethal liver injury.^[68] The results revealed that the keratin hydrogel was as effective as the commercial products at improving the survivability and significantly increased the survival rate from 0% in the negative control to 75%. The keratin hydrogel and the zeolite-based hemostat also led to lower blood loss with respect to chitosan-based bandage. The hydrogel was also found to have enough adhesiveness when it was deposited onto the bleeding site as it was not washed away in most cases, even by severe bleeding. The authors claimed that the keratin hydrogel not only

can stimulate thrombin formation via absorption of fluid from the blood and by concentrating clotting factors but it also is capable to physically seal the wounded area provide a porous scaffold for formation of granulation tissue.^[68]

In a study by Li et al., insulin was conjugated to human hair keratin via the EDC/NHS reaction (Ins-K) to enhance full-thickness skin regeneration with synergy of keratin's excellent hemostatic and wound healing effects and insulin's collagen deposition regulation ability. In this study the potential of Ins-K to promote hemostasis and wound healing was assessed in rat models of hemorrhaging liver and a full-thickness skin wound, respectively.^[69] Insulin has been shown to accelerate wound healing by promoting cellular migration and it enhances re-epithelialization via stimulating angiogenesis.^[69–70] In this study, similar to keratin hydrogel, Ins-K hydrogels were also prepared through mixing the Ins-K conjugate powders with ultrapure water followed by overnight incubation at 37 °C, allowing the occurrence of crosslinking of the disulfide bonds, formation of hydrogen bonds and hydrophobic interactions. The results revealed that the rheology properties, water absorption and porosity of Ins-K hydrogel were comparable to those of the keratin hydrogel and Ins-K was degraded in vitro after 56 days. The in vivo hemostatic evaluation in a hemorrhaging liver rat model revealed that in comparison to the control group, both keratin and Ins-K hydrogels significantly inhibited bleeding from the injured site and resulted in significantly lower blood loss. Interestingly, Ins-K hydrogel was found to have higher hemostatic capacity with respect to keratin hydrogel as it significantly reduced the amount of blood loss and time to hemostasis. The wound healing characteristic of Ins-K hydrogel was also investigated in vivo and the results showed that as compared to keratin hydrogel, the Ins-K hydrogel with ability for sustained release of insulin exhibited a superior healing effect, leading to smoother skin tissues at the excision area.^[69–70] Overall, the study showed that conjugating insulin to keratin enhanced hemostasis, wound healing, full-thickness skin regeneration and inhibited the scar formation by collagen arrangement regulation. However, the study did not elucidate the effect of insulin on hemostatic function of Ins-K hydrogel and more studies are required to effectively exploit the insulin effect on blood coagulation.

Sun et al. added sodium carboxymethyl cellulose into keratin-catechin nanoparticles (KE-NPs) suspensions and let them to stir at room temperature for 2 h, leading to formation of cellulose/KE-NPs nanocomposite hydrogel (KEC) for hemostatic applications (Figure 6).^[71] Here, KE-NPs nanoparticles were prepared through combination of keratin extracted from human hair^[72] with epigallocatechin-3-gallate (EGCG), which is the main ingredient of catechins inducing the self-assembly of nanoparticles. In this study, it was demonstrated that while keratin has amino groups, carboxyl groups, and hydrophobic domains, catechin consists of phenyl rings and phenolic hydroxyl groups, and therefore the hydrogen bonding and hydrophobic interactions between the groups eventually result in the formation of nanoparticles. As the proportion of the KE-NPs as crosslinker was increased from 0% to 1.5%, the adhesion strength of the KEC hydrogel on pig skin at 2 different time points (day 1 and day 14) was shown to increase from ≈ 8 to ≈ 18 kPa. Further increase in nanoparticles content, however, diminished the adhesive strength of the hydrogel, which was correlated to functional

groups consumption in the hydrogel with 1.5% KE-NPs. The resulting KEC hydrogel also showed excellent cytocompatibility toward L929 and human umbilical vein endothelial cells (HUVEC), which was ascribed to the biocompatibility of keratin, cellulose, and catechin, and the promoting effect of keratin and catechins on tissue regeneration as well as the mild condition of preparation process. The results from in vitro blood clotting experiments using pig whole blood showed that addition of more KE-NPs nanoparticles led to the formation of a larger blood clot. In addition, the in vivo study in rat models of liver puncture and tail amputation demonstrated that combination of KE-NPs nanoparticles and cellulose improved the hemostatic performance of the composite hydrogel with respect to the use of either cellulose hydrogel or the nanoparticles alone as they could synergistically accelerate hemostasis and reduced the amount of bleeding (Figure 6B–G). The acceleratory effect of keratin on thrombin activation and platelet aggregation as well as hemostasis efficacy of cellulose were found to be important factors affecting the hemostatic response of the KEC hydrogel.^[67a] It was concluded that the hydrogel can be suitable for different types of wounds such as narrow and deep wounds or large area defect wounds.

Postoperative rebleeding is a major clinical problem in intracerebral hemorrhage (ICH) treatment and is believed to be one of the decisive factors leading to poor outcomes after ICH surgery. Thus, injection of efficient hemostatic agents such as hydrogels into a wound site after hematoma evacuation can be a promising strategy to prevent postoperative rebleeding. Good mechanical properties, injectability, hemostatic capability, and biocompatibility are crucial factors to consider when designing an ideal brain sealant to treat ICH rebleeding.

In an interesting work, He et al. fabricated hemostatic keratin hydrogels (K-gels) via a rehydration method from human hair keratin extracts and its therapeutic effects in the treatment of ICH rebleeding was assessed in rat brain in vivo (Figure 7).^[73] To prepare the K-gels at different concentrations (30, 35, and 40% (w/v)), ultrapure water was used to reconstitute the lyophilized keratin powders. The homogeneous distribution was achieved through vigorously mixing the mixture by vortexing followed by stirring at 37 °C to crosslink and form the gels. Based on the results, the K-gel with 35% keratin was found to be suitable for intracranial implantation as it exhibited several desirable properties including high porosity, porous structure, suitable rheological properties and good injectability. To assess the in vivo hemostatic function of the K-gels to treat rebleeding after ICH, different doses of collagenase were injected into the rat brain to induce postoperative rehemorrhage and formation of hematomas with different volumes. The results obtained revealed that intracranial implantation of the K-gels led to a reduction in volume of hematoma when rebleeding occurred. Magnetic resonance imaging (MRI) and ImageJ statistics also confirmed the hemostatic effect of the K-gel on cerebral hemorrhaging. The hematoma volume was decreased after injection of collagenase with different doses compared with the group treated by the vehicle and it could markedly decrease bleeding (hematoma volume in collagenase dose of 0.6 U: 60.87 ± 16.43 mm³ vs 231.86 ± 32.28 mm³, respectively) (Figure 7B,C). The injection of K-gel also improved survival in rats within 24 h and led to a higher survival rate of 75% in comparison to 17.6% found with the vehicle group. The results also demonstrated that the K-gels were almost degraded

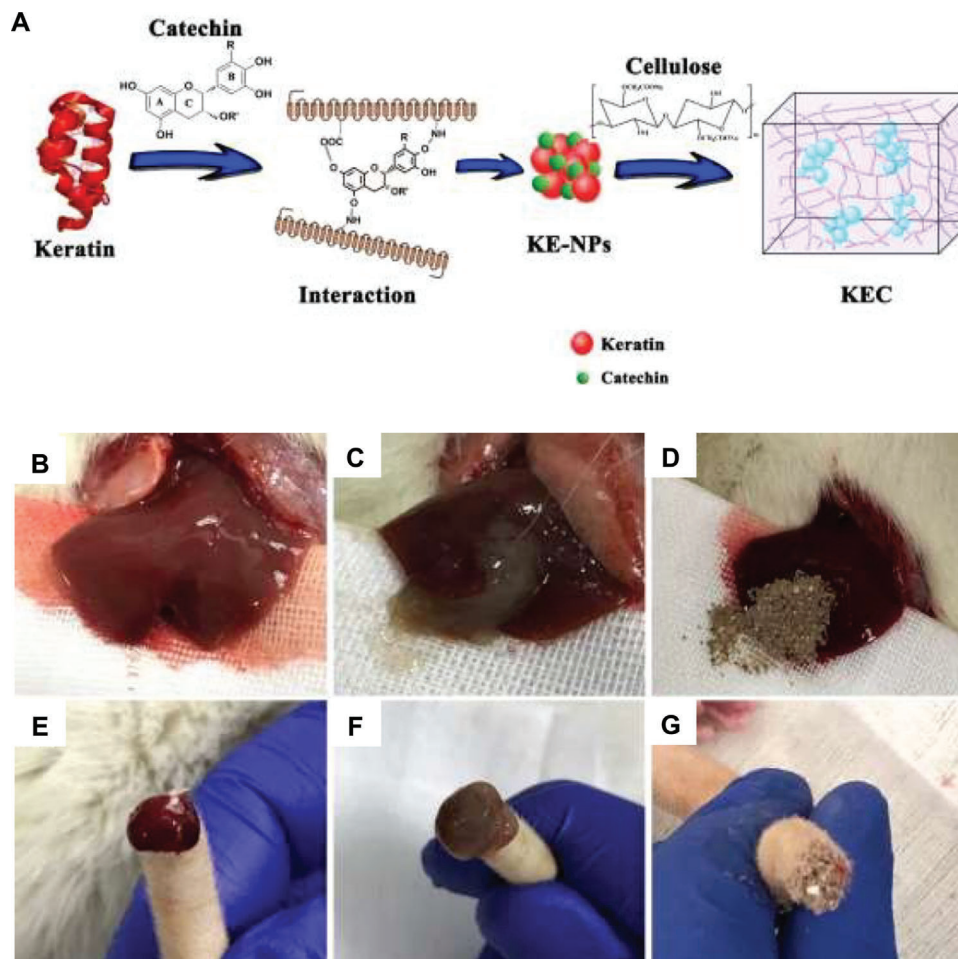


Figure 6. A) Schematic diagram depicting the formation of KE-NPs and thereby construction of KEC hydrogel. B) Untreated (control), C) KEC and D) KE-NP-treated liver hemorrhage in rat models after 5 min. E) Untreated (control), F) KEC, and G) KE-NP-treated tail bleeding in rat models after 5 min. Reproduced with permission.^[71] Copyright 2018, The Royal Society of Chemistry.

in the brain over a period of 28 days. In addition to promising hemostatic efficacy and excellent biocompatibility *in vivo*, the K-gel was also found to relieve brain damage, highlighting its potential to improve therapeutic outcomes for ICH through stemming postoperative rebleeding.

3.3. Silk

Silk is a widely recognized natural fibrous protein produced by arthropods (e.g., silkworms, bees, spiders, and mites). Silk fibroin (SF) derived from the most common silkworm, *Bombyx mori*, has been broadly utilized in biomedical and pharmaceutical applications thanks to its unique physicochemical properties, high biocompatibility, biodegradability and tunable mechanical properties.^[74] Interestingly, low molecular weight SF has been shown to have a stimulatory effect on hemostasis via promoting the activation of the coagulation cascade (the intrinsic pathway), shortening the time for fibrin formation, increasing the blood clot strength and acting as a physical barrier to blood loss.^[75] SF has also shown high potential to boost wound healing due to its stimulating effect on migration and proliferation of differ-

ent cell types contributing to various stages of the wound healing process.^[76] However, owing to inappropriate mechanical and adhesive characteristics within wet and dynamic environments, SF-based biomaterials have not yet fully satisfied the requirements to be used as ideal surgical sealants.^[77]

Polyphenol chemistry has been also utilized to construct hydrogels with improved properties.^[78] Tannic acid (TA) is a naturally derived polyphenol that has served as a remarkable source of pyrogallol and catechol groups and has been shown to offer advantages such as excellent antibacterial efficiency, antioxidant, and anti-inflammatory effects.^[79] Most impressively, TA can stimulate blood clotting via the interactions of its phenolic hydroxyl groups with blood.^[80] It is also noteworthy that TA's polyphenol groups possess strong binding affinity to nucleophiles (e.g., thiol, amines, and amido bond), which can be therefore firmly attached to proteins and peptides.^[81]

Inspired by mussel foot proteins' hierarchically assembled nanostructures which also accounts for mussel underwater adhesion, Bai and co-workers introduced TA into SF to develop a SF-based sealant (SFT) with hierarchically assembled nanostructure and tough adhesion ability to wet and dynamic surfaces (Figure 8).^[82] The working principle behind the formation of this

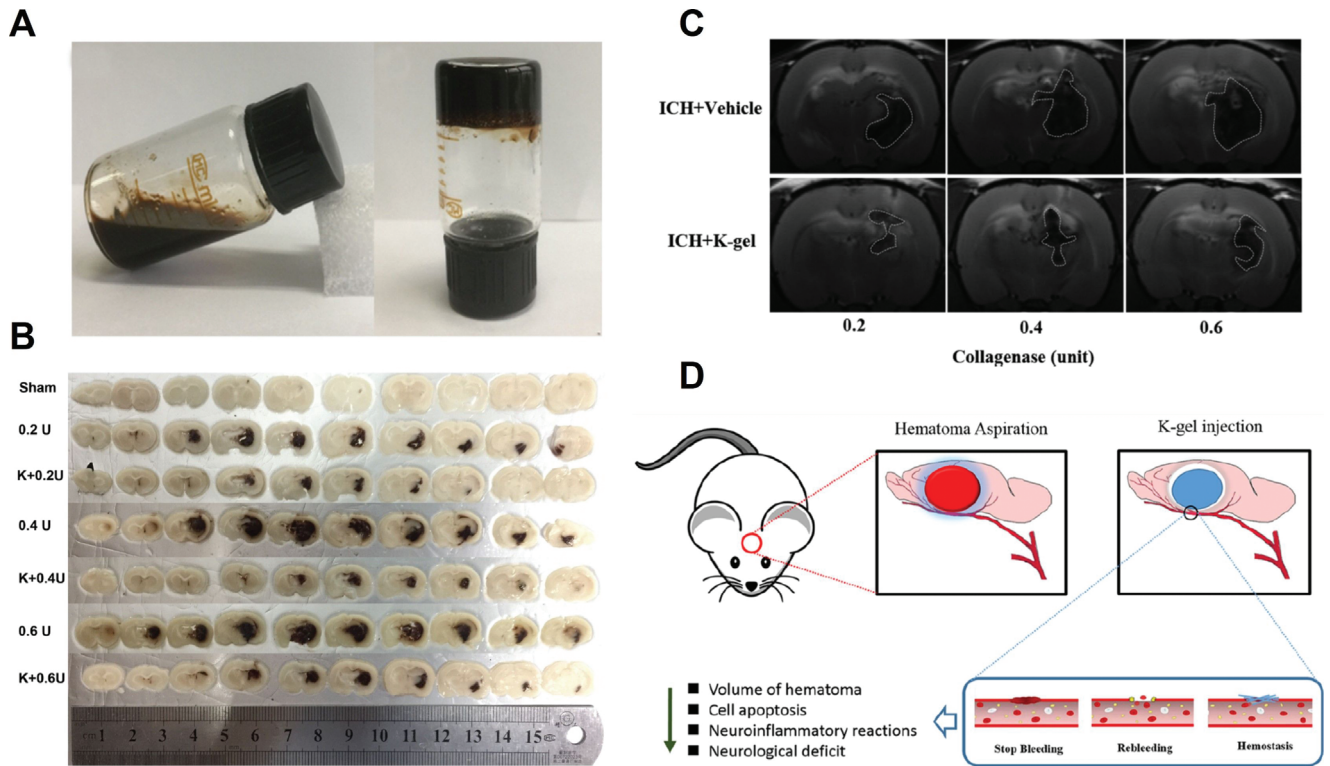


Figure 7. A) Photograph of keratin solution and inverted vial test of developed K-gels. B) Tissue slice of the sham-, collagenase (0.2, 0.4, and 0.6 U)- and K-gel-treated groups (K + 0.2U, K + 0.4U, and K + 0.6U). C) MR images showing hematoma volume at 24 h post-ICH in the treatment groups. D) Schematic illustration of influence of K-gels injection into the hematoma area which can improve the ICH surgery outcome by ceasing postoperative rebleeding. Reproduced with permission.^[73] Copyright 2019, American Chemical Society.

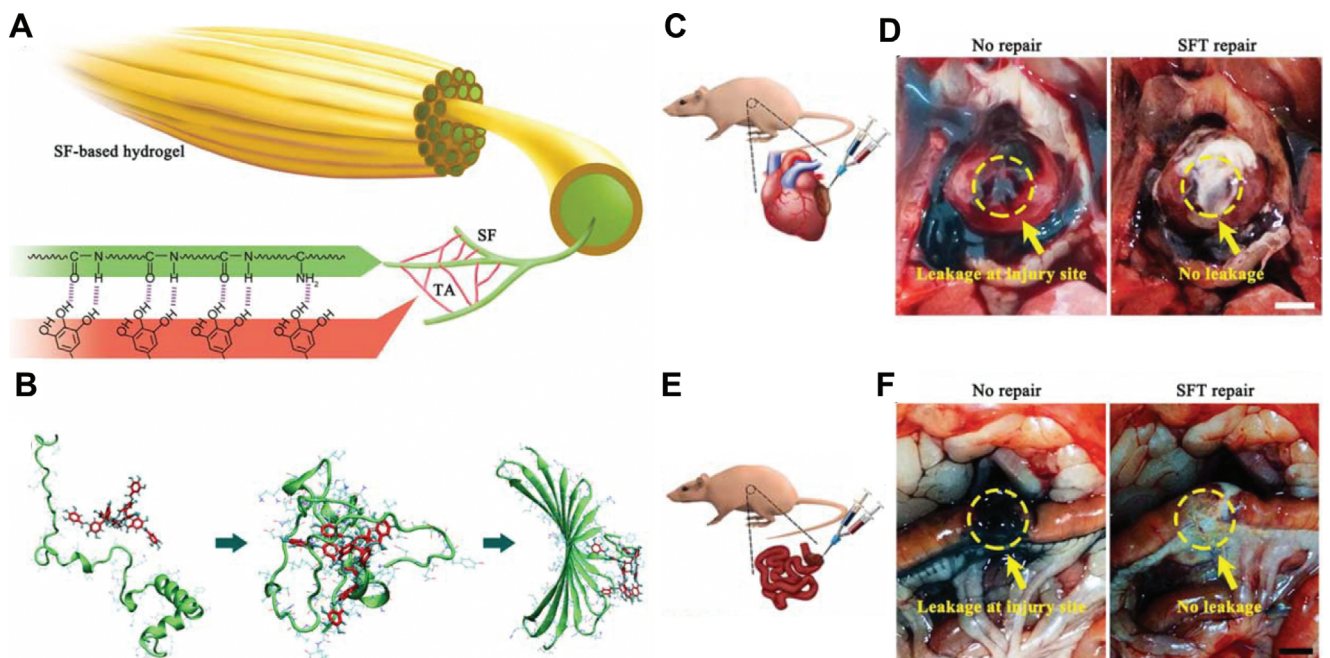


Figure 8. A) Schematic diagram demonstrating the hierarchical structure of SFT. B) Simulation steps of conformation changes occurred during the coassembling process between TA and SF. C) Schematic showing in vivo SFT's hemostatic performance in rat heart bleeding model. D) Comparison of SFT sealed and unsealed heart injury site. E) Schematic representation of in vivo SFT's sealing ability in rat intestine injury model. F) Comparison of SFT sealed and unsealed intestinal injury sites. Reproduced with permission.^[82] Copyright 2019, The Royal Society of Chemistry.

hydrogel sealant is based on the intermolecular interactions between the polyphenol group of TA and nucleophiles present in the SF structure which trigger the coassembly of TA and SF to generate a hierarchical nanofibrillar structure. It was noted that SF conformation transitions from random coil to β -sheet and this effect was driven by hydrogen bonds and electrostatic interactions between TA and SF as well as π - π stacking interactions during the coassembly process. This study indicated that introducing 0.3 g mL^{-1} of TA to 5 wt% SF endowed the resulting adhesive gel with significantly improved mechanical toughness and strong time-dependent adhesion strength, which was ascribed to the hydrogel unique hierarchically assembled nanostructures with β -sheet conformation. The SFT hydrogel could attach to tissues wetted with blood stronger than two available sealants and was shown to adhere to diverse wet tissue surfaces including porcine liver, heart, lung, and intestine. The hydrogel also presented good cytocompatibility toward human synovial fibroblasts (HSF), in vivo fast degradation profile, and outstanding antibacterial performance. The degradation ratios of the sealant were found to be 84.7% (by volume) and 80.4% (by weight), 45 days after implantation. More specifically, the hydrogel showed excellent in vitro hemostatic capacity as the blood clotting was reduced from $5.6 \pm 0.2 \text{ min}$ in the control to $0.8 \pm 0.3 \text{ min}$, which was associated with the strong binding affinity of the phenolic moiety present in SFT to nucleophiles in blood proteins, thereby promoting aggregation and activation of platelet and clotting factors. When covering the hemorrhaging site in a rat liver bleeding model in vivo, the SFT hydrogel also significantly enhanced hemostasis and reduced blood loss to $35.2 \pm 8.6 \text{ mg}$ that was found to be significantly lower than that in cyanoacrylate group ($170.5 \pm 21.1 \text{ mg}$). The application of the hydrogel in a rat model of heart bleeding additionally confirmed its hemostatic efficacy within highly dynamic environments as it resulted in instant wound sealing without secondary bleeding. The sealing ability of SFT was further examined in an intestine incision model in the rat and no leaking from the injured sites was observed following SFT application (Figure 8C–F). The SFT hydrogel also demonstrated to have potential to repair cutaneous wounds and resulted in effective wound healing when tested in a rat skin incision model. The SFT hydrogel not only accelerated the wound closure and re-epithelialization but also displayed higher wound contraction with respect to the commercial sealant, indicating its stimulatory effect on the wound healing process. It was reported that the developed SFT as a surgical sealant can potentially be used for sutureless sealing of wounds under wet and dynamic conditions.

4. Natural Polysaccharide-based Hemostatic Hydrogels

4.1. Chitosan

Chitosan consisting of randomly distributed D-glucosamine and N-acetyl-D-glucosamine units is a widely used natural polysaccharide in wound healing applications owing to its superior biocompatibility, low toxicity, low allergenicity, biodegradation, antimicrobial activity, mucoadhesive properties, and hemostatic activity.^[83] Chitosan is found to play a constructive role in various phases of wound healing. In the process of hemostasis, platelet

activation and aggregation play an initial and vital role.^[84] Chitosan has been shown to have enhancing effect on platelet function through increasing GPIIb/IIIa (a platelet surface receptor) expression and $[\text{Ca}^{2+}]_i$ mobilization, thereby inducing potent platelet aggregation.^[84] Chitosan's hemostatic effect can be also associated to the presence and abundance of positively charged amino acid groups that attract negatively charged residues on red blood cell (RBCs) membranes and proteins through electrostatic interaction, leading to strong hemagglutination at the injured sites.^[85] However, it should be noted that chitosan can also induce hemolysis leading to externalization of hemoglobin which is a potent platelet activator, nitric oxide quencher and inflammatory agent.^[86] Therefore, chitosan-based hemostatic products cannot be utilized intravenously. Although this hemolytic property may be of benefit for topical hemostatic dressings since cell-free hemoglobin can activate platelets, they cannot be utilized intravenously or systemically because of thrombotic risk. In the inflammatory phase of wound healing, chitosan is reported to regulate the secretion of the inflammatory mediators.^[87] Chitosan has been also found to enhance functions of inflammatory cells such as macrophages,^[88] and polymorphonuclear leukocytes,^[88b] thereby promoting granulation and organization of wounds.^[89] Chitosan has been also demonstrated to facilitate fibroblast proliferation, angiogenesis and deposition of collagen as well as it can boost hyaluronic acid production at the injured site, leading to faster wound healing.^[90] Considering the outstanding characteristics of chitosan, it can be an ideal polymer to engineer hemostatic hydrogels.

It has been well documented that incorporation of inorganic materials into a chitosan matrix can also boost its hemostatic potential.^[91] Sundaram et al. fabricated a shear-thinning injectable composite hydrogel (2%Ch–4%nWH) through incorporation of 4% w/w nanowhitlockite (nWH: $\text{Ca}_{18}\text{Mg}_2(\text{HPO}_4)_2(\text{PO}_4)_{12}$) into 2% chitosanhydrogel which was prepared by changing the pH to 6.5 using NaOH (Figure 9).^[92] The resultant composite hydrogel exhibited shear-thinning behavior and showed improved storage modulus with respect to the pure chitosan hydrogel. Moreover, the composite hydrogel was shown to be injectable in vitro when tested in a syringe maintaining a smooth and continuous flow. The hydrogel also indicated no disturbance after 72 h when assessed using an inversion test. The cytocompatibility of the hydrogel was analyzed using HUVEC. While nWH at higher concentration (>4%) decreased the cell viability, 2%Ch–4%nWH and 2%Ch displayed good biocompatibility.^[92] The hydrogels were also found to be hemocompatible as their hemolysis percentage was less than 5%. Moreover, with increasing nWH concentration up to 6% w/w within Ch hydrogel, the in vitro blood clotting time was found to be much shorter with respect to those of 2%Ch hydrogel and blood alone and 2%Ch–4%nWH hydrogel exhibited the lowest blood clotting time of $3.5 \pm 1.2 \text{ min}$ after 48 h incubation with recalcified human whole blood. The hemostatic potential of the 2%Ch–4%nWH hydrogel was further examined in rat liver and femoral artery injury models in vivo (Figure 9D). The results illustrated that application of 2%Ch–4%nWH hydrogel onto the wound sites could effectively control the bleeding and greatly reduced the time to achieve hemostasis and the mass of blood loss in liver and femoral artery injury models compared to the control, 2%Ch hydrogel and a commercial hemostatic agent made

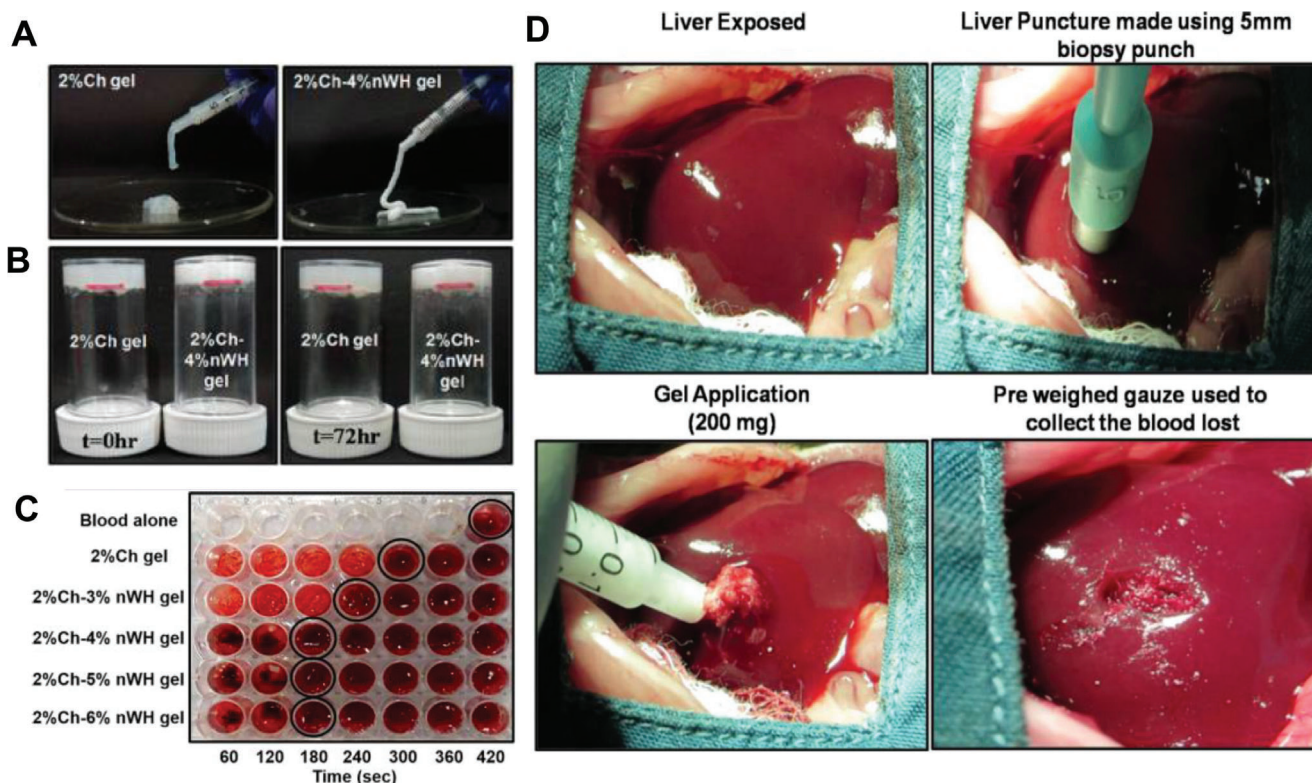


Figure 9. A) Injectability and B) inversion tests of engineered hydrogel systems. C) Blood clot formation in contact with hydrogels as a function of time. D) Photographic images depicting creation of a model of liver injury in rat and achieving hemostasis after injection of the hydrogel. Reproduced with permission.^[92] Copyright 2019, American Chemical Society.

of thrombin and gelatin. The higher blood clotting activity of 2%Ch–4%nWH hydrogel was correlated to the synergistic effect of the therapeutic Ca^{2+} (acting as cofactor to stimulate the blood clotting cascade), Mg^{2+} (helping to stabilize the native conformation of factor IX) and PO_4^{3-} (initiating the extrinsic pathway of coagulation cascade) ions released from nWH and amine groups of Ch hydrogel that are believed to stimulate the blood clotting cascade.^[92] The author proposed the engineered hydrogel to cease bleeding during crucial emergency situations.

In a further study by Sundaram et al., the effect of nanobio-glass incorporation (5%nBG (w/w %)) on the hemostatic activity of Ch hydrogel was also elucidated both in vitro and in vivo using rat liver and femoral artery injury models.^[93] The prepared shear-thinning injectable hydrogel exhibited good injectability, biocompatibility with HUVEC and hemocompatibility. Incorporation of the 5%nBG into Ch hydrogel increased the storage modulus from 10.02 ± 1.07 to 42.01 ± 1.5 kPa. Moreover, the in vitro clotting time was found to be much lower in the Ch hydrogel containing 5%nBG than in the 2%Ch and control samples. It was demonstrated that the incorporation of nBG into Ch matrix promotes blood clotting via releasing the therapeutic ions, Si^{4+} (activating coagulation factor XII), Ca^{2+} , and P, together with protonated amine group of Ch that would stimulate blood clot formation by aggregating the blood cells.^[93] In vivo experiments also proved the higher hemostatic efficiencies of 2%Ch–5%nBG hydrogel with respect to 2%Ch hydrogel as it resulted in faster blood clot formation and lower blood loss in both liver and femoral

artery injuries in rat models. It was suggested that the developed shear thinning injectable hydrogel may have potential to control bleeding during traumatic conditions and major surgeries.

By taking advantage of the unique features of TA, Geng and his co-workers developed sprayable and injectable hydrogels using O-carboxymethyl chitosan (CMCS), TA and 1,4-benzenediboronic acid (BDDBA) with effective hemostatic effect. The CMCS was crosslinked into a network by TA (acting as a molecular glue).^[94] The CMCS–TA–BDDBA hydrogels formation was believed to be driven by physical crosslinking (electrostatic interactions and hydrogen bonding) between CMCS and TA as well as covalent binding between pyrogallol and catechol groups of TA and BDDBA. The results revealed that the gelation time and mechanical properties of the CMCS–TA–BDDBA hydrogels could be tuned by varying the concentrations of TA, CMCS and the ratios of BDDBA/TA. It was shown that introducing BDDBA into the CMCS–TA bicomponent system not only increased the storage modulus from 7.2 Pa for CMCS–TA hydrogel to 2.5×10^4 Pa but also decreased the gelation time from 1 min to 10 s. However, when the BDDBA/TA molar ratio was increased to 4:1, the mechanical strength of the resulting hydrogel was decreased as hydrogen bonds between TA and CMCS were disrupted by excess BDDBA molecules which compete with CMCS for interaction with TA's pyrogallol or catechol groups. The resulting hydrogel also displayed injectability, sprayability and self-healing properties which make it well-suited for hemostatic applications. The authors ascribed the enhancement in self-healing properties to

the formed boronate ester bonds and hydrogen bonds. Furthermore, MCF-7 human breast cancer cells in contact with the hydrogel degradation products demonstrated biocompatibility ($\approx 80 - \approx 100$), depending on the concentrations of the degradation products. In vivo investigations in a mouse model of liver hemorrhage showed that the hydrogel with BDBA/TA ratio of 1:1 possessed efficient hemostatic effect as it significantly reduced total bleeding amount from 180 ± 20 mg and 240 ± 35 mg in gauze-treated and nontreatment groups, respectively, to 55 ± 19 mg. The hydrogel was assumed to act as an efficient physical barrier to achieve hemostasis. The strong interactions of TA and CMCS with blood components via hydrogen bonds, covalent bonds and cation- π interactions, which led to efficient blood clotting, were found to be the potential mechanism behind the hemostatic effect of the hydrogel.^[94] These results suggested the hydrogel as a local hemostatic agent, being potentially suitable for reducing bleeding amount.

One of the most widely used strategies to prepare hydrogels is Schiff base reactions due to high reaction rates and mild reaction conditions which lead to formation of imine bonds.^[95] In a study by Huang et al., injectable self-sealing hydrogels based on CMC and benzaldehyde-terminated four-arm PEG (PEG-BA) were developed and their self-healing performance, injectability, and hemostatic ability were evaluated (Figure 10).^[30] The CMC/PEG-BA hydrogels with various mass ratios and different total solid content (4–6%) were prepared through a Schiff base reaction between amine groups of CMC and aldehyde groups of PEG-BA. According to the results of rheological analysis, when the ratio of CMC to PEG-BA was 1:2 ($R = 1/2$) and the total solid content increased from 4% to 6%, the storage modulus of CMC/PEG-BA hydrogel increased from 944.55 to 3162.06 Pa. While combination of CMC and PEG-BA resulted in the formation of a hydrogel within 100 s at 25 °C, the hydrogel was formed instantly at physiological temperature (37 °C). Macroscopic self-healing evaluation and quantitative analysis of CMC/PEG-BA ($R = 1/2$, $T = 6$) confirmed its self-healing efficacy, as the separated hydrogel stripes took 5 min to heal with no external intervention and showed efficient self-healing capability at physiological temperature.^[30] The CMC/PEG-BA hydrogel also showed injectability when tested using 20 G needles due to the existence of reversible Schiff base linkages in its structure making it capable of spontaneously deforming or quick reformation the broken matrices, thereby further confirming its self-healing ability (Figure 10D,E). Both MTT assay and fibroblast cell 3D encapsulation studies showed excellent cell viability up to 24 h and 7 days, respectively, indicating nontoxicity and biocompatibility of the hydrogel. The formed CMC/PEG-BA hydrogel additionally exhibited superior hemostatic efficacy compared with gauze pad and the negative control (no treatment) when applied on the rabbit liver incision. In comparison to gauze pad and the negative control group, the application of CMC/PEG-BA hydrogel without compression not only decreased blood loss to 0.29 ± 0.11 g, but also significantly reduced the time to achieve hemostasis to 120 ± 10 s.^[30] The authors claimed that the hydrogel, serving as a physical barrier, remained at the bleeding site and could efficiently stop bleeding without being swept away by blood flow. Histological evaluation also revealed that while the application of sterile gauze with compression on the incision site led to a large gap between interfaces of the wound, the hydrogel trapped RBCs and

filled the gaps. Overall, these hydrogels were found to be potential hemostatic materials as they exhibit the ability to be injected into surgical sites or trauma and are capable of stopping bleeding by forming a strong barrier entrapping blood components.

A series of antibacterial and self-healable injectable hydrogels were developed by Zhao et al. through crosslinking quaternized chitosan-g-polyaniline (QCSP) by benzaldehyde group functionalized poly(-ethylene glycol)-co-poly(glycerol sebacate) solutions (PEGS-FA) via an aromatic Schiff base reaction.^[96] The resulting QCSP3/PEGS-FA hydrogels showed excellent conductivity and antioxidant activity. The experimental results demonstrated that with increasing PEGS-FA concentration in the hydrogel, not only the stability of the hydrogel network, storage modulus and adhesive strength were increased but also the gelation time was reduced from 374 to 86 s in the hydrogel with the highest crosslinker concentration, which was stemmed from increased crosslinking density of the hydrogel network. The adhesive strength of the hydrogels with higher concentration of PEGS-FA was found to be slightly lower compared to thrombin and fibrinogen-based glue. The QCSP3/PEGS-FA hydrogels also exhibited rapid self-healing behavior owing to dynamic covalent Schiff base links between benzaldehyde groups from PEGS-FA and amine groups from QCSP. The hydrogel blood compatibility, in vitro cytocompatibility toward L929 cells as well as its antimicrobial effect against *Escherichia coli* (*E. coli*) and *Staphylococcus aureus* (*S. aureus*), which was attributed to antibacterial effects of QCSP and PEGS-FA, were further proved in this study.^[96] In vivo studies also confirmed the potential of the QCSP3/PEGS-FA1.5 composition as an injectable hydrogel for hemostasis and skin wound healing. The results indicated that the total blood loss in a mouse liver injury model was substantially decreased from 2025.9 ± 507.9 mg in the control group (no treatment) to 214.7 ± 65.1 mg in the QCSP3/PEGS-FA1.5 group. The leading cause of hemostatic effect of the hydrogel was related to the synergism between chitosan's intrinsic hemostatic efficacy, quaternary ammonium groups and polyaniline segments as well as adhesive property of the hydrogel. The hydrogel was also found to have superior wound healing efficacy compared to the hydrogel without polyaniline component (QCS3/PEGS-FA1.5) and a commercial film dressing due to showing highest percentage of wound closure after 15 days treatment, promoting thickness of granulation tissue, increasing collagen production, exhibiting free radical scavenging capacity and enhancing the expression of growth factors participating in the wound healing process.^[96] The authors proposed that the hydrogels can be good candidates for cutaneous wound healing.

Qu and co-workers prepared injectable chemically/physically crosslinked double network QCS/PF hydrogels as joint skin wound dressing via employing two kinds of dynamic crosslinking approaches, including the Schiff base reaction (covalent bonds) between benzaldehyde-terminated Pluronic F127 (PF127-CHO) and quaternized chitosan (QCS) and micelle physical crosslinking interaction (noncovalent interaction) of PF127 under physiological conditions.^[97] An increase of PF127-CHO concentration from 14.4% to 24% (wt/vol) in the hydrogel network resulted in a decrease in gelation time from 90 to 20 s. The hydrogels showed desirable degradation properties, good stretchability, rheological and mechanical properties, as well as great self-healing performance, which were ascribed to the combining

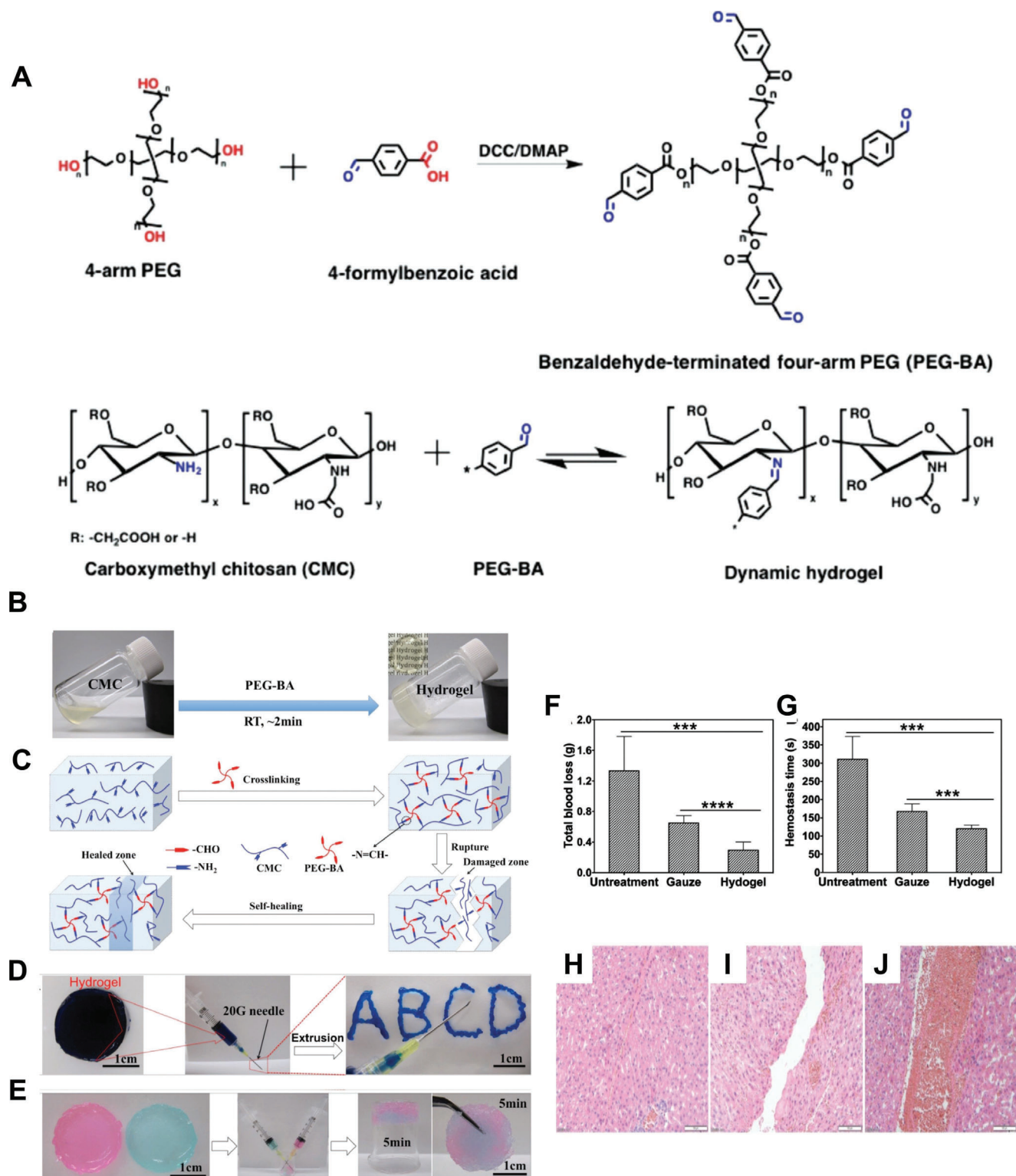


Figure 10. A) The chemistry behind the hemostatic CMC/PEG-BA hydrogel. B) Photographs illustrate gel formation via interaction of CMC with PEG-BA. C) Schematic depiction of chemical reactions involved in gelation and self-healing characteristic of CMC/PEG-BA hydrogel. D,E) Images displaying the injectability and self-healing properties of the hydrogel. F,G) Total blood loss (g) and hemostasis time (s) after applying the hydrogel and gauze pad compared with the negative control. Histological assessment of H) untreated liver surface and injured liver surface treated by I) sterile gauze, and J) CMC/PEG-BA. Reproduced with permission.^[30] Copyright 2016, Wiley-VCH GmbH.

effect of both covalent and noncovalent interactions. Increasing PF127-CHO content also led to a gradual increment in adhesive strength, which was attributed to the Schiff base interaction between aldehyde groups and amine groups from PF127-CHO and the surrounding tissue surface, respectively, as well as hydrophobic and electrostatic interactions between chitosan and cell membrane's phospholipid molecules. The adhesive strength of the hydrogels (6.1 ± 1.2 kPa) was found to be comparable with that of commercial thrombin and fibrinogen-based glue. These formed hydrogels were also found to exert antimicrobial activities against *E. coli* and *S. aureus* and QCS/PF1.0 hydrogels had better cytocompatibility toward L929 cells after 3 days incubation. The authors of this study also encapsulated curcumin in the hydrogel matrix (Cur-QCS/PF1.0) and found that the incorporation of curcumin with antioxidant activity into the micellar hydrogel could stimulate different stages of wound healing. Most importantly, in vivo application of QCS/PF1.0 hydrogel in mouse liver injury model led to significant decreases in blood loss in comparison to the control, which was correlated with the hemostatic property of QCS, its short gelation time (≈ 55 s), high adhesive properties and stable gelation network.^[97] In vivo wound healing studies in mouse skin defect model also demonstrated that both QCS/PF1.0 and Cur-QCS/PF1.0 hydrogels have better wound healing effect compared to a commercial dressing, as the hydrogels resulted in higher granulation tissue thickness, superior collagen deposition, higher and lower expression of wound healing-related factors and pro-inflammatory factors, respectively, and Cur-QCS/PF1.0 hydrogels were found to be more effective in promoting the wound healing process.^[97]

In another study, mixing different contents of a modified chitosan, *N*-(2-hydroxypropyl)-3-trimethylammonium chitosan chloride (HTCC) and polydextran aldehyde (PDA, 2.5 wt%), formed an antibacterial and bioadhesive injectable hydrogel (HTCC-PDA) in situ crosslinked by imine bonds for wound sealing applications.^[98] Increasing the content of HTCC from 1 to 2.5 wt% resulted in decreasing the gelation time from >60 to 10 s and increasing the mechanical stiffness of the hydrogels from 175 to 1528 Pa, which was attributed to the greater availability of amine groups for imine bond formation. The hydrogel also exhibited the maximum adhesive strength in the range of 4.05–7.4 kPa. These injectable hydrogels exerted HTCC content-dependent antibacterial activities against *E. coli*, *S. aureus*, and *P. aeruginosa* as well as drug-resistant bacteria and the hydrogel with the highest HTCC content (2.5 wt%) was found to have the highest antimicrobial effect. This antibacterial hydrogel was also found to be biocompatible and no inflammation response was detected, suggesting its promise for wound healing application.^[98] Negligible hemolysis was observed for all the adhesives when they were exposed to human erythrocytes, highlighting their hemocompatibility. The hemolysis ratio of an adhesive containing 2.5 wt% HTCC was found to be only 2–4%. Notably, hemostatic effect of the hydrogel was evaluated using hemorrhaging liver mouse model and the results showed that the use of HTCC-PDA (2.5 wt% HTCC) hydrogel decreased total blood loss after 3 min, from 168 mg in the control group (no treatment) to 50 mg. Higher wound healing ratio was also observed for the hydrogel compared to the control when tested in an in vivo rat skin wound model. The hydrogel has been also shown to prevent bacterial sepsis in a mouse cecal ligation and puncture model and demonstrated the

highest survival rate compared to the control (62.5% vs 12.5%).^[98] The authors of the study speculated that the engineered bioadhesive hydrogels could potentially be utilized as efficient and antibacterial sealants in surgical sites.

Hydrophobically modified chitosan (hmCS), known as an amphiphilic chitosan derivative,^[99] is composed of hydrophobic alkyl side chains and is found to have superior hemostatic potential and antibacterial effect than those of chitosan, which were attributed to the capability of hydrophobic alkyl chains to aggregate RBCs on the injured site via inserting their membranes and killing bacteria via strong hydrophobic interactions.^[100] It has been reported that hm-CS has capability to transform liquid blood into a gel. This ability is predicted to stem from the self-assembly of hm-CS chains so that their hydrophobic groups anchor into the hydrophobic interiors of RBCs membranes, thereby connecting the RBCs into a 3D network.^[100a] However, hmCS solution is not a perfect hemostat to arrest bleeding owing to its weak mechanical strength.

Oxidized dextran (OD) and hmCS were used to prepare hmCS/OD hydrogel, which was demonstrated to have potential application to accelerate hemostasis and infected wound healing.^[101] Increments in the concentration of OD, from 1 to 4 wt%, led to a decrease in gelation time and an increase in the storage modulus and adhesive strength. Additionally, the hmCS/OD hydrogels were found to not only have self-healing effect attained by the Schiff base reaction between OD and hmCS and the hydrophobic interaction of aliphatic side chains but also to display injectability as the hmCS/OD mixed solution could be injected through a syringe both in vitro and in vivo rat models and formed a hydrogel. The hydrogels also showed excellent antibacterial effect against *S. aureus* and *P. aeruginosa* and no significant toxic effect toward NIH-3T3 fibroblast cells was observed.^[101] The in vitro and in vivo hemostatic function of the hydrogels was evaluated using heparinized rat whole blood (HWB) and liver hemorrhage model. The in vitro results showed that grafting of hydrophobic aliphatic side chains onto CS can improve the coagulation behavior of CS as mixing 0.5 or 1.0 wt% of hmCS with HWB decreased blood clotting time from 448 s in 0.5 wt%CS/HWB to 57 and 26 s, respectively. The blood clotting activity of hmCS/HWB was further improved by adding OD solution so that 0.5 wt%hmCS/OD and 1.0 wt%hmCS/OD led to shorter blood clotting time of HWB compared to 0.5 wt%CS/OD (21 and 10 s vs 141s). The in vivo results also revealed that the application of 1.0 wt%hmCS/OD (hydrogel with 2 wt% of OD, Gel2) over the bleeding site resulted in significantly lower total mass of bleeding with respect to 0.5 wt%hmCS/OD and 0.5 wt%CS/OD hydrogels.^[101] The authors speculated that the adhesive property of the hydrogel, electrostatic interaction between cationic CS and blood cell membranes as well as hydrophobic interactions are the leading cause for its higher hemostatic activity. Furthermore, when Gel2 was applied to a full thickness infected rat skin-defect model, it demonstrated to have higher ability to accelerate the wound healing as compared to traditional gauze as it resulted in wound closure of 99.8% and higher collagen deposition at day 15 postsurgery, which was correlated to its efficient antibacterial activity against *P. aeruginosa*.^[101]

In a recent effort, Liu et al. fabricated an in situ forming hemostatic hydrogel based on Schiff base reaction between aldehyde hydroxyethyl starch (AHES) and amino carboxymethyl chitosan

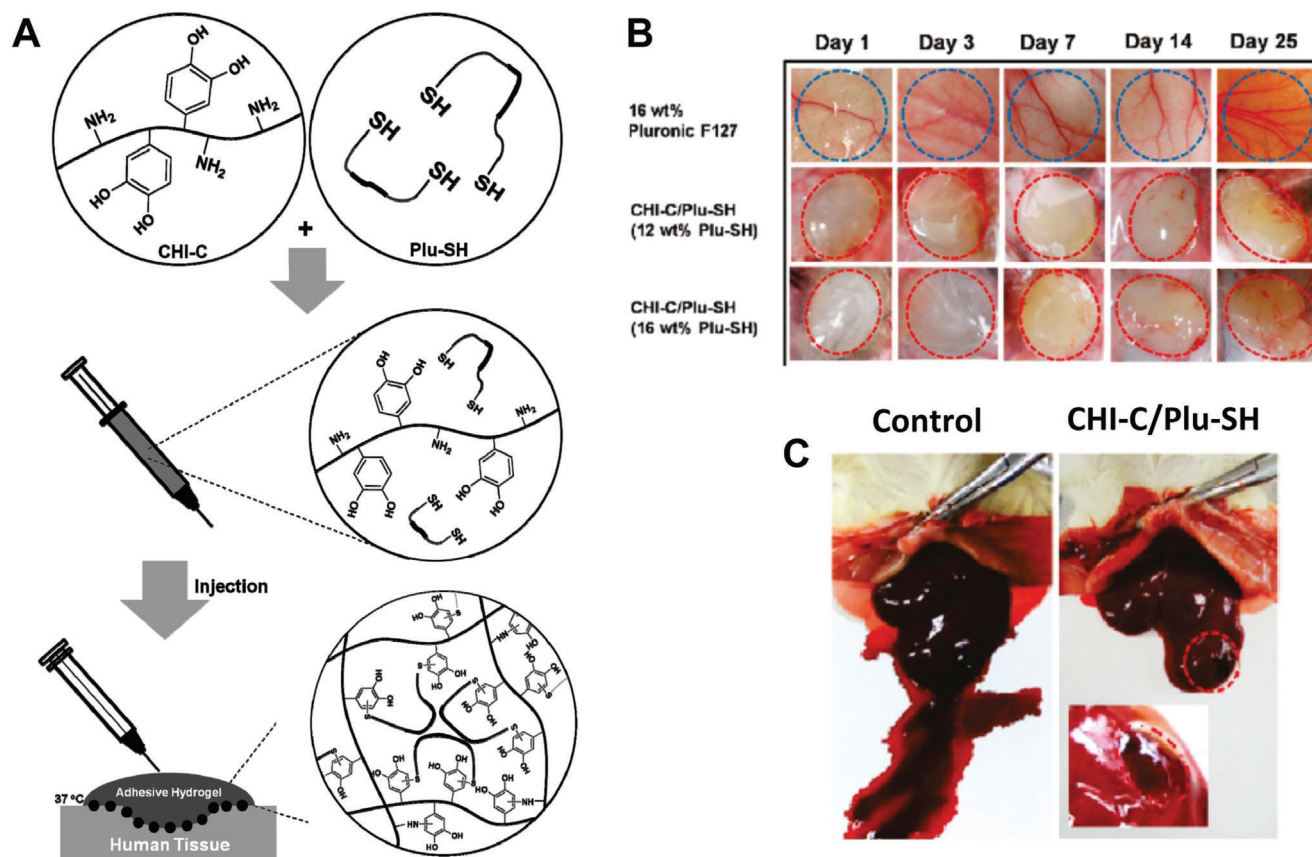


Figure 11. A) The chemistry behind the formation of CHI-C/Plu-SH adhesive hydrogel. B) Photographic images of engineered hydrogels injected in the mouse subcutaneous region. C) Photographic image illustrating the amount of blood loss absorbed on the filter papers after treating rat damaged liver with CHI-C/Plu-SH hydrogel, compared with the control. Reproduced with permission.^[104] Copyright 2011, American Chemical Society.

(ACC) which were prepared by oxidizing HES and modifying CC with sodium periodate and ethylenediamine, respectively.^[102] The study found that the amino and aldehyde group contents of the resulting hydrogel were dependent on the amount of sodium periodate and ethylenediamine so that with increasing molar ratios of sodium periodate and ethylenediamine to HES and CC, respectively, more aldehyde and amino groups were introduced into ACC and AHES molecular chains. Remarkably, following increments of amino and aldehyde group contents and subsequently increasing crosslinking density, gelation time, swelling ratio, and degradation rate were decreased. The tensile strength of the resulting hydrogel also reached the highest value of 42.73 ± 1.18 kPa. In vitro cell studies indicated that while increasing aldehyde content increased cytotoxicity of the resulting hydrogels toward bone marrow mesenchymal stem cells (BMSCs) occurred, cell adhesion and proliferation were enhanced with increasing positively charged amino group content, resulting in facilitation of cell membrane adhesion with negative sites, therefore providing better conditions for cell growth. In vivo results from injection of AHES/ACC hydrogel onto the cut wound of a SD rat liver model showed that it had significantly better hemostatic effect when compared with medical gauze. The hemostatic efficacy was assumed to be achieved by forming a 3D network to physically block bleeding from the wound and due to interaction of positively charged amino groups with negatively charged platelets.

Furthermore, histological assessment of rats' liver and other vital organs such as kidney, heart, lung, and spleen treated with the hydrogels, revealed its excellent biocompatibility in vivo. In the authors' opinion, such AHES/ACC hydrogels with efficient hemostatic property are promising candidates as hemostatic wound dressings and tissue adhesives.

Another favorable strategy to prepare polymeric hydrogels is Michael addition reactions which is a chemical crosslinking method involving the addition of a nucleophile to a α,β -unsaturated carbonyl compound.^[103]

Inspired by the remarkable mussel adhesion mechanisms, the mixture of a thiolated Pluronic F127 (Plu-SH, a temperature-sensitive polymer) and catechol-functionalized chitosan (CHIC) formed injectable and thermosensitive CHI-C/Plu-SH hydrogels in situ (**Figure 11**) that could potentially arrest bleeding when injected into bleeding sites.^[104] In the authors' opinion, combining chemical and physical crosslinking is a good strategy resulting in fabrication of a hydrogel which benefits from the advantages of both methods. The findings showed that addition of Plu-SH into CHI-C could not only result in rapid gelation but it can also increase the mechanical strength of the hydrogels. It was postulated that introduction of catechol groups onto CHI could lead to in situ crosslinking of the CHI's amine groups and Plu-SH, leading to formation of a robust hydrogel. Additionally, the hydrogels could be rapidly gelated under physiological

conditions due to instantaneous gelation of temperature-sensitive Plu-SH via physical crosslinking. The results also showed that crosslinking via quinone (oxidized form of catechol)-thiol bond is a contributing factor to the increased gel stability. The stability of CHI-C/Plu-SH hydrogels was further evaluated in vivo through injection of the hydrogels into subcutaneous regions of mice. The findings indicated that while the hydrogels with 16 and 12 wt%Plu-SH showed high stability and their relative remaining weights after 25 days were 97.5 ± 5.8 and $75.0 \pm 8.8\%$, respectively, 16 wt%Plu was degraded after 1 day (Figure 11B). Additionally, the CHI-C/Plu-SH hydrogel was found to be biocompatible when tested in this model and showed good adhesion properties. The author proposed that the reaction of the quinone with amine groups and thiol via Michael addition and Schiff base formation reaction^[32b,105] is the underlying mechanism behind the hydrogel adhesion properties. Experiments using a rat hemorrhaging liver injury model further revealed that the CHI-C/Plu-SH hydrogel can be a potential hemostatic hydrogel as it could solidify after injection in the bleeding site and it strongly adhered onto the surrounding tissue, thereby accelerating hemostasis. Benefitting from the blood clotting activity of chitosan and high adhesivity, CHI-C/Plu-SH hydrogels showed the lowest total blood loss compared to those of Plu-SH hydrogels and the control. Although the hemostatic efficiency of 2 wt%CHI-C solution was found to be similar to that of CHI-C/Plu-SH hydrogels, it had slower gelation kinetic rate and it was therefore easily washed away by buffer or body fluids before a strong gel could be formed.^[104]

Hydroxybutyl chitosan (HBC), prepared by conjugating hydroxybutyl groups to amino and hydroxyl groups of chitosan, is a derivative of chitosan possessing controlled temperature-responsive properties, good water solubility, and biocompatibility,^[106] and it has recently shown promise in accelerating wound healing processes.^[107] However, due to lack of great adhesiveness in wet condition, its clinical application for hemostasis is limited.^[108] One of the powerful tools to endow HBC-based hydrogels with strong adhesion properties is mussel-inspired chemistry.

In one study, a series of antibacterial thermosensitive HBC-based hydrogels with strong adhesive properties was prepared when HBC was mixed with neutral CS solution and dopamine (HCS-DOPA) in different concentrations (0, 0.5, 1.0, and 2.0 mg mL⁻¹), and their potential as hemostatic materials was evaluated.^[108] Upon increase of temperature from 4 to 37 °C, the hydrogels underwent a sol-gel transition showing a rapid increase of storage modulus. The gelation time was found to be accelerated by increasing the concentration of polydopamine (PD), formed spontaneously through polymerization of dopamine at almost neutral solution, so that HCS-DOPA hydrogels with the highest PD content exhibited faster gelation time (19.67 s) compared to HCS (82.67 s). The composite hydrogel with higher PD content showed higher compressive strength and adhesive strength than those of other hydrogels, which was attributed to Michael addition reaction between amino groups of the CS and HBC with catechol of PD, imparting good mechanical and adhesive properties to the composite hydrogels. Furthermore, the HCS-DOPA hydrogels were shown to be cytocompatible toward L929 cells and exerted better antibacterial effects against *S. aureus* and *E. coli*. with respect to the control group and HCS. The

hemocompatibility and hemostatic capability of the composite hydrogels were further evaluated in vitro. The hydrogels showed nonhemolytic properties with hemolysis rate <3.0% and accelerated in vitro blood coagulation. With increasing concentration of dopamine, from 0 to 2.0 mg mL⁻¹, the clotting time was significantly diminished, from 253.8 and 208 s, in the control and HCS sample, respectively, to 112.4 s, due to synergistic effect of HCS and dopamine on the coagulation process. Moreover, SEM images indicated more aggregation of blood cells on HCS-DOPA-2, confirming its higher hemostatic efficacy.^[108] However, further in vitro and in vivo hemostatic experiments are required to validate these findings.

Interest in the Michael addition reaction between thiols and maleimide groups benefiting from the fast reaction kinetics at physiological pH has increased considerably. In a recent study by Nie et al., a novel fast curable hemostatic hydrogel was developed in situ via Michael reaction between thiolated chitosan (CSS) and a polypeptide crosslinker, maleimide-modified ϵ -polylysine (EPLM), and its capabilities to arrest bleeding was investigated in vivo using a rat liver injury model.^[109] The results revealed that while the molar ratio of maleimide group to thiol groups exhibited negligible effect on gelation time and storage modulus of the hydrogels, the substitution degree (DS) of maleimide and CSS concentration had crucial impacts on these characteristics of CSS/EPLM hydrogels. It was demonstrated that increasing the DS of maleimide from 5% to 30% and the CSS concentration from 2 to 4 wt%, efficiently improved the crosslinking rate and led to formation of a hydrogel with faster gelation time (15 ± 3 s) and higher storage modulus. The CSS/EPLM hydrogels' adhesive strength (with fixed DS of 30%) was assessed using gelatin coated glass as adherent to simulate tissue. The adhesive strength was found to increase with increasing CSS concentration and reached a maximum of ≈ 87.5 kPa for CSS/EPLM-6 (CSS concentration: 4 wt%). The CSS/EPLM hydrogels also displayed remarkably better adhesion strength with respect to thrombin and fibrinogen-based glue, ascribed to multi-interactions (e.g., hydrogen bonding, ionic attraction, and covalent bonding) between CSS/EPLM and gelatin. The authors also speculated that higher CSS concentration not only may lead to introducing more thiol and maleimide groups to the hydrogel, which would further result in formation of more thiol-maleimide linkages and improvement of the hydrogel cohesive force, but also increased interactions between hydrogel components and gelatin matrix, thereby enhancing the adhesive force. It was also found that cationic groups provided by EPLM, which enhance the interaction of the hydrogel and gelatin, contribute to the highest adhesive strength of CSS/EPLM-6. In addition to excellent cytocompatibility to L929 cells, the hydrogel demonstrated effective hemorrhage controlling effect after being applied in vivo using a dual syringe. It could significantly reduce blood loss from 106.7 mg in the control to 28.3 mg after 3 min. Although the CSS/EPLM-6 exerted similar hemostatic action to that of pure CSS solution, it was found to be a more promising hemostatic material compared to CSS, which was easily washed out of the wound site, corresponding to the synergistic effect of the efficient hemostatic function of CS and the good adhesiveness of the hydrogels.^[109] The engineered hydrogels have been proposed to be used as hemostatic material and adhesive sealant.

In a study by Du et al., hydrocaffeic acid-modified chitosan (CS-HA) was synthesized and then mixed with different concentrations of presynthesized hmCS lactate, leading to formation of adhesive hydrogels in situ after oxidizing with sodium periodate.^[110] The chemistry behind the hydrogel formation was based on Michael addition reactions or Schiff base reaction between amine groups of both hmCS lactate and CS-HA with *o*-quinone groups (oxidized form of CS-HA's catechol groups), intermolecular crosslinking of the CS-HA via a coupling reaction which could be triggered by *o*-quinone groups, and hydrophobic interactions of hydrophobic alkyl chains. While higher sodium periodate concentrations led to shorter gelation time (<20 s), increasing concentration of hmCS lactate solution up to 1 wt% (Gel 3) also improved the mechanical properties of the hydrogel and resulted in higher adhesive strength and burst pressure with respect to the sole hmCS lactate and CS-HA. The increased adhesion property of Gel 3 was correlated to the covalent bond formation between *o*-quinone groups and tissue's thiol and amine groups as well as improved mechanical properties, leading to an increase of the adhesive and cohesive forces. The composite CS-HA/hmCS lactate hydrogels also resulted in lower BCI values and higher levels of RBCs and platelet adhesion and aggregation compared to CS-HA, which was ascribed to hmCS lactate's protonated amine groups and hydrophobic alkyl chains. More importantly, application of the composite hydrogels in vivo in a rat hemorrhaging liver model further proved the superior hemostatic efficacy of the hydrogels as it led to lower total blood loss and shorter clotting time than those of CS-HA and hmCS lactate. The composite hydrogels were not only shown to be cytocompatible toward 3T3 fibroblasts but also they exerted higher antibacterial effects against *S. aureus* and *P. aeruginosa*, and Gel 3 demonstrated in vitro anti-infection properties against *S. aureus* and *P. aeruginosa*-infected pigskin. In vivo degradation behavior of Gel 3 was evaluated via subcutaneous implantation in rats and the inflammatory response was also monitored. The results revealed that the gel can be degraded in vivo and the number of inflammatory cells observed after 1 week was obviously reduced with increased postimplantation time. Furthermore, the gel efficiently resulted in wound closure in a rat full-thickness skin incision model compared with suture-treated incisions and it stimulated wound healing.^[110] The results of the study suggested that CS-HA/hmCS lactate hydrogels possess great potential for sutureless closure of surgical incisions.

Another chemical crosslinking reaction used to engineer chitosan-based hydrogels in situ is enzymatic crosslinking. Recently, enzyme-catalyzed in situ crosslinkable hydrogels have become appealing for various biomedical applications owing to their unique merits such as tunable physicochemical properties, biocompatibility and mild crosslinking conditions.^[111]

Accordingly, in one study by Lih et al., PEG was modified with tyramine, followed by grafting onto a chitosan backbone, which could rapidly form curable and hemostatic adhesive hydrogels in situ within 5 s via enzymatic crosslinking with horseradish peroxidase (HRP) and hydrogen peroxide (H_2O_2).^[112] Based on the results, when the concentrations of the chitosan-PEG-tyramine (CPT) conjugate was 10 wt%, the gelation time was decreased to 5 s with increasing the concentration of HRP to 0.063 mg mL⁻¹. Moreover, mechanical properties and adhesive strength of the hydrogels were found to be tuned through changing the con-

centrations of H_2O_2 (0.015–0.060 wt%) so that the hydrogel with the highest H_2O_2 concentration demonstrated the highest elastic modulus (8 kPa) and a greater adhesive strength (97 kPa) to porcine skin. The CPT hydrogels also appeared to have higher adhesiveness with respect to a current thrombin and fibrinogen-based glue, which was ascribed to the capability of chitosan to bind to the negatively charged sialic acid group available on the mucus membrane as well as its interaction with the phospholipids of cell membranes.^[113] In vivo hemostatic ability of the CPT hydrogel was assessed in a mouse liver injury model. The CPT solutions containing HRP and H_2O_2 were applied to the bleeding site via a dual syringe kit. The results demonstrated that the synergy between adhesive and hemostatic properties of chitosan gave the CPT hydrogels excellent capability to arrest bleeding so that it could significantly reduce the blood loss with respect to the control. In comparison to commercial products and suture, the CPT hydrogel also indicated superior in vivo wound healing effect when it was evaluated in rat skin incision. According to histological examinations, no visible fibrosis was observed after 2 week, which was correlated to the wound healing effect of chitosan.^[112] In the authors' opinion, the engineered in situ curable CPT hydrogels with efficient hemostatic and wound healing properties are promising bioadhesives for biomedical applications.

Although photocrosslinkable hydrogels based on natural polymers (e.g., GelMA, methacryloyl chitosan (MC), methacrylated alginates and hyaluronic acid) have shown advantages such as biocompatibility and tunable physical features,^[114] they lack enough adhesion and mechanical properties which may limit their applications for wound healing.

Interestingly, to address these issues, Wang et al. fabricated a novel chitosan based-double-network hydrogel using a double strategy.^[115] Firstly, carbon-carbon double bond and catechol groups were chemically attached to chitosan to synthesize MC and catechol-modified MC (CMC). A double-network hydrogel (LFe-CMC-MC) based on MC and CMC was then engineered in situ via photocrosslinking of carbon-carbon double bonds (induced by blue light) and catechol-Fe³⁺ chelation. A swift gelation within 30 s was observed for LFe-CMC-MC, L-CMC, and LFe-CMC hydrogels compared to Fe-CMC hydrogel (80 s) which was prepared using only Fe³⁺ triggered crosslinking. LFe-CMC-MC hydrogel was also found to have better mechanical performance with respect to other hydrogels, which was attributed to its higher crosslinking-network density resulting from its double network and double crosslinking design. Interestingly, results revealed that the end-product not only exhibited stronger adhesive property (shear strength: 18.1 kPa) on porcine skin compared to other hydrogels and a thrombin and fibrinogen-based glue (shear strength: 3.0 kPa), but also displayed strong adhesion to various surfaces (e.g., rubber glove, steel, glass, polytetrafluoroethylene, polypropylene, and polyethylene) and porcine muscle even under vigorous water flushing. This result was ascribed to enhanced mechanical performance (cohesive forces) and catechol groups of catechol-Fe³⁺ chelation (adhesive force), which can covalently (via interaction with imidazole, thiol, and amino groups) and noncovalently (hydrogen bonds) attach to biological tissues (Figure 12).^[115] The hydrogels also displayed in vitro cytocompatibility, hemocompatibility, in vivo biodegradation and biocompatibility as well as high antibacterial activity against both antibiotic

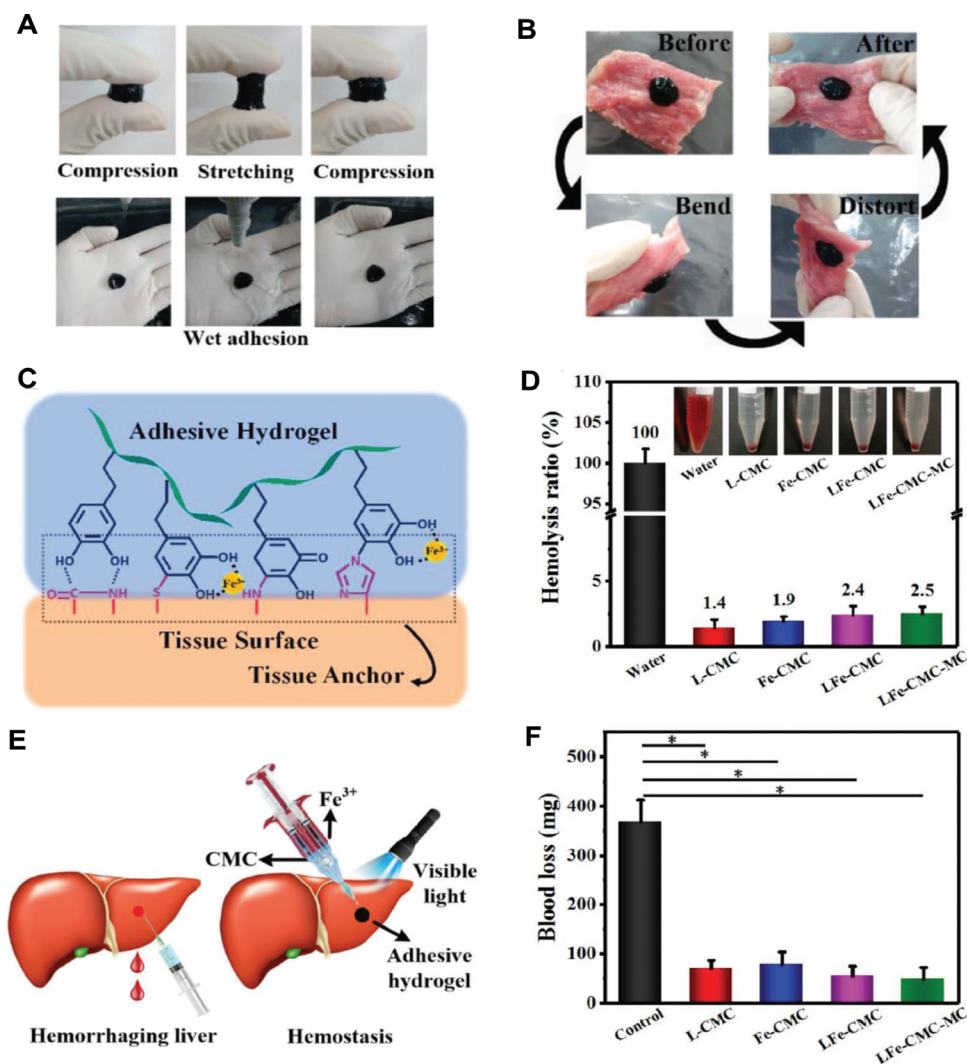


Figure 12. A) Images indicating the strong adhesion of LFe-CMC-MC hydrogel to a rubber glove surface under repeated compressing, stretching and even under vigorous water flushing. B) Photograph indicating adhesion of in situ-forming LFe-CMC-MC hydrogel on porcine muscle tissue; no detachment was seen when undergoing bending and distorting. C) The chemistry behind the adhesion of hydrogel to biological tissue. D) Hemolysis ratio of the hydrogels which was less than 3% for all hydrogels, indicating their hemocompatibility. E) Schematic diagram depicting a liver injured by needle pricking and employing hydrogels to achieve hemostasis. F) Quantitative results of blood loss (mg) from a hemorrhaging liver. Reproduced with permission.^[115] Copyright 2019, Wiley-VCH GmbH.

and nonantibiotic resistant bacteria, which was correlated to chitosan's protonated amino groups and produced quinone groups by Fe^{3+} oxidation that have ability to kill bacteria.^[116] More impressively, hemostatic assessment in a mouse liver injury model revealed that chitosan's intrinsic hemostatic function and the hydrogels' excellent tissue adhesive ability were supposed to lead to a synergistic effect, which created an improved hemostatic performance in hydrogels: only 50–70 mg of blood loss was observed in the hydrogel groups in comparison to that of control (367 mg). Wound healing effects of the hydrogels were also assessed in a mouse full-thickness cutaneous defect model infected with *S. aureus* and the results showed that in comparison to the L-CMC and phosphate buffer solution (PBS) group, other hydrogels had greater promoting effect on the wound healing process, attributed to their enhanced mechanical performance, tissue adhesion and antibacterial activity. However, the authors indicated

that although these hydrogels formed by blue light (400–500 nm) can be employed to achieve hemostasis of superficial wounds, for application in internal wounds an optical fiber would be required due to poor blue light penetration into body tissue.^[115]

4.1.1. Chitosan-Based Cryogels

Cryogels, a type of hydrogels developed by polymerization at subzero temperatures, have remarkable shape-memory abilities, interconnected macroporous structure, excellent flexibility and syringe-injectability, which make them promising candidates for biomedical applications.^[117]

A series of antibacterial injectable shape memory cryogels composed of glycidyl methacrylate functionalized quaternized chitosan (QCSG) and carbon nanotubes (CNT) were synthesized

by Zhao et al. via cryopolymerization under -20°C and their potential for hemostatic and wound healing applications was evaluated using various animal models.^[118] The results of the study revealed that incorporation of CNT led to formation of cryogels with robust mechanical strength, rapid recovery behavior, stability, excellent conductivity, drug encapsulation ability, and near-infrared (NIR) photothermal capacity which significantly boosted antibacterial activity against both Gram-positive and Gram-negative bacteria. Once in contact with water and blood, the cryogels demonstrated outstanding shape memory property and quick recovery speed in less than 1 s and the cryogels with up to 4 mg mL^{-1} CNT presented huge potential for hemostatic applications. In addition to demonstrating cytocompatibility, the cryogels showed excellent hemocompatibility and the preparation QCSG/CNT4 was found to have the lowest hemolysis ratio at the highest dispersion concentrations. In vitro whole blood clotting studies also showed that QCSG/CNT0 has a good blood-clotting ability which was further improved after addition of CNT in different concentrations. In comparison to the blank group, the engineered cryogels, particularly QCSG/CNT4, exhibited efficient hemostatic effect when tested in the mouse liver injury and tail amputation models and resulted in significantly shorter hemostasis time and less blood loss. They were also found to be much better than gelatin sponge and gauze. The hemostatic functions of both QCSG/CNT0 and QCSG/CNT4 composites were evaluated in a standardized rabbit liver bleeding model as compared to commercial Combat Gauze and the cryogel was found to lead to significantly lower blood loss. To assess the hemostatic performance of the cryogel in a lethal noncompressible rabbit liver defect model, the cryogels were squeezed and loaded into a syringe. After injection of the cryogel into irregular, deep, and narrow wounds, they instantly absorbed and concentrated the blood and shape recovery occurred, thereby filling the irregular wound site. The QCSG/CNT4 sample resulted in less blood loss of 0.2 g as compared to both the blank group and the gelatin sponges with different diameters. It was additionally found that QCSG/CNT4 composite could promote wound healing in a mouse full-thickness skin defect model better than the QCSG/CNT0 material and a commercial wound dressing. These injectable shape memory cryogels were proposed as promising candidates for lethal noncompressible hemorrhage and wound dressing applications.^[118]

To overcome dual challenges of hemorrhage and multidrug-resistant bacteria infections in clinical wound care, Hou et al. developed a series of antibacterial polysaccharide-peptide cryogels composed of glycol chitosan methacrylate and ϵ -polylysine acrylamide (GC-EPL) by cryogelation method and evaluated their hemostatic and wound healing properties in vivo.^[119] It was stated that while addition of EPL slightly increased the swelling ratio, the mechanical strength was slightly reduced. The cryogel containing 0.25% (w/v) of EPL-A demonstrated the lowest BCI with respect to the blank, commercial products and GC, indicating its higher blood clotting rate. The hemostatic function of the cryogel was further assessed in a rat liver bleeding model and it resulted in the lowest blood loss as compared to the control, commercial products, GC cryogel and nonporous GC-EPL hydrogel. It was found that the synergy between chitosan's hemostatic effect, EPL incorporation and the macroporous structure allows the cryogel to have effective hemostatic performance. The presence of EPL, an antimicrobial polypeptide, additionally endowed the

resultant cryogels with efficient antibacterial properties against *E. coli* and methicillin-resistant *S. aureus* (MRSA) and the cryogel with higher concentration of EPL showed higher bacterial killing efficiency. The biocompatible cryogel also exerted a strong antibacterial effect against MRSA in a mouse skin wound infection model which further accelerated the wound healing process.^[119]

4.2. Hyaluronic Acid

HA, a major constituent of the ECM, is a natural anionic polysaccharide comprising repeating disaccharide units of D-glucuronic acid and N-acetyl-D-glucosamine.^[120] HA hydrogel is found to be a potential candidate for a variety of tissue engineering applications due to its outstanding physicochemical and biological properties including excellent gel-forming properties, biocompatibility, biodegradability, efficiency to increase cell attachment and cell migration and intrinsic swelling property.^[121] HA has been known to promote wound healing and its superior wound healing efficacy is evident through keratinocyte proliferation and migration, improving granulation tissue formation, stimulating angiogenesis, and promoting tissue regeneration.^[122] Owing to these remarkable characteristics, HA is therefore chosen as a suitable biopolymer to make hemostatic hydrogels.

In a study by Sakoda et al., adipic dihydrazide-modified HA (HA-ADH) was conjugated with imidazole-modified inorganic polyphosphate (PolyP-Im) to get HA-PolyP.^[123] The HA-PolyP was then mixed with aldehyde-modified HA (HA-CHO) to form a hemostatic injectable hydrogel (HAX-PolyP) via Schiff base reaction between hydrazide groups of HA-PolyP and aldehyde groups of HA-CHO.[†] The results revealed that the gelation time of the injectable HAX-PolyP hydrogel became longer when the degree of PolyP modification (17.6–209.6 s) and the amount of HA-PolyP (9.3–216.8 s) were increased.[†] It was also found that while increasing the HA-PolyP ratio increased hydrogel swelling, degradation times of the hydrogels were similar and took nearly 3 weeks to complete degradation, irrespective of the HA-PolyP content. In vitro cytotoxicity evaluation indicated that the HAX-PolyP hydrogel was biocompatible with MeT-5A human mesothelial cells, RAW264.7 mouse macrophages, and NIH3T3 mouse fibroblasts and no severe toxicity was observed. In vivo intraperitoneal and subcutaneous injection of the hydrogel into mice models further confirmed the biocompatibility of the hydrogel, showing no inflammation and peritoneal adhesion as well as no clot formation in the lungs. It has been reported that intravenous administration of PolyP with degree of polymerization of 60–100 induces pulmonary embolization.^[124] The developed HAX-PolyP with lower degree of polymerization of PolyP, however, did not induce pulmonary embolism following subcutaneous and intraperitoneal administration. It was explained that peritoneally and subcutaneous injection of HAX-PolyP leads to a gradual release of PolyP over a long period of time, which would be degraded by the tissue enzymes, thereby preventing its migration into the bloodstream. Most importantly, study of hemostatic efficacy of HA-PolyP using a Sonoclot coagulation and platelet function analyzer demonstrated that although the conjugation of HA with PolyP had no significant influence on clotting time, it led to formation of a thick fibrin clot with higher strength and resistance to fibrinolysis with respect to HA-ADH and normal saline.

The contribution of conjugated PolyP to the efficient hemostatic capacity of the HAX-PolyP hydrogel was additionally proved in a mouse liver bleeding model. Based on the results, while the amount of blood loss following hydrogel injection was almost the same compared with a commercial thrombin and fibrinogen-based glue, it was significantly lower compared with the HAX and nontreated control.^[123] In the authors' opinion, when the conjugated PolyP comes into contact with blood, it can potentially accelerate contact pathway initiation leading to the activation of coagulation factor V and factor XI and fibrin clot stabilization, thereby enhancing the HAX-PolyP's hemostatic effect.

To improve hemostatic efficacy and tissue adhesiveness of HA, Liang and co-workers grafted dopamine onto HA (HA-DA) using EDC/NHS chemistry, followed by crosslinking with different concentrations (1, 3, and 5 wt%) of polydopamine-coated reduced graphene oxide (rGO@PDA) using HRP and H₂O₂.^[125] The results revealed that concentration of rGO@PDA is a contributing factor to the outstanding features of the HA-DA/rGO hydrogels as increasing the rGO@PDA concentration from 0 to 5 wt% led to improvement in crosslinking and stability, decreasing gelation time from 557.4 ± 51.2 to 157.7 ± 33.8 s and increasing mechanical properties. The rGO@PDA also endowed the hydrogels with good conductivity, antioxidative properties, efficient self-healing ability, and photothermal antimicrobial activities both in vitro and in vivo against *E. coli* and *S. aureus*.^[1] In comparison to blank and HA-DA/rGO0, HA-DA/rGO3 with 10 min of NIR irradiation resulted in complete bacterial killing. Furthermore, when an antibacterial drug, doxycycline, was encapsulated into HA-DA/rGO3, it exerted the highest antibacterial properties against the bacteria compared with drug free HA-DA/rGO3 and PBS.^[125] The results verified that these hemocompatible and cytocompatible hydrogels have good adhesive strength, resulting from interaction of reactive catechol and quinone groups from hydrogels with amine and thiol group found in proteins via Michael type reaction. Increasing the rGO@PDA ratio in the hydrogel network also increased the degradation rate from 50.2% for HA-DA/rGO0 to 58.2% for HA-DA/rGO5 after about 1 month. Combining with tissue adhesiveness, the HA-DA/rGO3 hydrogels additionally stimulated blood coagulation in vivo in a liver bleeding mouse model and led to significant decrease of blood loss with respect to the control group. In addition, the rGO@PDA incorporation into HA-DA hydrogel network also contributed to accelerating the wound healing process in a mouse full-thickness skin defect model as injection of both HA-DA/rGO3 and HA-DA/rGO3/Doxy hydrogels resulted in higher healing ratio, collagen deposition, thicker granulation tissue, epidermis, more hair follicles, and blood vessels and reduction in tumor necrosis factor- α (TNF- α) expression and upregulation of CD31 production, when compared with HA-DA/rGO0 and a commercial film dressing.^[125] In the authors' opinion, these injectable adhesive hydrogels are highly promising for full thickness skin repair.

In another interesting work, conjugation of HA with serotonin, a blood coagulating mediator,^[126] led to formation of a hemostatic and adhesive hydrogel within 20–30 s via enzymatic crosslinking in the presence of HRP and H₂O₂ (Figure 13).^[127] The physical crosslinking between serotonin's indole groups was also assumed to have a contribution to the formation of HA-serotonin hydrogel.^[128] The results manifested that gelation time, average storage modulus and adhesive force of the

serotonin-conjugated hydrogel were tunable depending on the concentration of HRP and H₂O₂. When the hydrogel was treated with hyaluronidase, it was found to be completely degraded after 7 h. The hydrogel was also proven to have both tissue adhesive and anti-fouling properties. Adhesiveness of the hydrogels was assumed to be governed by Schiff-base reaction between proteins' amine groups and dione groups from oxidized products of serotonin.^[129] Besides, the lack of adhesive moieties after gelation completion and the resistance to cell adhesion due to interaction of negatively charged HA with water, were found to lead to the hydrogel's anti-biofouling effect.^[130] The author speculated that these characteristics probably prevent abnormal tissue adhesion after hemostasis. This anti-adhesion effect of the hydrogel was further confirmed in a mouse abdominal wall abrasion model as 7 days after operation no abnormal tissue adhesion was observed compared to the control.^[127] Besides these characteristics, high cell viabilities were noted for HASCs and HepG2 cells encapsulated in the hydrogel. The serotonin-conjugated HA hydrogel demonstrated outstanding hemostatic performance in vitro as it not only increased the level of platelet factor 4 and factor V released from platelet alpha-granules^[131] but also it led to an increase in blood clot formation. It also decreased blood clotting time compared with a commercial thrombin and fibrinogen-based system in a dose-dependent manner. Results from an in vivo study in a mouse liver hemorrhage model also indicated a significant promotion of hemostasis, as the mass of bleeding in a model treated with the hydrogel was significantly lower than those in thrombin and fibrinogen-based glue and in the "no treatment" group. The hydrogel was also found to exhibit lower abnormal tissue adhesion following surgery with respect to other groups. Finally, the application of the serotonin-conjugated HA hydrogel in liver hemorrhage of hemophilic mice confirmed its capability to accelerate hemostasis as the amount of bleeding was significantly reduced in the hydrogel treated group in comparison to the control group.^[127] It was thus concluded that the prepared hemostatic adhesive has a great potential to improve hemorrhage control, and therefore it may improve the outcomes of surgical procedures.

4.3. Alginate

Alginate, a negatively charged natural polysaccharide derived from seaweed and marine algae, is a widely used polysaccharide in biomedical fields benefiting from biocompatibility, low toxicity, tunable gelation properties and low cost.^[132] It is well known that alginate can crosslink via divalent cations (e.g., Ca²⁺) which further boosts its hemostatic properties through activation of the coagulation cascade and acceleration of platelet aggregation.^[132c,133] Owing to its unique capability of high-water absorbency, alginate dressings are known to promote the wound healing process. They can absorb wound fluid to form a hydrogel that minimizes bacterial infections, thereby stimulating rapid re-epithelialization and formation of granulation tissue.^[134] However, ionically crosslinked alginate gels lack long-lasting stability under physiological conditions, adequate tissue adhesiveness and mechanical properties, which has led to increasing interest in the fabrication of alginate hydrogels through covalently crosslinking methods.^[132c,135]

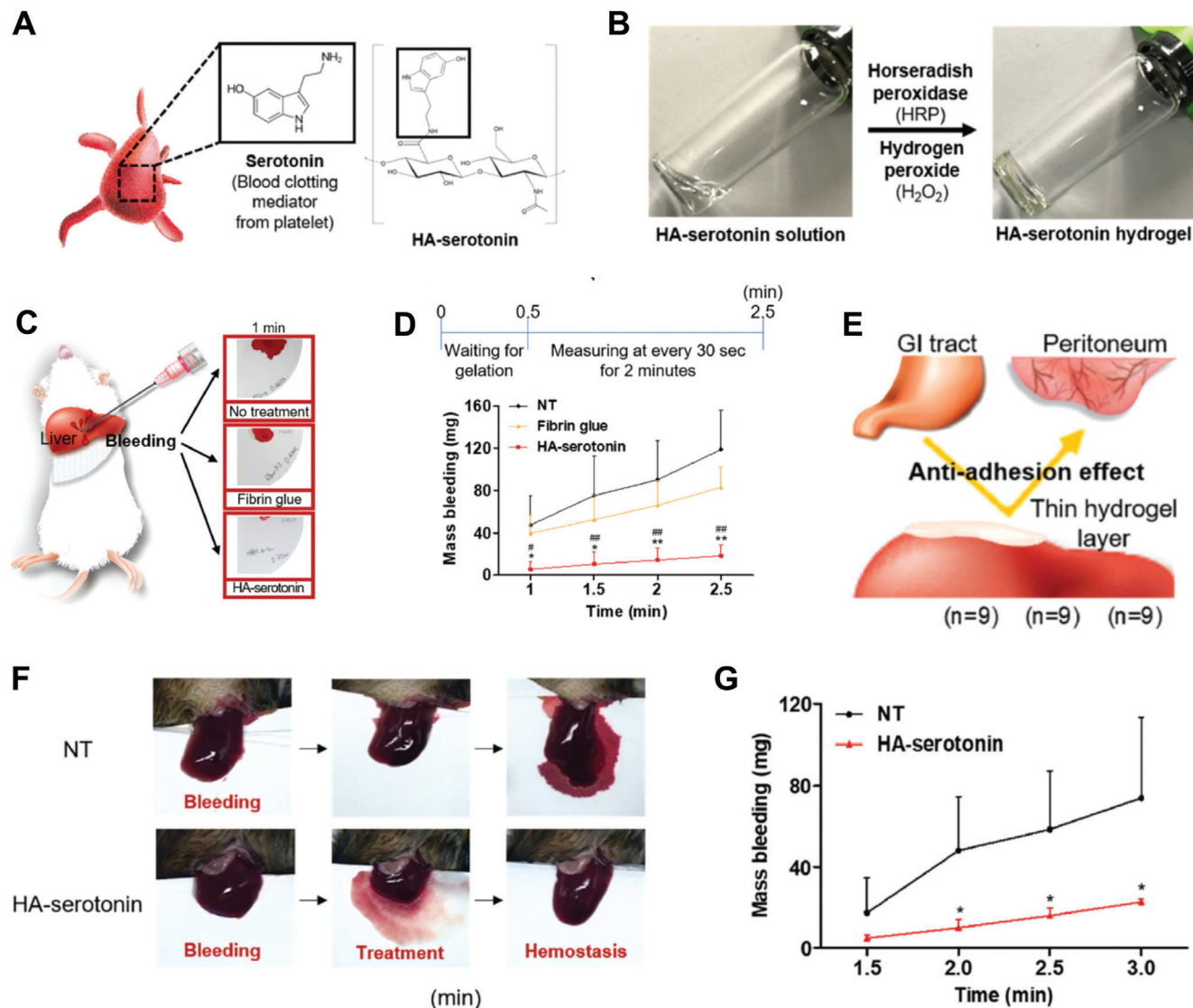


Figure 13. A) Schematic representation of the chemical structure of HA-serotonin hydrogel synthesized via conjugation of serotonin to HA backbone. B) The HA-serotonin hydrogel formation via enzymatic oxidation process. C) Photographs of filter papers showing the level of bleeding from mouse damaged liver after treatment with HA-serotonin hydrogel compared with thrombin and fibrinogen-based glue and control (non-treatment). D) Mass bleeding (mg) in HA-serotonin-treated mice compared to those in the glue and control groups. E) Schematic depiction of anti-adhesion behavior of the hydrogel to peritoneum and gastrointestinal (GI) tract by a thin layer formation on the bleeding sites. F) Hemostatic abilities of HA-serotonin hydrogels compared with the control in a hemophilia mouse model of liver hemorrhage along with G) the quantitative results of mass bleeding (mg). Reproduced with permission.^[127] Copyright 2019, The Royal Society of Chemistry.

Inspired by mussel adhesion chemistry, Song et al. developed dopamine-conjugated oxidized sodium alginate-polyallylamine (Dopa-OA/PAA) hydrogel glue with strong tissue adhesiveness properties for hemostatic application (Figure 14).^[135] In this study, OAs with different degrees of oxidation (OA-30, OA-60, and OA-90) were first obtained using different concentrations of sodium periodate followed by mixing with PAA to yield OA hydrogel glue through Schiff base reaction. It was proven that two polymers formed a stable hydrogel glue and OA-30 exhibited shorter gelation time of 4.1 s with respect to OA-60 and OA-90. However, it was found that OA glue would be too rigid over time to use as a hemostatic material and could be easily detached from the tissue, therefore reducing its hemostatic effect.^[135] To endow

the hydrogel with good tissue adhesiveness and flexibility, the author introduced dopamine into the OA network to form Dopa-OA through Schiff base reaction and it was combined with PAA to obtain Dopa-OA/PAA. Interestingly, the dopa-containing hydrogel demonstrated fast gelation time, lower rigidity, higher adhesive strength and higher elongation compared with OA glue (Figure 14B,C). The subsequent *in vivo* hemostatic experiment in a liver hemorrhage mouse model revealed that the amount of blood loss was significantly reduced with the application of Dopa-OA/PAA (29.7 mg) and OA glue (35.2 mg) in comparison to the control group (97.4 mg). However, in comparison to the OA glue that was easily detached from the wound tissue before attaining hemostasis, the Dopa-OA/PAA with higher stickiness, adhesiveness and

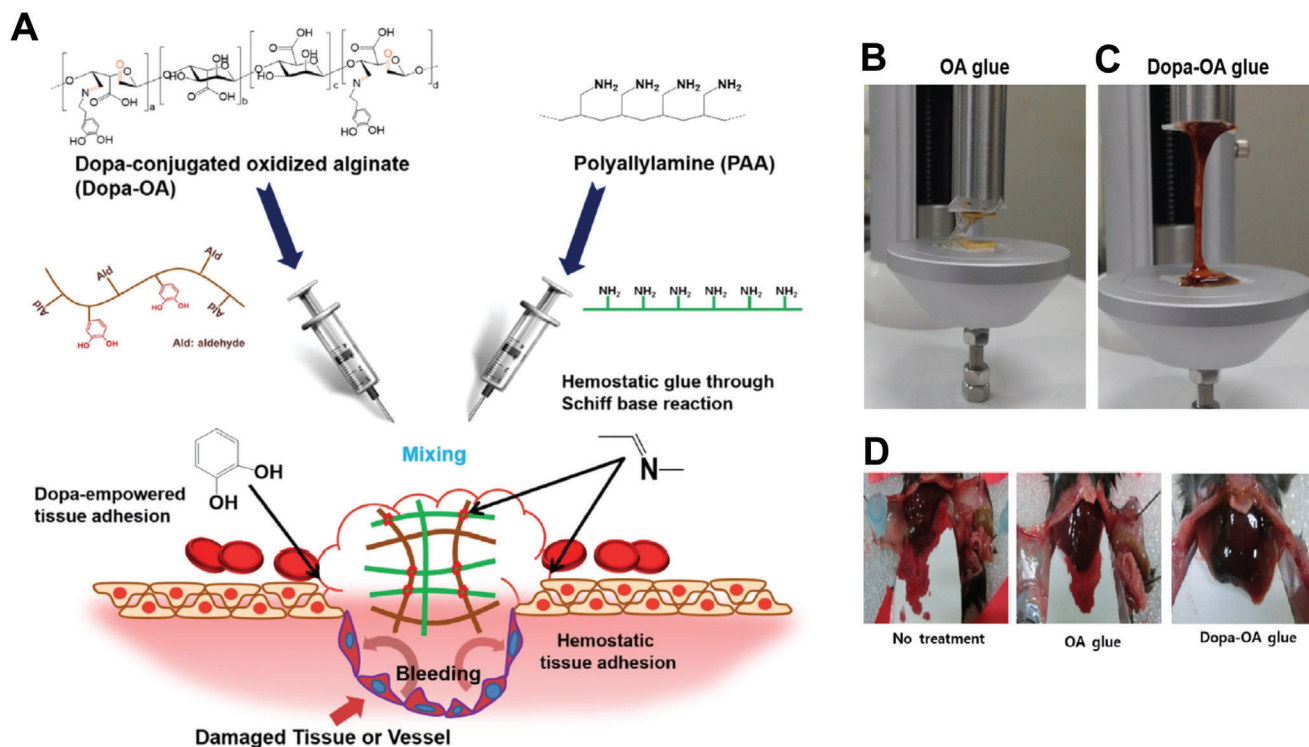


Figure 14. A) The chemistry behind the formation of Dopa-OA hydrogel glue. B,C) The Dopa-OA hydrogel displayed higher tensile strength than OA glue. D) Hemostatic performance of Dopa-OA glue with respect to OA glue and the control, when used in a mouse liver injury model. Reproduced with permission.^[135] Copyright 2019, Springer Nature.

elasticity was found to be a superior hemostatic hydrogel as it remained attached to the bleeding site, therefore stopping bleeding. The authors considered that the remarkable characteristics of the Dopa-OA/PAA material arose from Schiff base reaction between aldehyde groups and quinones of Dopa-OA and the amine groups of tissue proteins, enabling the hydrogel to attach strongly to the wound site.^[135] This engineered hydrogel glue has potential for hemorrhage control in trauma or surgical settings.

It is known that by simple crosslinking reaction, OA as crosslinking agent can form hydrogels when it is mixed with CMC or gelatin for use in drug delivery and tissue engineering applications.^[136] However, this strategy may not be suitable to construct the hydrogel as an efficient hemostat as the resulting hydrogel may lack strong adhesiveness, a critical factor that needs to be considered when designing a hydrogel for hemostatic applications.

To overcome such challenge, in a recent study, an in situ forming adhesive injectable hybrid hydrogel (CMC-GEL/OSA) generated from Schiff base linkages between OSA's aldehyde groups and amino groups from gelatin and CMC, was developed for hemostasis application.^[137] The possible presence of hydrogen bond crosslinking between OSA and CMC was also confirmed. In this study, the aim was to improve the adhesive properties and mechanical strength of the hydrogel through increasing the amino group content, which further enhanced the crosslinking network, therefore increasing hydrogel strength. Based on the results, the double-network hydrogel was found to be injectable by adjusting the concentration of OSA, CMC, and gelatin, and demonstrated a sol-gel transition time of 30 s. Evaluation of ad-

hesion strength of the CMC-GEL/OSA hydrogels revealed that increasing the gelatin concentration from 0 to 40% w/v increased the adhesive strength from ≈ 3 to 11 kPa due to providing more amino groups which promote Schiff base reaction. The double crosslinking network also boosted the gel strength.^[137] In addition to exhibiting good rheological properties, the resulting hydrogel also showed long-lasting bacteriostatic effect against *E. coli* and *S. aureus* when it was loaded with a synthetic antibiotic (levofloxacin) and no cytotoxicity was observed when the hydrogel was incubated with L929 mouse fibroblast cells. In vivo injection of the hydrogel over the bleeding site in a rat hemorrhaging liver model also illustrated its appealing potential as a hemostatic material. It was able to arrest bleeding efficiently and reduced the amount of blood loss from 0.228 g in untreated liver to 0.036 g and it additionally diminished hemostasis time from 349 s in untreated liver to 62 s. The CMC-GEL/OSA also outperformed gauze pressing, resulting in significantly lower blood loss and hemostasis time due to the synergistic effect arising from the hemostatic efficacy of CMC and gelatin as well as the good adhesiveness of the hydrogel.^[137]

4.4. Carrageenan

Carrageenan (CA), an anionic sulfated polysaccharide extracted from edible red seaweeds, comprises long linear chains of D-anhydrogalactose and D-galactose and, based on sulfonic groups number, it is categorized into Kappa (κ), Iota (ι), and Lambda (λ)-carrageenan.^[138] Among those, κ CA has been found

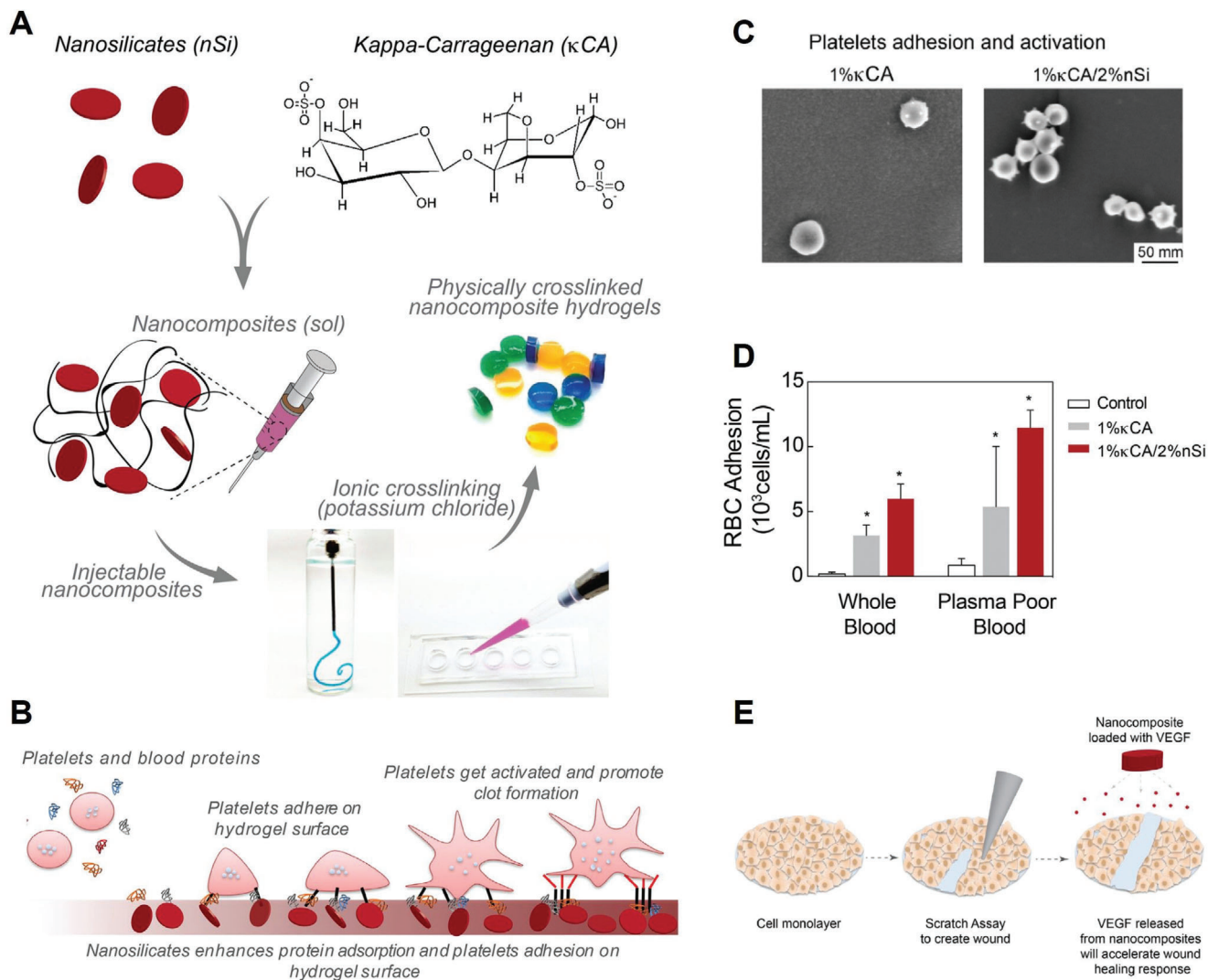


Figure 15. Schematic diagram illustrating A) the preparation of the nanoengineered injectable κ CA/nSi hydrogel and B) possible interaction mechanism between nSi and platelets, resulting in platelet adhesion and activation. C) SEM micrographs showing that more platelets were adhered to the surface of 1% κ CA/2%nSi compared with those in 1% κ CA. D) Effect of the developed hydrogel systems on RBCs adhesion. E) Schematic diagram depicting the scratch wound assay. The scratch wound healing could be stimulated by releasing VEGF which in turn can promote cell migration. Reproduced with permission.^[28] Copyright 2018, Elsevier.

to be a promising candidate for tissue engineering applications owing to its resemblance to natural glycosaminoglycans, mechanical strength and excellent gel forming ability.^[139] κ CA containing one negatively charged sulfated group (OSO_3^-) per disaccharide is known to produce rigid and strong gels in the presence of monovalent cations (e.g., potassium ions) owing to strong ionic interactions between the ions and sulfate groups.^[28] However, ionically crosslinked κ CA hydrogels were found to be unstable under physiological conditions and their degradation characteristic and mechanical properties are not adequately controllable.^[139a,140]

To overcome these limitations, Lokhande and co-workers engineered a series of mechanically strong κ CA shear-thinning injectable hydrogels via physically reinforcing with 2D nSi and assessed their potential for hemostatic and wound healing application (Figure 15).^[28] In this study, the nanocomposite hydro-

gels were fabricated via combination of 1 wt% κ CA and nSi (up to 2 wt%) followed by ionically crosslinking via potassium chloride (KCl). Physically reinforcing κ CA hydrogel network with nSi not only imparted shear-thinning behavior and increased storage modulus but also improved hydrogel physiological stability. While the κ CA was completely degraded within 72 h, the weight loss of the nanocomposite hydrogel was <20% after 72 h. Such improvements in the characteristics of the hydrogels were attributed to the electrostatic interactions between positively charged edges of nSi with OSO_3^- groups of κ CA. The interaction between κ CA and nSi can be also facilitated by K^+ . The hydrogels were also found to be biocompatible toward human mesenchymal stem cells (hMSCs) and the cells displayed higher adhesion and spreading on the κ CA/2%nSi sample compared to pure κ CA gel. The authors of the study argued that while translation of previously reported gelatin/nSi hydrogels with maximum

mechanical stiffness of $\approx 1\text{--}10$ kPa into clinical practice would be difficult, κ CA hydrogel with 2% nSi had higher compressive modulus of 84.5 ± 18.5 kPa at 37°C , which could allow it to efficiently withstand blood pressure at the bleeding site, therefore leading to achieving more efficient hemostasis. Results of hemostatic studies additionally revealed that introduction of higher amount of nSi (2%) into κ CA led to a significant reduction in clotting time compared to pure κ CA and the control. Interestingly, addition of 2% nSi into κ CA significantly promoted blood cell aggregation and platelet adhesion and activation to the surface of the hydrogel (Figure 15C,D). It is reported that negatively charged surfaces can initiate intrinsic coagulation pathway and activate platelets.^[141] It was therefore hypothesized that the negative surface charge of κ CA which became more negative owing to inclusion of nSi as well as increased adsorption of proteins onto the surface of the hydrogel contribute to the efficacious hemostatic ability of the hydrogels, allowing more adhesion of blood component and acceleration of hemostasis (Figure 15C,D).^[28]

Moreover, the in vitro wound healing effect of the nanoengineered hydrogel was assessed with scratch and migration assays using HUVECS. The results indicated that vascular endothelial growth factor (VEGF)-encapsulated κ CA/2% nSi hydrogel with sustained release capacity of VEGF led to the highest wound closure and enhanced HUVECS migration with respect to κ CA and κ CA/2% nSi, highlighting its ability to accelerate wound healing. In the author's opinion, κ CA-nSi hydrogels as an injectable hemostat are suitable for penetrating injuries and for percutaneous intervention during surgical procedure. However, further in vivo investigation is required to fully elucidate the efficacy of the hydrogels for hemostatic and wound healing applications.

5. Synthetic Polymer-Based Hemostatic Hydrogels

5.1. Polyethylene Glycol

Synthetic polymers are appealing materials to engineer hydrogel systems due to possessing controllable chemical and physical properties.^[142] Polyethylene glycol (PEG), comprising repeated ethylene glycol units ($-\text{CH}_2-\text{CH}_2-\text{O}-$), has been broadly investigated as one of the attractive hydrophilic synthetic polymers for a wide range of biomedical applications due to its high hydration capacity, excellent biocompatibility, nontoxicity, high structure flexibility and nonimmunogenicity.^[143] Considering these unique advantages, hydrogels prepared from PEG are therefore known to be excellent candidates for biomedical applications.^[142,144]

Over the past few decades, PEG-based sealants have been shown to possess enormous merits for hemostatic applications. Although a PEG-based sealant composed of two different tetrafunctional PEG macromers has been indicated to achieve adjunctive hemostasis via mechanically sealing areas of leakage,^[20a,145] there are safety concerns with the sealant that limit its applications. For instance, it was reported that it can swell up to 400 percent which may lead to nerve compression; It should not be applied in place of mechanical closure (e.g., sutures, staples, etc.) and also has a limited shelf life, which requires special precautions and handling.^[20a] Recently, efforts have been devoted toward engineering PEG-based hydrogels in order to being able

to meet the requirement of an ideal material for hemostatic applications.

Bu et al.^[146] constructed bacteria-responsive in situ 4-arm-PEG-based hydrogels with potential hemostatic and antibacterial effects through incorporating Schiff base moieties into the crosslinked network and further loading with vancomycin as an antibiotic (Figure 16).^[147] In this study, 3 different hydrogels were first prepared via simply combining 4-arm PEG amine (4-arm-PEG-NH₂), 4-arm PEG succinimidyl (4-arm-PEG-NHS) and benzaldehyde-functionalized PEG (4-arm-PEG-CHO) with different ratios (Gel 1 (1:1:0), Gel 2 (1:0.7:0.3), and Gel 3 (1:0.5:0.5)) in PBS (pH = 7.4) using a dual syringe. The prepared hydrogels not only showed instant gelation (20–25 s) when solid content was increased to 15%, but also exhibited highly porous structures, and high swelling capacities, thus allowing them to effectively facilitate blood cell and coagulation factors concentration. The results showed that although Schiff base formation in the network of Gels 2 and 3 led to a decrease of mechanical strength compared to that of Gel 1 formed by amidation reaction, the gels were found to have higher adhesion ability, which made them strong enough to withstand pressures much higher than normal arterial blood pressure.^[146] According to the authors, while formation of amide bond between Gel 1 and tissue led to adhesion, the working mechanism behind the higher adhesiveness of the other hydrogels stemmed from amide bonds, Schiff bases and $\pi-\pi$ stacking interactions between networks of the hydrogels and tissue proteins, allowing them to strongly attach to the tissues.^[148] The pH-responsive release of vancomycin was investigated in a buffer solution at pH 5 (to mimic the weakly acidic condition where bacteria can reproduce) and pH 7.4. It was found that incorporation of Schiff base moieties into the hydrogel network allowed the release of vancomycin faster and to a higher extent at pH 5, endowing the vancomycin-loaded hydrogels with bacteria-sensitivity.

These hydrogels also displayed efficient in vitro antibacterial properties against *S. aureus*. The vancomycin-loaded Gel 2 was found to be a superior antibacterial agent compared to those of gauze, vancomycin, and Gel 2 alone, when tested in vivo in a rabbit skin infection model. The cytotoxicity evolutions also indicated that the hydrogel systems were biocompatible toward 3T3 mouse fibroblasts even after encapsulation with vancomycin. Most remarkably, the in vivo hemostatic evaluation revealed that while application of the Gel 2 in the rabbit liver laceration model and pig skin led to cessation of bleeding and achieved complete hemostasis when it was applied on the wounds for 30 s, the bleeding in the gauze-treated group did not stop even after 5 min. It was found that, firstly, Gel 2 provided a physical barrier to control bleeding, and then its high absorption capacity led to concentration of the blood components and platelets, thereby resulting in quick hemostasis. The hemostatic efficacy of Gel 2 was additionally verified in rabbit femoral artery injuries. Taken together, these findings suggested that the prepared PEG-based hydrogel systems with efficient antibacterial and hemostatic properties may have the potential to be utilized for first aid treatment in critical situations.^[146]

Later, the same group engineered ammonolysis-based Tetra-PEG hydrogel integrating fast degradability, controllable dissolution properties and outstanding hemostatic capabilities in vivo through introducing cyclized succinyl ester groups into the

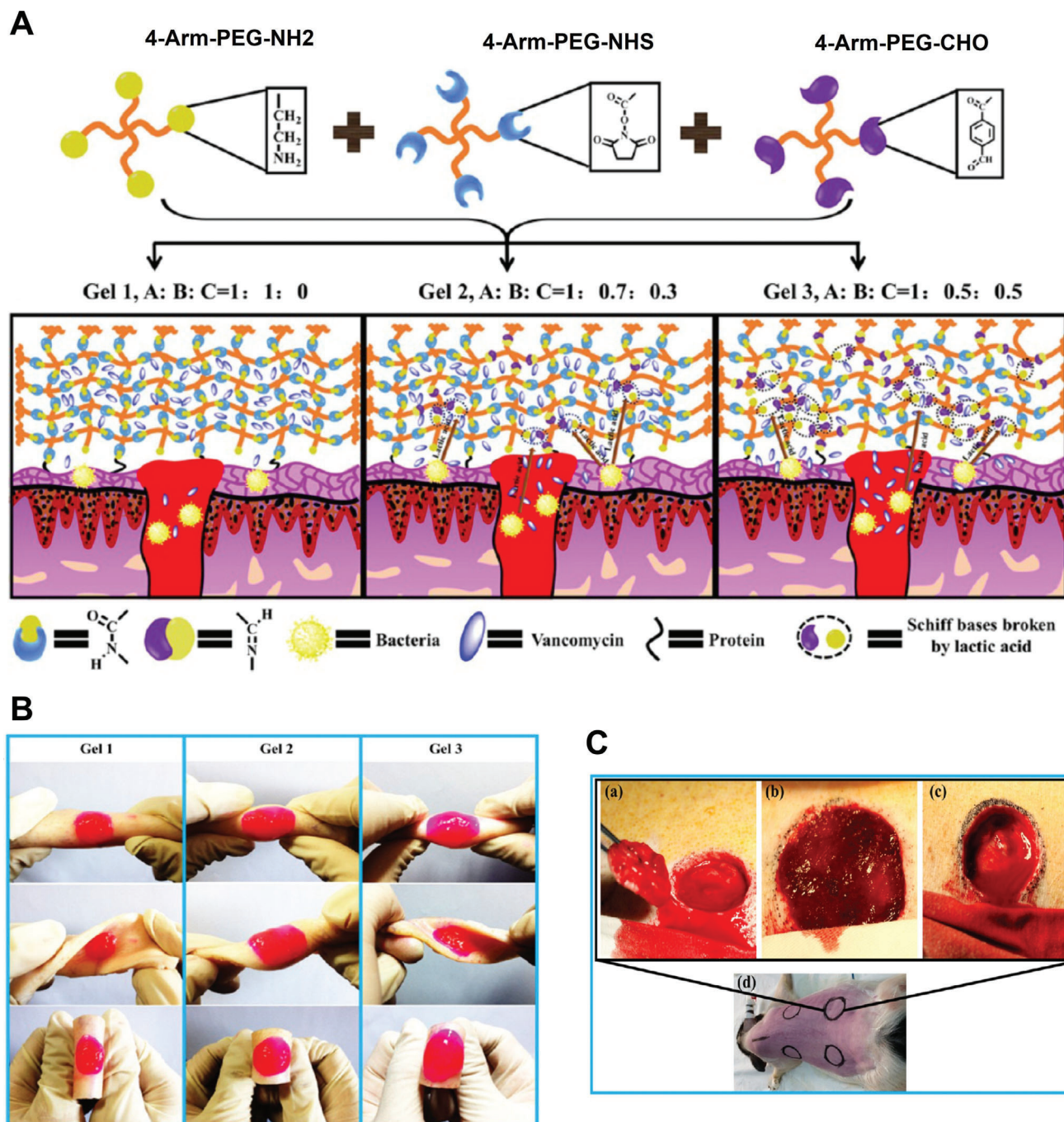


Figure 16. A) Schematic presentation of vancomycin-loaded hemostatic hydrogel preparation and adhesion to tissues. B) Photographs representing the adhesion of hydrogels to pig skin. C, a–d) Photographic images displaying the hemostatic effect of b) Gel 2 in a laceration model of pig skin as compared to c) gauze. Reproduced with permission.^[146] Copyright 2016, American Chemical Society.

hydrogel network.^[149] The hydrogel was prepared in situ from mixing tetra-PEG-NH₂ and tetra-PEG succinimidyl succinate (tetra-PEG-SS) in PBS using a dual-syringe and its suitability to be used as hemostatic sealant was assessed and compared to another tetra-PEG hydrogel composed of tetra-PEG-NH₂ and tetra-PEG succinimidyl glutarate (tetra-PEG-SG). The resulting SS and SG hydrogels displayed fast gelation time (≈ 6 s), higher adhesion and compression strength and larger bursting pressure with re-

spect to those of a current thrombin and fibrinogen-based system, suggesting their ability to firmly attach to the tissue and their stability. The SS hydrogel also exhibited controllable dissolution properties as it could be cleaned on flat porcine skin and on skin with holes in less than 2 and in 5 min, respectively, via cysteamine-soaked swabs with a slight external force. Assessment of in vitro and in vivo degradation profiles of the hydrogels demonstrated that the degradation rate of tetra-PEG hydrogels

can be enhanced by introducing succinyl ester. In comparison to SG that showed slow degradation *in vitro* as well as *in vivo* inducing foreign body reaction and fibrous capsule formation, the SS hydrogel displayed very fast degradability both *in vitro* (in 3 days) and in a rat liver damage model (in 5 days) with no adverse effects. Its degradation products were found to be excluded by urination, as confirmed by fluorescence of urine and feces. The authors suggested that no long-term inflammatory response and tissue adhesion would be promoted by SS with respect to SG due to its rapid degradation, as confirmed by the subcutaneous and muscle implantation experiments. *In vivo* implantation of both SS and SG hydrogels into rabbit liver injury additionally achieved faster and efficient hemostasis in less than 30 s than that of the gauze. Moreover, the SS hydrogel indicated superior healing effect compared to SG hydrogel and the gauze as no inflammatory response and tissue adhesion postoperation was observed in SS-treated livers, which correlated with its fastest degradation rate to inhibit the inflammatory response and the capability to create a barrier to stop adhesion to the surrounding tissue and second bleeding. The SS hydrogel was also proven to efficiently reduce time to hemostasis in not only the anticoagulated rabbit model (as compared with those of the gauze and the commercial system) but also in a porcine spleen injury model even under anticoagulated situations.^[149] According to the author's suggestion, this hydrogel sealant can be an optimal choice for *in vivo* visceral hemostasis, drug delivery vehicles as well as *in vivo* antifouling materials.

Injectable mussel-inspired bioadhesive hydrogels (iCMBAs) were generated by mixing PEG, dopamine and citric acid with sodium periodate, and their capacities to promote hemostasis and sutureless wound closure were evaluated.^[150] The amide bond formation between dopamine's NH_2 groups and citric acid unreacted COOH groups as well as esterification reaction between PEG and citric acid were involved in the adhesive hydrogel's synthesis. The results of this study demonstrated that using smaller molecular weight of PEG ($M_n = 400$), higher amount of dopamine (0.5 mol) and increasing the sodium periodate to prepolymers ratio (8%) led to faster formation of the adhesive injectable hydrogel in 18 ± 2 s at 37°C , compared to other compositions. The iCMBAs with different formulations also demonstrated higher adhesion strength of 33.4 ± 8.9 to 123.2 ± 13.2 kPa to wet porcine small intestine submucosa compared with that of commercially available thrombin and fibrinogen-based glue (15.4 ± 2.8 kPa), which was ascribed to the capability of produced *o*-quinone from oxidation of catechol to react with tissue proteins through Schiff base reaction and Michael addition. The study also found that the crosslinked iCMBAs hydrogel possessed rubber-like (elastomer) behavior, controllable degradation rate, and excellent cytocompatibility both *in vitro* and *in vivo*. Additionally, *in vivo* injection of iCMBAs in the rat skin incision model showed that the adhesive hydrogel has efficient hemostatic effects as it could immediately cease bleeding and closed the wound after a few min and no blood leakage was observed at the injured site compared with suture. In the author's opinion, the hemostatic property of iCMBAs is associated with its capability to create a mechanical barrier to blood loss and to form insoluble interpolymeric complexes via interaction of its carboxyl groups with blood proteins. The hydrogel was also found to accelerate the wound healing process and showed minimal inflamma-

tory reaction according to the histological evaluation. In contrast to suture-closed skin that had tensile strength of 810 ± 355 kPa, the iCMBAs-treated skin showed superior tensile strength of 1250 ± 315 kPa, suggesting the acceleratory effect of iCMBAs on tissue reconstruction.^[150] Furthermore, the adhesive hydrogel exhibited complete *in vivo* degradation so that no trace of polymer was observed after 28 days, which was ascribed to the presence of degradable ester bonds in the iCMBAs backbone formed by esterification reaction between PEG and citric acid.

6. Other hydrogels

In addition to gelatin, keratin, silk, chitosan, hyaluronic acid, alginate, carrageenan, and PEG, other polymers have been utilized to prepare hemostatic hydrogels and promising results have been attained.

For instance, a novel self-healing and injectable agarose-based hydrogel was formed by a Schiff base reaction between dialdehyde-functionalized PEG (DF-PEG) and agarose-ethylenediamine conjugate (AG- NH_2).^[151] The resulting hydrogel (AD hydrogel) not only demonstrated fast gelation time of 10–15 s, it also presented self-healing performance after 5 min, good mechanical strength and injectability.^[152] In comparison to AG and AG-PEG hydrogels, the AD hydrogel was shown to have higher adhesive strength to porcine skin and displayed the greatest bursting pressure even higher than the normal arterial blood pressure. The high adhesive capability of AD hydrogel was attributed to both the Schiff base linkages and hydrogen bonds between amino groups in tissue and hydrogel's residual aldehyde as well as π - π stacking interactions formed between proteins of the surrounding tissue and the hydrogel.^[146,148b] The cell viability analysis also revealed that the hydrogel composed of biocompatible DF-PEG and AG- NH_2 ^[153] is cytocompatible with HUVEC, as its extract was found to maintain high cellular viability (>80%). Furthermore, after the AD hydrogel was applied in the bleeding site of a rabbit liver model, it could stanch bleeding very rapidly and significantly reduced the total amount of bleeding from 0.71 ± 0.09 g and 1.17 ± 0.13 g in gauze-treated and negative control groups, respectively, to 0.19 ± 0.03 g. A sharp reduction in hemostasis time was also observed for the AD hydrogels group with respect to the gauze and the control group, which was ascribed to its swelling property and porous structure, thereby allowing the accumulation of platelets and RBCs via absorbing wound exudate.^[151]

A series of hemostatic hydrogels made of ϵ -polylysine grafted with pnitrophenylchloroformate-PEG-tyramine conjugate (PNC-PEG-TA) was rapidly formed *in situ* through HRP/ H_2O_2 enzymatic crosslinking reaction.^[154] ϵ -polylysine is a naturally occurring homopolyamide that has been known to possess good biodegradability, anti-infection activity and biocompatibility.^[155] It was found that gelation time is affected by the concentration of HRP and the polymer so that the gelation time was drastically reduced to 2 s in the hydrogel with higher concentration of HRP and polymer due to increasing degree of crosslinking. At fixed HRP (0.12 mg mL^{-1}) and PPT conjugates content (10 wt%), the hydrogels also displayed slower degradation rate, the highest storage modulus and adhesive strength with increasing concentration of H_2O_2 up to 0.08 wt%, which can be attributed to the effect on crosslinking density. It is noteworthy to

mention that the PPT hydrogel was found to have higher adhesive strength than that of commercially available thrombin and fibrinogen-based glue. In addition to the concentration of H_2O_2 , the good water-solubility of ϵ -polylysine was also believed to contribute to the strong adhesiveness of the PPT hydrogel, which facilitates hydrogel formation, subsequently providing tighter interaction between negatively charged mucus membrane and cationic ϵ -polylysine.^[1109,156] The cytotoxicity studies revealed that the modification of ϵ -polylysine with PEG can reduce its cytotoxicity as the PPT hydrogel showed good biocompatibility toward fibroblast L929 cells. The hemostasis and wound-healing properties of the PPT hydrogel were additionally assessed in vivo using rat hepatic hemorrhage and skin thickness incision models, respectively. The authors emphasized that the synergy between the hemostatic property of polylysine, which is found to provoke platelet aggregation and fibrinogen gelation, and the hydrogel's strong adhesive properties, allowed the PPT hydrogel to rapidly seal the bleeding site through plug formation, therefore reducing the total blood loss from 211.5 ± 10.3 mg in the control group to 65.2 ± 4.6 mg. In comparison to sutures, commercial products, the PPT hydrogels also exhibited superior wound closure and wound healing effect as the wound was completely recovered at 14 days post-treatment with reduced fibrosis and newly formed dermis.^[154]

Dopamine was also conjugated to acid-terminated poly(organophosphazene) (AP) through amide bond linkages to form an injectable thermosensitive hydrogel at body temperature and its hemostatic activity was assessed using a mouse liver injury model.^[157] While AP revealed no viscosity due to its high hydrophilicity, the conjugated hydrogel was capable of initiating sol-gel transition at the body temperature with viscosity of 356.25 Pa s. This behaviour was ascribed to dopamine conjugation that affects the hydrophilic-hydrophobic balance through the conversion of AP's hydrophilic carboxyl group to less hydrophilic dopamine group. The injectable hydrogel displayed in vivo biodegradability of 85% by 21 days and low cytotoxicity toward NIH3T3 cells, suggesting its suitability for hemostatic applications. In vivo results from injection of the hydrogel into the bleeding point in rat liver injury model revealed that it had efficient hemostatic efficacy and it led to significantly less blood loss than that of the control.^[157] The engineered hydrogel is suggested to achieve hemostasis in clinical settings.

In a study by Chen et al. a novel mussel-inspired injectable γ -PGA-DA hydrogel composed of dopamine and poly(γ -glutamic acid), a natural biocompatible polymer produced by a *Bacillus subtilis* strain,^[158] was formed in situ via the HRP/ H_2O_2 enzymatic crosslinking reaction and its hemostatic effectiveness in a mouse hemorrhaging liver model was assessed.^[159] To prepare γ -PGA-DA conjugates, the γ -PGA backbone was modified with dopamine through carbodiimide coupling reaction using EDC/NHS chemistry. The results revealed that by varying the concentrations of polymer, H_2O_2 , and HRP, the hydrogel gelation, swelling ratio, inner morphology, and biodegradation behavior were shown to be tuned. Notably, with increasing concentrations of polymer, H_2O_2 and HRP to 8.0 wt%, 10.0×10^{-3} M and 20.0 U mL⁻¹, respectively, the gelation time decreased to 25 s, which was ascribed to increased crosslinking density, formation of a tighter network structure and rapid catechol free radicals generation. The hydrogels showed stronger adhesion capability

on the wet surface of porcine skin in comparison to thrombin and fibrinogen-based glue, depending on the degree of catechol substitution. This effect stemmed from several chemical covalent and physical noncovalent crosslinking interactions between the catechol groups of the hydrogels and tissue.^[81,129,160] The excellent biocompatibility of the hydrogels toward L929 mouse epidermal cells was also reported in this study. More importantly, in vivo applications of hydrogels in a mouse hemorrhaging liver model reduced the amount of bleeding from 479.7 and 199.7 mg in the control and the commercial glue, respectively, to 117.5 mg by adhering and covering the hemorrhaging site. The governing factors behind the efficient hemostatic function of γ -PGA-DA hydrogels were found to be the hydrogel porous structure allowing to capture more blood, and the interaction of remnant catechol quinones with tissue proteins and carbohydrates as well as blood plasma leading to more efficient cell attachment. After achieving hemostasis, the hydrogel was also found to be beneficial for blood vessel regeneration, further confirming its suitability as a hemostatic agent.^[159] In the author's opinion, the engineered hydrogels can be used as local hemostatic agents, tissue adhesives, and for other medical applications.

In a similar study by Han et al., two adhesive and antibacterial mussel-inspired injectable hydrogels based on γ -PGA-DA conjugate were formed in situ within 2 s via the HRP/ H_2O_2 enzymatic crosslinking reaction and their feasibility as an efficient hemostatic agent was evaluated.^[161] To prepare the hydrogels, PD conjugate was first prepared by modifying the γ -PGA with dopamine through EDC and NHS chemistry followed by dissolving PD into PBS (PBS-PD) and cirsium setosum extracts CSE-PD, respectively. The CS, the above ground part of *Cephalanoplos segetum* Kitam, has been shown to have a significant impact on hemostasis and it possesses the capability to accelerate platelet aggregation and adhesion.^[162] The experimental results showed that mechanical properties and adhesion strength (13–30 kPa) of the PD hydrogels could be enhanced with increasing the H_2O_2 concentration (from 2% to 3%), which was attributed to increasing crosslinking density. Introducing CSEs into the PD system not only endowed adhesive hydrogels with a higher antibacterial efficacy against *E. coli* and *S. aureus* in comparison to PBS-PD, but also led to the formation of a hydrogel with superior hemostatic capability. The results of blood clotting studies revealed that CSE-PD possesses higher hemostatic efficacy than those of the PD control and PBS-PD. When it was incubated with sheep blood, the material exhibited a significantly lower hemoglobin absorbance value, indicating its higher clotting ability. Furthermore, more platelets were adhered to the surface of CSE-PD material.^[161] However, in vivo experiments need to be performed to evaluate the actual potential of these novel hydrogels for hemostatic applications.

In another interesting work, a water-triggered hyperbranched polymer adhesive (HBPA) composed of PEGDA, pentaerythritol tetraacrylate (PETEA) and dopamine was engineered via Michael addition reaction between dopamine's amine group and multivinyl monomers.^[163] It was found that when HBPA with hydrophilic catechol side branches and a hydrophobic backbone encounters water, the hydrophobic backbone swiftly aggregated and formed gum like coacervates, thereby dispelling water molecules on the surface of the substrate. This would allow the adhesive to expose more catechol groups outward, resulting in strong

adhesion to diverse substrates even in wet conditions. The adhesive was found to be solidified in 10 s upon contacting water and demonstrated good degradability. To endow the adhesive with hemostatic capability, long chains of alkyls (octylamine (HBPA-OA), dodecylamine (HBPA-DDA), and decylamine (HBPA-DA)) were introduced into the adhesive's structure. It was found that these hemostats possess injectability which allow them to reach deep wounds and therefore stop bleeding. The *in vitro* experiment showed that while HBPA-DA and HBPA-DDA led to complete blood clotting, ascribed to the effect of the longer chain of alkyl on blood clotting, HBPA did not form solid clots. Impressively, in comparison to plain cotton swab that resulted in a large amount of blood loss in femoral artery bleeding in a rat model, application of HBPA-DDA-impregnated cotton swab led to the stop of bleeding and no blood flow was identified after removing the cotton swab. Furthermore, when the HBPA-DDA was injected into the bleeding site of a liver bleeding in a rat model, it rapidly stopped bleeding and showed greater hemostatic efficacy (93%) compared to that of gauze (26%). Alongside its hemostatic effect, the adhesive was shown to develop a barrier layer against blood flow. The hemostatic capability of HBPA-DDA was also assessed in the pig's liver with a puncture wound and it could successfully arrest bleeding in 4 s. The adhesive also showed complete *in vivo* degradability in 10 days and biocompatibility when it was subcutaneously injected into rats. The authors of the study proposed this interesting hemostatic system as first aid in emergency situations.^[163]

As mentioned earlier, in addition to using dopamine to impart efficient adhesiveness to hydrogels, another strategy to engineer adhesive hydrogels is to use TA, which is rich in catechol and pyrogallol groups, and, interestingly, it can act as both chemical crosslinker and catechol group provider. However, it has been argued that like dopamine-based adhesive hydrogels, their adhesive strength still needs to be improved.

A recent study reported that incorporation of different amounts of kaolin (KA) into polyacrylamide-TA (PAAm-TA) hydrogel networks as physical crosslinker and hemostatic accelerator led to formation of a series of mechanically tough hydrogels with improved hemostatic efficacy and adhesive strength.^[164] All PAAm-TA-KA hydrogels showed superior mechanical strength, capability of self-recovery, flexibility and stretchability compared to PAAm-TA hydrogel, which were attributed to physical and chemical interactions between KA, TA and PAAm chains. However, incorporation of the highest amount of KA into the hydrogel network resulted in reduction in mechanical properties due to formation of short PAAm chains between crosslinking points. The KA incorporation also enhanced the adhesive strength of the resulting hydrogels to porcine skin compared to PAAm-TA and the highest adhesive strength value was observed in the hydrogel with the highest concentration of KA. The underlying causes of this enhancement of adhesive strength have been shown to stem from high toughness which favors energy dissipation and the presence of a large amount of catechol groups contributing to the intimate interfacial adhesion forces from the noncovalent bonds and chemical covalent bonds. Furthermore, the PAAm-TA-KA hydrogel with the highest amount of KA was found to be sufficiently adhesive to adhere tightly to various surfaces (e.g., ceramic, glass, rubber, paper, polypropylene, iron, and rubber suction bulb) and human skin as well as wet porcine myocardium.

The authors emphasized that this hydrogel also offers benefit with respect to many traditional medical adhesives as it can be effortlessly peeled off from the skin without producing pain and leaving any residue. The adhesion strength of the hydrogels was further examined by the bursting pressure test and all PAAm-TA-KA hydrogels exhibited bursting pressure higher than the one obtained with PAAm-TA and human arterial blood pressure. Notably, in comparison to PAAm-TA and the control, the prepared adhesive hydrogels yielded shorter times to hemostasis when they were pasted onto the bleeding site in a rat femoral artery model. This behavior was ascribed to their stronger adhesion strength and to the acceleratory effect of KA on the coagulation cascade. From the results, it was found that the prepared adhesive hydrogels have efficient capability to stop bleeding from a broken artery. The PAAm-TA-KA hydrogels were also found to be cytocompatible as they promoted L929 fibroblast attachment and proliferation.

Inspired by a defensive mucus of the *Arion subfuscus* slug, Li et al. prepared a family of bilayered tough adhesives comprised of an adhesive surface made of a primary amine-containing polymer (e.g., gelatin, collagen, polyallylamine, chitosan, and polyethylenimine) and a dissipative matrix composed of a hydrogel that contains both covalently and ionically crosslinked polymer (e.g., a hydrogel like alginate-polyacrylamide).^[29a] These adhesives could be used either as a preformed patch or as injectable solution for tissue repair. The authors found that while the adhesive surface can be bonded to the diverse wet surfaces via physical interpenetration, covalent bonds, and electrostatic interactions, the dissipative matrix dissipates energy by hysteresis, thereby synergistically resulting in higher adhesion energies on wet surfaces. It was also reported that the bridging polymer could be covalently bonded to the hydrogel matrix, which could be further facilitated by two coupling agents such as EDC and Sulfo-NHS. The results showed that owing to the high concentration of primary amines, adhesives made of chitosan and polyallylamine demonstrated high adhesion energies ($>1000 \text{ J m}^{-2}$). Notably, the use of adhesives led to high adhesion energies when tested on the pig skin and beating pig heart covered with blood (adhesion strength: $83 \pm 31 \text{ kPa}$). The burst pressures reported for these adhesives were 206 and 367 mmHg without and with a plastic backing, respectively, which were considerably higher than the values for the arterial blood pressure and commercial surgical sealants. The hemostatic efficiency of the adhesives was also assessed in rat models with a circular liver laceration and they showed comparable performance to SURGIFLO. The *in vitro* and *in vivo* studies also showed that the adhesives were biocompatible.^[29a]

7. Discussion, Conclusion, and Outlook

Depending on the type of hemorrhage and wound location, many hemostatic materials and technologies with the ability to effectively manage bleeding have been steadily developed. While to control bleeding from externally visible and accessible (often compressible) injuries there are several successful options in the form of dressings, gauzes, bandages, foams, sprays, adhesives, gels, powders, granules, tourniquets, and tamponades, to manage internal bleeding (often noncompressible), transfusion of blood products are needed to achieve proper hemostatic resuscitation.

Blood loss during operations and surgical procedures has always been a concern and therefore management of bleeding is very important. Despite development and commercialization of a variety of hemostats, sealants, and adhesives that are currently successfully utilized in various surgical disciplines, these products may face obstacles to efficiently achieve hemostasis and promote wound healing in some situations. Therefore, swift and efficient hemorrhage control during surgical procedures is still a significant challenge. To address unmet needs, the development of polymeric hydrogels with multifunctional characteristics has been rapidly growing over recent years.

In the present review, we have described the recent advances in the development of polymeric hydrogel systems as hemostatic agents, sealants or adhesives, with emphasis on the polymer backbone, nature of the crosslinking, physiological, and biological properties, as well as mechanical properties. More importantly, their hemostatic potential both *in vitro* and *in vivo* has been discussed. Most of the hydrogel systems described here have been developed to arrest surgical bleeding and the studies utilized accessible wounds to evaluate hemostatic capability. **Table 2** provides a summary of the *in vitro* and *in vivo* characteristics, including hemostasis time, amount of blood loss, antibacterial and wound healing effects, adhesive strength, gelation time, and bursting pressure, of a wide range of polymeric hydrogel systems.

As discussed in this article, these hydrogels that are widely engineered from natural and synthetic polymers such as gelatin, keratin, silk, chitosan, alginate, hyaluronic acid, carrageenan, and PEG, offer a suite of exciting properties and mostly show potential to stop localized bleeding in accessible sites.

It was found that the incorporation of synthetic silicate nanoplatelets, nanobioglasses, and nanowhitlockite into hydrogel networks improves their hemostatic performance and, interestingly, the hydrogels showed shear-thinning ability, a crucial characteristic that allows the hydrogels to be injected into a bleeding site using minimally invasive approaches. Cryogel systems with shape recovery behavior were also found to have potential for deep and irregular hemostasis.

Sufficient internal strength, high adhesive bonding capability and fast wound sealing are also considered as primary requirements for *in vivo* applications. A hemostatic hydrogel must adhere strongly to the tissue of choice even under high fluid pressures, wet and dynamic conditions, while preserving its mechanical strength and thereby rapidly halting blood loss without migrating away from the target tissue site. In comparison to some of the current available sealants that may fail to meet the wet bonding requirements, adhesive polymeric hydrogel systems constructed by mimicking the hierarchical nanostructure and chemical composition of mussel foot proteins as well as the ECM composition, demonstrated instant hemostasis capacity with high adhesion to wet tissue particularly in highly dynamic biological environments (e.g., the beating heart). Some of the polymers highlighted in this article were modified with catechol which not only showed good hemostatic properties but also demonstrated strong adhesion properties. While in some studies current thrombin and fibrinogen-based glue was shown to be easily washed away from the injured site, some of the developed hydrogels could withstand the high blood pressure as they exhibited higher burst pressure which would make them promis-

ing sealing agents for hemostasis. The resulting hydrogels also showed superiority over some of commercial products in accelerating wound healing in the investigated conditions, implying their excellent biocompatibility. The loading of the hydrogels with antibacterial substances also endowed them with antibacterial efficacy, an extremely important functionality which needs to be considered when designing a product for hemostatic and wound healing applications.

Despite recent progress attained in the field of polymeric hydrogel systems for hemostatic and wound healing applications, as discussed in this review, there are numerous challenges that need to be overcome before these hydrogel-based technologies can be translated for clinical applications. The challenges are highlighted as follows:

- Several hemostatic hydrogels have so far been fabricated from natural and synthetic polymers. However, although natural polymers have been shown to possess many advantages, they lack adequate mechanical properties. On the other hand, although synthetic polymers lead to formation of stronger hydrogels and their chemistry and structure are easily controllable, they have lower biocompatibility. Therefore, combination of natural and synthetic polymers can be a highly desirable approach leading to engineering hemostatic hydrogels which tap into the favourable characteristics of both realms. Even though few studies highlighted in this article have reported hemostatic hydrogels based on combination of natural polysaccharides and/or proteins with synthetic polymers (mostly PEG), further studies are still required to focus on the design and synthesis of these hydrogels. In addition to PEG, other types of synthetic polymers such as polyacrylamide and poly(vinyl alcohol) can be also used.
- Although a variety of chemical and physical crosslinking methods have been reported to prepare hemostatic hydrogels, none of these approaches on their own can satisfy the requirements of an ideal hemostatic hydrogel. The fast *in situ* gelation (ideally <5 s) is one of these crucial requirements that needs to be considered when designing a hemostatic hydrogel for blood clotting and to achieve swift hemostasis under critical conditions as it prevents gels to diffuse away from the bleeding site. The application of hydrogels as hemostatic material and adhesive sealant also demands suitable mechanical strength to prevent their failure, thereby providing efficient hemostasis. However, several chemically crosslinked hydrogels reported here displayed long gelation time. Additionally, it has been found that, compared with hydrogels prepared by chemical crosslinking, physical hydrogels usually have lower mechanical properties. Therefore, one of the best strategies to circumvent these limitations is developing mechanically strong double-network hemostatic hydrogels via combining chemical and physical bonds which endow hydrogels with robust mechanical properties and fast gelation, respectively. Only few studies have attempted to prepare double-network hydrogels and therefore more effort is required to engineer these types of hydrogel systems for hemostatic applications.
- While a gel needs to be rapidly formed upon application on the incision site, it should maintain a balance between its cohesive strength (internal molecular forces formed within the adhesive hydrogel's layer) and adhesive strength (force between

Table 2. Summary of hemostatic polymeric hydrogels.

Polymeric system	Hydrogel preparative technique	Time to hemostasis (in vitro or in vivo)	In vivo model and wound type	Blood loss in treatment groups	Biocompatibility effect/wound healing	Antibacterial capability [%]	Adhesive strength/in vitro bursting pressure	Relaxation time	Ref.
Gelatin-based hemostatic hydrogels									
Gelatin + silicate nanoparticles	Physical crosslinking	In vitro clotting time [min]		A circular liver laceration model in rats (1 cm diameter)	After 5 and 10 min Control >2 g 9NC75 <1 g	Exhibited insignificant cytotoxic effect with RAW macrophages and was biocompatible in vivo when assessed by dorsal subcutaneous implantation in rats	-	-	[51]
		Control	5.3						
		6NC0	5.4						
		6NC25	4.5						
		6NC50	3.6						
		6NC75	3.2						
		6NC100	2.5						
		9NC0	5.5						
		9NC25	2.7						
		9NC50	3.9						
9NC75	1.4								
9NC100	1.3								
GelMA +HA-NB + LAP	Photocrosslinking with UV light and Schiff base reaction	Bleeding was stopped in a few seconds.		A large incision (3 cm) in rabbit's livers was made by surgical scissors	Blood loss in rabbit liver injury Control GelMA/HA-NB/LAP Commercial thrombin-fibrinogen-based glue	Showed biocompatibility toward L929 fibroblastic cells and C3H cells; showed cytocompatibility in vivo with no necrosis and minimal inflammation	-	1.384 ± 0.0006 s for 5%GelMA/1.25%HA-NB/0.1%LAP 82.137 ± 4.005/290 ± 18 mmHg for 10%GelMA/2.5%HA-NB/0.2%LAP 7.063 ± 2.940/<100 mmHg for commercial sealants	[61]
		Bleeding was stopped in a few seconds.							
		No blood leakage was seen when hemostatic forceps were removed after 30 s.							
		Bleeding was stopped within 30 s.							
		Puncture injury model (6 mm diameter) in pig hearts							
		Tail cut model in rats (class I hemorrhage)							
		Liver wedge resection model in rats (class II hemorrhage)							
		More extensive liver wedge resection model in rats (class IV hemorrhage)							
		In vitro hemostatic time [min]							
		Biogel with 0% BIL							
Biogel with 5% BIL		4.875 ± 0.12							
Biogel with 20% BIL		1.13 ± 0.13							
GelMA+ BIL + LAP (BioGel) + LAP (BioPEG)	Photocrosslinking with visible light	Mean losses of TBV		Controls GelMA BioGel	Showed biocompatibility toward primary C2C12 cells with cell viabilities of 98.5 ± 0.5 for BioGel and 97 ± 1.0% for BioPEG. In vivo subcutaneous implantation led to less or no inflammatory responses	-	0.23 ± 0.02 kPa/9.17 ± 0.66 kPa for Biogel with 0% BIL 2.25 ± 0.02 kPa/101.74 ± 2.12 for Biogel with 20% BIL 7.01 ± 0.20 kPa/25.60 ± 0.99 kPa for BioPEG with 0% BIL 38.70 ± 0.30 kPa/69.42 ± 1.59 kPa for BioPEG with 20% BIL	120 s and 60 s light exposure were used to for GelMA and PEGDA, respectively	[32c]
		15.4%							
		8.27 ± 2.77%							
		6.64 ± 2.62%							
		19.8%							
		34.5 ± 2.9%							
		16.2 ± 4.6%							
		12.06 ± 0.98%							
		9.282 ± 1.522%							
		48.72%							
Both									
successfully stopped blood loss									
Class I hemorrhage									

(Continued)

Table 2. Continued.

Polymeric system	Hydrogel preparative technique	Time to hemostasis (in vitro or in vivo)	In vivo model and wound type	Blood loss in treatment groups	Biocompatibility effect/wound healing	Antibacterial capability [%]	Adhesive strength/in vitro bursting pressure	Gelation time	Ref.
Hyaluronic acid + gelatin	Chemically crosslinked using EDC/NHS (amid bonds)	BioGel completely stopped bleeding within 2 min Class II hemorrhage BioGel completely stopped bleeding after the 7th min	Needle puncture (5 mm in depth) injury model in rat's liver	Control	Displayed no significant cytotoxicity toward 3T3-E1	-	Bursting pressure: 9.64 ± 7.55 kPa for sc-G 24.71 ± 11.58 kPa for HA/G 2.51 ± 1.61 kPa for a commercial thrombin and fibrinogen-based glue	90 s for sc-G 50 s for HA/G	[63]
				Sc-G HA/G Commercial thrombin-fibrinogen-based glue					
Cellulose + KE-NPs (KEC)	Physically crosslinking (hydrogen bonding and hydrophobic interactions)	Liver puncture model Control <275 s Cellulose <225 s KE-NPs <225 s KEC <150 s	Rat liver puncture model (5 mm deep wound was created by scalpel)	Liver puncture model Control <275 mg Cellulose <225 mg KE-NPs <225 mg KEC <100 mg	Showed cytocompatibility toward fibroblast L929 and HUVEC	-	Adhesive strength: 18.21 kPa at 1.5% ratio of KE-NPs 8.61 kPa at 2.5% ratio of KE-NPs	-	[71]
			Rat tail amputation model (5 cm length of the tail was cut using surgical scissors)						
			Tail amputation model Control <175 mg Cellulose <125 mg KE-NPs <125 mg KEC <75 mg						
Silk-based hemostatic hydrogels SF + TA	Coassembly (physical crosslinking)	Control 5.6 ± 0.2 min SF + TA <6 min (0.05) SF + TA <2 min (0.1) SF + TA 0.8 ± 0.3 min (0.15) SF + TA (0.3)	Liver injury in a rat model (made by an 18G needle) Heart injury in a rat (made by a 23G needle)	Control >400 mg SFT 35.2 ± 8.6 mg Commercially available sealant 170.5 ± 21.1 mg	Showed cytocompatibility toward HSF, although it showed inflammatory response after subcutaneous implantation in rats, the response was gradually diminished Displayed high efficiency in wound healing process with highest wound contraction (95%).	Exhibited efficient antibacterial effect against <i>S. aureus</i> and <i>E. coli</i>	Adhesive strength: SFT 86.1 ± 6.4 kPa in wet porcine skin within 1 min >125 kPa in blood for 20 min >75 → 125 kPa on diverse tissue surfaces Cyanocrylate <25 kPa in blood for 20 min Commercial thrombin fibrinogen-based glue <25 kPa in blood for 20 min	The adhesive gel was instantly formed upon mixing the SF and TA solutions	[82]

(Continued)

Table 2. Continued.

Polymeric system	Hydrogel preparative technique	Time to hemostasis (in vitro or in vivo)	In vivo model and wound type	Blood loss in treatment groups	Biocompatibility effect/wound healing	Antibacterial capability [%]	Adhesive strength/in vitro bursting pressure	Gelation time	Ref.
Chitosan-based hemostatic hydrogels									
Ch + nWH	Physical crosslinking induced by pH	In vitro blood clotting time [min] Whole blood 5.5 ± 1 2%Ch 3.5 ± 1.2 2%Ch- 4%nWH	Lethal liver injury model in rats (made by a 5 mm biopsy punch) Lethal femoral artery injury model in rats (a 24 gauge needle was used to puncture the artery)	Liver injury model Sham ctrl 2%Ch- 4%nWH Femoral artery injury model Sham ctrl 2%Ch- 4%nWH Sham ctrl 2%Ch- 4%nWH	Displayed good biocompatibility toward HUVEC	-	-	-	[92]
Ch + 5%nBG	Physical crosslinking induced by pH	Liver injury model Sham ctrl ≈150 s 2%Ch- ≈62 ± 3 s 4%nWH	Femoral artery injury model Sham ctrl ≈400 s 2%Ch- 229±9 s 4%nWH	Liver injury model Sham ctrl 2%Ch 2%Ch- 5%nBG	Sham ctrl 2%Ch- 4%nWH	-	-	-	[93]
CMC +PEG-BA	Schiff base reaction	In vivo hemostasis time [s] Control 311 ± 62 CMC/PEG-BA 120 ± 10 Sterile gauze 167 ± 21	An incision (length: 1 cm) was made by a scalpel in rabbit's liver	Control CMC/PEG-BA Sterile gauze	Nontoxic toward human primary dermal fibroblast cells with cell viability of 90.7 ± 6.8%	-	-	100 s at 25 °C Instantly gelled at 37 °C	[30]

(Continued)

Table 2. Continued.

Polymeric system	Hydrogel preparative technique	Time to hemostasis (in vitro or in vivo)	In vivo model and wound type	Blood loss in treatment groups	Biocompatibility effect/wound healing	Antibacterial capability [%]	Adhesive strength/in vitro bursting pressure	Gelation time	Ref.
QCSP + PEGS-FA	Schiff base reaction	–	Liver injury model in mouse (made by a 20 G needle)	Control QCSP3/PEGS-FA1.5 2025.9 ± 507.9 mg 214.7 ± 65.1 mg	Showed cytocompatibility toward L929 with cell viability of 95% resulted in higher wound contraction (≈100%, day 15) and granulation tissue thickness (> 750 μm) than those of QCSP3/PEGS-FA1.5 and commercial film dressing	killing ratio for <i>E. coli</i> and <i>S. aureus</i> QCSP3/PEGS-FA0.5 (24% and 91%) QCSP3/PEGS-FA1.0 (99% and 100%) QCSP3/PEGS-FA1.5 (99% and 100%) QCSP3/PEGS-FA2.0 (99% and 100%)	Adhesive strength: 1.5 kPa for QCSP3/PEGS-FA0.5 0.5 kPa for QCSP3/PEGS-FA2.0 about 5 kPa for commercial thrombin fibrinogen-based glue	374 ± 67 s for QCSP3/PEGS-FA0.5 86 ± 2 s for QCSP3/PEGS-FA2.0	[96]
QCSP + PF127-CHO	Schiff base reaction	–	Liver injury model in mouse (made by a 20 G needle)	Control QCSP/PF1.0 616.7 ± 157.0 mg 80.1 ± 7.13 mg	Showed cytocompatibility toward L929 QCSP/PF1.0 hydrogels led to better wound healing effect with ≈100% wound contraction	Displayed outstanding killing ratio of >90% for both <i>E. coli</i> and <i>S. aureus</i>	Adhesive strength: 4.4 ± 1.3 kPa for QCSP/PF 0.8 6.1 ± 1.2 kPa for QCSP/PF1.3 about 5 kPa for a commercial thrombin fibrinogen-based glue	≈90 s for QCSP/PF 0.8 <20 s for QCSP/PF1.3	[97]
HTCC + PDA	Schiff base reaction	–	Punctured liver in mice model (made by a needle)	Control 2.5 wt% HTCC-2.5 wt%PDA 168 mg 50 mg	Showed hemocompatibility toward human erythrocytes; showed no inflammation when was subcutaneously injected in mice Percentage of wound closure: Control 58 ± 7% 2.5 wt% HTCC-2.5 wt% PDA 78 ± 9%	Efficacy against higher bacterial concentration of 10 ⁹ CFU mL ⁻¹ : <i>E. coli</i> (88–94%) <i>S. aureus</i> (93–98%) MRSA (79%) VRE (75%) <i>K. pneumoniae</i> (78%)	Adhesive strength: 4.05–7.4 kPa	>60 s for HTCC-PDA (1 wt% HTCC) 10 s for HTCC-PDA (2.5 wt% HTCC)	[98]
hmCS + OD	Schiff base reaction and hydrophobic interaction	57 s hmCS/HWB 26 s 1.0 wt% 448 s hmCS/HWB 141 s 0.5 wt% 21 s CS/HWB 10 s 0.5 wt% CS/HWB/OD 0.5 wt% hmCS/HWB/OD 1.0 wt% hmCS/HWB/OD	Rat liver puncture model (a 16G needle was used to puncture liver)	0.5 wt% CS/OD 0.5 wt% hmCS/OD 1.0 wt% hmCS/OD 136 mg 53 mg 15 mg	No significant toxic effect toward NIH-3T3 fibroblast cells was displayed. Percentage of wound closure at day 15: 99.8%	Efficacy against bacterial concentration of 10 ⁸ CFU mL ⁻¹ <i>S. aureus</i> (95.0%) <i>P. aeruginosa</i> (96.4%)	Adhesive strength: 3.8 kPa for hmCS/OD (1 wt%) 8.9 kPa for hmCS/OD (4 wt%)	343 s for hmCS/OD (1 wt%) 90 s for hmCS/OD (4 wt%)	[101]

(Continued)

Table 2. Continued.

Polymeric system	Hydrogel preparative technique	Time to hemostasis (in vitro or in vivo)	In vivo model and wound type	Blood loss in treatment groups	Biocompatibility effect/wound healing	Antibacterial capability [%]	Adhesive strength/in vitro bursting pressure	Relation time	Ref.	
AHES + ACC	Schiff base reaction	In vivo hemostasis time [s] Control (medical gauze) AHES/ACC >≈150 1.8 ± 5.42	Liver injury in a rat model (made by scalpel (0.5 × 2 cm ²))	Control (medical gauze) AHES/ACC >500 mg <200 mg	Shown biocompatibility toward BMSCs	–	Adhesive strength: 42.73 ± 1.18 kPa for HES-4/ACC-3 <20 kPa for a commercial thrombin fibrinogen-based glue	The gelation times for the different formulations were shorter than 20 s.	[102]	
CSS + EPLM	Michael addition reaction	–	Liver injury in a rat model (made by an 18 G needle pricking)	After 3 min Control Pure CSS CSS/EPLM-6 106.7 mg <30 mg 28.3 mg	Nontoxic to fibroblast L929 cells	–	Adhesive strength: ≈87.5 kPa for CSS/EPLM-6 <30 kPa for a commercial thrombin fibrinogen-based glue	15–215 s	[109]	
CS + PEG + tyramine	Enzyme-mediated crosslinking using HRP and H ₂ O ₂	–	Mouse models of liver injury (made by a 20 G needle pricking)	After 3 min Control CPT 154 mg 59 mg	Superior wound healing effects in the rat's skin incision than those of commercial sealants, and suture	–	Adhesive strength: 17–97 kPa for CPT About 5 kPa for a commercial thrombin fibrinogen-based glue	About 5 s at highest concentration of HRP	[110]	
QCSCG + CNT0	Cation-π interaction, hydrophobic interaction, and chemical crosslinking	Mouse liver injury model Blank group Gelatin sponge QCSCG/CNT0 QCSCG/CNT2 QCSCG/CNT4 QCSCG/CNT6 Gauze group 190 s 73 s 83 s 82 s 78 s 101 s	Mouse liver injury model (pricking the liver using a 16 G needle) Mouse-tail amputation model (surgical scissors were used to cut the 50% of the tail)	Mouse liver injury model Blank group Gelatin sponge QCSCG/CNT0 QCSCG/CNT2 QCSCG/CNT4 QCSCG/CNT6 Gauze group > 180 mg Cryogels with 2 and 4 mg/mL CNT resulted in lower blood loss.	Shown biocompatibility toward L929 cells (>90% cell viability) 100% wound contraction was observed at 15th day in mice treated with QCSCG/CNT0, QCSCG/CNT4 and a commercial wound dressing	After only 1 min NIR irradiation, QCSCG/CNT4 showed 92%, 96%, and 95% killing ratios for <i>S. aureus</i> , <i>E. coli</i> , and <i>P. aeruginosa</i> , respectively. After only 1 min NIR irradiation, QCSCG/CNT4 groups showed 100% killing ratios for all the bacteria.	–	–	[118]	
		Mouse-tail amputation model QCSCG/CNT0 QCSCG/CNT2 QCSCG/CNT4 QCSCG/CNT6 117 s 107 s 91 s 60 s		Mouse-tail amputation model Blank group Gauze Gelatin sponge QCSCG/CNT0 QCSCG/CNT2 QCSCG/CNT4 QCSCG/CNT6 204 mg 28 mg 32 mg 20 mg 19 mg 23 mg 19 mg						

(Continued)

Table 2. Continued.

PolymERIC system	Hydrogel preparative technique	Time to hemostasis (in vitro or in vivo)	In vivo model and wound type	Blood loss in treatment groups	Biocompatibility effect/wound healing	Antibacterial capability [%]	Adhesive strength/in vitro bursting pressure	Gelation time	Ref.
		Rabbit liver defect hole	Rabbit liver volume defect model (biopsy needle and surgical scissors were used to make a columniform liver volume defect (diameter: 5 mm and height: 5 mm))	Rabbit liver volume defect model					
		Blank group Gelatin sponge D1 Gelatin sponge D2 QCSG/CNT0 QCSG/CNT4	Blank group Gelatin sponge D1 Gelatin sponge D2 QCSG/CNT0 QCSG/CNT4	>15 g 7.1 g 2.6 g 0.8 g 0.2 g					
CC + EPL	Radical polymerization	–	Rat liver injury model (pricking the liver using a 16 G needle)	Untreated CC CC-EPL CC-EPL-HG Gelatin foam Gauze	Showed biocompatibility toward HDF and hBMSC	Bacteria killing efficiency [%] MRSA	–	–	[119]
				>1 g >0.1 g ≈0.1 g ≈0.4 g >0.4 g >0.4 g			– 78.84 96.53 99.42 99.61		
				Control GC GC-EPL-1 GC-EPL-2 GC-EPL-4 <i>E. coli</i> Control GC GC-EPL-1 GC-EPL-2 GC-EPL-4			– 68.59 93.09 99.11 99.84		
Hyaluronic acid-based hemostatic hydrogels HA-ADH + PolyP-Irn	Schiff-base reaction	Within 3 min in all cases	A wide resection (5 mm) in mouse liver was made by a scalpel	HAX-PolyP Commercial thrombin-fibrinogen-based glue	HAXPolyP was found biocompatible toward RAW264.7, NIH3T3 and MeT-5A Suggested good biocompatibility in vivo mouse peritoneum without severe inflammation in surrounding tissues		–	Below 5 min	[123]
				<0.1 g <0.1 g					
				Blood loss after 2.5 min					(Continued)

Table 2. Continued.

Polymeric system	Hydrogel preparative technique	Time to hemostasis (in vitro or in vivo)	In vivo model and wound type	Blood loss in treatment groups	Biocompatibility effect/wound healing	Antibacterial capability [%]	Adhesive strength/in vitro bursting pressure	Gelation time	Ref.
HA + serotonin	Enzyme-mediated crosslinking using HRP and H ₂ O ₂	—	A mouse model of liver injury (made by an 18 G needle puncture) Liver injury in hemophilic mice (made by an 18 G needle)	Control HA-serotonin Commercial thrombin-fibrinogen-based glue Blood loss after 3 min Control HA-serotonin	HepG2 cells, HADSCs and HepG2 cells were highly viable when encapsulated in HA-serotonin Unusual immune response was not observed in the hydrogel-treated areas	—	—	Within 20–30 s	[127]
Alginate-based hemostatic hydrogels									
CMC + gelatin + OSA	Schiff base reaction and hydrogen bond crosslinking	In vivo hemostasis time [s] Control 349 CMC-GEL/OSA 62	A wound (length: 1 cm and depth: 2 mm) was made by a scalpel in rat's liver	Control CMC-GEL/OSA	Showed no cytotoxicity toward fibroblast L929 cells with >100% viability of the cells	levofloxacin loaded-CMC-GEL/OSA exhibited obvious inhibition zone against <i>E. coli</i> and <i>S. aureus</i>	Adhesive strength: 11 kPa for CMC-GEL/OSA	30 s	[137]
Carraageenan- κ CA + nSi	Physically crosslinking (Ionic interaction and hydrogel bond)	Control κ CA 1% κ CA/2% n Si	—	—	Showed cytocompatibility toward hMSCs 1% κ CA-2% n Si/VEGF resulted in virtually complete wound closure after 36 h than those of 1% κ CA (\approx <30) and 1% κ CA/2% n Si (\approx <30)	—	—	<2 min	[28]
PEG-based hemostatic hydrogels 4-arm-PEGNH ₂ + 4-arm-PEG-NHS + 4-arm-PEG-CHO	Schiff base reaction or amidation reaction	Gel 2 For both injuries (laceration models of rabbit liver and pigskin), no bleeding was observed after the gel was applied for 30 s	Laceration model of rabbit liver (an incision with length of 1 cm and depth of 0.5 cm in was made by a	—	3T3 mouse fibroblasts viability was over 80% and 90% when concentrations of hydrogels and loaded vancomycin in hydrogels were up to 10 mg mL ⁻¹ and 15 mg mL ⁻¹ , respectively	Gel 3 showed highest antibacterial effect against <i>S. aureus</i> . Gel 2 loaded with vancomycin exerted higher in vivo antimicrobial effect in rabbit skin infected with RN6390-GFP bacteria	Bursting pressure: Gel 1: 116.5 \pm 4.4 mmHg Gel 2: 164.7 \pm 21.9 mmHg Gel 3: 197.6 \pm 49.8 mmHg	20–25 s for solid content of 15 wt%	[146]

(Continued)

Table 2. Continued.

Polymeric system	Hydrogel preparative technique	Time to hemostasis (in vitro or in vivo)	In vivo model and wound type	Blood loss in treatment groups	Biocompatibility effect/wound healing	Antibacterial capability [%]	Adhesive strength/in vitro bursting pressure	Gelation time	Ref.
		Gauze Gel 2	on the wound sites. Not able to stop bleeding even after 5 min When hemostatic forceps were removed after 30 s, hemostasis was found to be completely achieved						
Tetra-PEG-NH ₂ + Tetra-PEG-SS (SS) and Tetra-PEG-NH ₂ + Tetra-PEG-SS (SG)	Chemically crosslinked via amide bonds	Rabbit liver injury model	surgical scalpel) Laceration model of pigskin (a cylinder wound with diameter of 3 cm and depth of 1 cm) was made by a surgical scalpel Rabbit model of femoral artery injury (the arteries were clipped by surgical scissors)						
		SS SG Gauze	<30 s <30 s >5 min	Three incisions (length: 30 mm and depth: 5 mm) were made by a scalpel in rabbits' liver An incision (length: 20 mm and depth: 5 mm) was made by a scalpel in rabbit liver treated by heparin Spleen injury (diameter: 25 mm and depth: 10 mm) in pig model treated with and without heparin			SS hydrogel displayed good biocompatibility without inducing inflammatory response as shown by subcutaneous and muscle implantation experiments in rats SS found to have potential to stimulate the wound healing process without any observable side effects	Adhesive strength: ≈20 kPa for SS and SG ≈17 kPa for a Commercial thrombin and fibrinogen-based glue Bursting pressure: ≈300 mmHg for SS ≈<200 mmHg for SG ≈<120 mmHg for a commercial thrombin and fibrinogen-based glue	Around 6 s [149]
		Heparin treated rabbit model SS Gauze	<5 min After 30 min, bleeding could not be stopped. After 20 min, bleeding could not be stopped by commercial glue.						

(Continued)

Table 2. Continued.

Polymeric system	Hydrogel preparative technique	Time to hemostasis (in vitro or in vivo)	In vivo model and wound type	Blood loss in treatment groups	Biocompatibility effect/wound healing	Antibacterial capability [%]	Adhesive strength/in vitro bursting pressure	Gelation time	Ref.
		Pig Spleen injury model							
		SS							
		Heparin treated pig model							
		SS							
		15 min							
Catechol-containing hydrogels									
DOPA + gelatin + FeCl ₃	Enzyme-mediated and Fe ³⁺ ions crosslinking	–	Liver injury in rat models by needle (18 G) pricking	After 1 min Control Gelatin DOPA-gelatin DOPA-Fe ³⁺ Gelatin	Shown cytocompatibility in vitro toward HASCs with absorption value comparable to control gelatin (0.95 ± 0.02 vs 1.01 ± 0.06) and in vivo with no obvious inflammation or fibrosis	–	–	Within seconds at 37 °C	[57]
Gel-SH/GelMA/PD-LAP	Photocrosslinking, Michael reaction and physical interaction	In vitro clotting time [min] Control 5.5 ± 0.5 Gel-0%PD-LAP 3.5 ± 0.5 Gel-2%PD-LAP 1.5 ± 0.5	–	–	Shown cytocompatibility in vitro toward L929 cells (cell viability: 105.7 ± 7.5 (%control) for Gel-2%PD-LAP vs 82.3 ± 3.6 (%control) for Gel-0%PD-LAP)	–	Adhesive strength: 68.7 ± 1 kPa for Gel-0%PD-LAP 116.1 ± 34 kPa for Gel-2 wt% PD-LAP	55 ± 5 s for Gel-0%PD-LAP 42 ± 5 s for Gel-2 wt% PD-LAP	[59]
CMCS + TA + BDBA	Physical crosslinking and covalent binding	–	Mouse liver puncture model (made by 23 G Needle)	Untreated Gauze Hydrogel	Shown biocompatibility toward MCF-7 human breast cancer cells	–	–	–	[94]
Plu-SH+CHIC	Michael addition reaction	–	Liver injury in a rat model (made an 18 G needle)	After 3 min Control CHI-C CHI-C/Plu-SH Plu-SH hydrogels	No obvious inflammation or massive fibrosis was observed around the injection site	–	Detachment stress 15.0 ± 3.5 kPa for CHI-C/Plu-SH (12 wt%)	Instantly gelled at a 37 °C	[104]

(Continued)

Table 2. Continued.

Polymeric system	Hydrogel preparative technique	Time to hemostasis (in vitro or in vivo)	In vivo model and wound type	Blood loss in treatment groups	Biocompatibility effect/wound healing	Antibacterial capability [%]	Adhesive strength/in vitro bursting pressure	Gelation time	Ref.
HBC + CS + dopamine	Michael addition reaction	Control HCS HCS-DOPA-0.5 HCS-DOPA-1 HCS-DOPA-2	–	–	The extract solutions of HCS-DOPA hydrogels showed no cytotoxicity toward fibroblast L929 cells	Inhibition zone diameter against <i>E. coli</i> and <i>S. aureus</i> : HCS (1.67 mm and 0.81 mm) PD (1.52 and 9.99 mm) HCS-DOPA-0.5 (1.69 mm and 6.49 mm) HCS-DOPA-1 (2.38 mm and 6.82 mm) HCS-DOPA-2 (3.77 mm and 13.52 mm)	Adhesive strength: <1020 ± 24 Pa for HCS <3117 ± 25 Pa for HCS-DOPA-2	82.67 s for HCS 19.67 s for HCS-DOPA-2	[108]
CS-HA + hmCS lactate	Michael addition, Schiff base reaction, coupling reaction and hydrophobic interactions	In vivo hemostasis time [s] Control 117 hmCS 56 lactate 73 Gel 1 45 Gel 2 32 Gel 3	An incision was made (length: 1 cm and depth: 0.5 cm) in rats' liver	Control hmCS lactate Gel 1 Gel 2 Gel 3	Shown cytocompatibility toward 3T3 fibroblast; showed hemocompatibility Promoted wound healing	Killing efficiency against: <i>S. aureus</i> Gel 1 (57%) Gel 2 (98%) Gel 3 (99.9%) <i>P. aeruginosa</i> Gel 2 (99.1%) Gel 3 (99.9%)	Adhesive strength: 3.8 kPa for 1 wt%hmCS 8.2 kPa for CS-HA/1 wt%hmCS lactate (Gel 3) Bursting pressure: 4 mmHg for 1 wt%hmCS 71 mmHg for CS-HA/1 wt%hmCS lactate (Gel 3)	<20 s at higher concentration of sodium periodate	[110]
HA-DA + rGO@PDA	Enzyme-mediated crosslinking using HRP and H ₂ O ₂	–	A mouse model of liver injury (made by a 20 G needle)	Control HA-DA/rGO3 74.2 ± 36.2 mg	Nontoxic to fibroblast L929 cells. HA-DA/rGO3 hydrogel showed highest cell proliferation Wound healing ratio: HA-DA/rGO3 (95.5%) HA-DA/rGO3/Doxy (98.0%) Commercial film dressing (90.2%) HA-DA/rGO3 group (92.8%)	In vitro and in vivo Bacteria survival ratios for <i>E. coli</i> and <i>S. aureus</i> after 10 min of NIR irradiation: HA-DA/rGO3 In vitro: almost completely killed both bacteria In vivo: (3.1%) for both bacteria HA-DA/rGO3 74.1% for <i>E. coli</i> 62.9% for <i>S. aureus</i> Inhibition zone diameter for HA-DA/rGO3/Doxy on day 1: 3.2 cm for <i>E. coli</i> 3.9 cm for <i>S. aureus</i>	Adhesive strength: Between 5.0 ± 0.5 and 6.3 ± 1.2 kPa 557.4 ± 51.2 s for HA-DA/rGO with 0 wt% rGO@PDA 157.7 ± 33.8 s for HA-DA/rGO with 5 wt% rGO@PDA	[125]	

(Continued)

Table 2. Continued.

Polymeric system	Hydrogel preparative technique	Time to hemostasis (in vitro or in vivo)	In vivo model and wound type	Blood loss in treatment groups	Biocompatibility effect/wound healing	Antibacterial capability [%]	Adhesive strength/in vitro bursting pressure	Relation time	Ref.
Dopa-OA + PAA	Schiff base reaction	–	Liver injury in mouse model of hepatic (made by a 21 G needle puncture)	Control Dopa-OA/PAA OA glue	–	–	655.1±34.4 gf mm ⁻² for OA-30 761.4±52.2 gf mm ⁻² for OA-90	4.1 s for OA-30 Instantly gelled after mixing Dopa-OA and PAA	[135]
Dopamine + AP (DCP)	Chemically crosslinked via amide bonds	–	Rat liver puncture model (an 18G needle was utilized to prick liver)	Control DCP	Shown low cytotoxicity (less than 20%) toward NIH3T3	–	–	–	[157]
γ-PGA + dopamine	Enzyme-mediated crosslinking using HRP and H ₂ O ₂	–	Rat liver injury model (an 18G needle was used to prick liver)	Blood loss at 120 s after surgery Control γ-PGA-DA Commercial thrombin-fibrinogen-based glue	Shown biocompatibility toward L929 mouse epidermal cells with cell viability above 80%	–	Adhesive strength 58.2 kPa for highest degrees of catechol substitution	660 s for γ-PGA-DA (2.0 wt%) 25 s γ-PGA-DA (8.0 wt%)	[159]
PAAm + TA + KA	Physical and chemical interactions	In vivo hemostasis time [s]	Femoral artery laceration model in rat (a surgical scissor was used to cut off femoral artery)	–	Shown cytocompatibility toward L929 fibroblasts	–	Adhesive strength ≈0.48 MPa for PAAm-TA-KA ≈0.025 MPa for PAAm-TA Bursting pressure 0.04–0.09 MPa for PAAm-TA-KA 0.02 MPa for PAAm-TA	–	[164]
Other hemostatic hydrogels									
AG-NH ₂ + DF-PEG (AD)	Schiff-base reaction	In vivo hemostasis time [s] Control 175 ± 22 AD hydrogel <10 gauze 72 ± 11	An incision (length: 1cm) was made by a surgical scalpel in rabbit's liver	Control AD hydrogel gauze	Shown cytocompatibility with HUVEC, with cell viability of >80%	–	Bursting pressure ≈>120 mmHg for AD hydrogel <30 mmHg for AG-PEG	10–15 s	[151]
PNC-PEG-TA conjugate + ε-polylysine (PPT)	Enzyme-mediated crosslinking using HRP and H ₂ O ₂	–	Penetrating injury was made by an 18 G needle in liver rat model of hepatic	Control PPT	Shown biocompatibility toward fibroblast L929 with cell viability of over 100% Exhibited superior wound healing ratio that those of other commercial products and suture	–	≈20–≈>120 kPa for PPT 6 kPa for a Commercial thrombin and fibrinogen-based glue	2 s at 0.12 mg mL of HRP	[154]

the adhesive hydrogel and the tissue surface) under wet environments and high fluid pressures.^[31] Strong adhesion is one of the key factors for an ideal hemostatic hydrogel that allows them to rapidly adhere to the tissues to stanch bleeding under high blood pressure even under wet and dynamic conditions, preventing the hydrogels from getting washed away from the bleeding point. While some studies have emerged demonstrating the adhesiveness of the resulting hydrogels, only few of them have tapped into the exciting properties of hydrogel adhesives and sealants to stanch bleeding in wet and mobile tissues and therefore more research effort is needed to design an efficient injectable hydrogel that is able to cease bleeding from wet, slippery, and dynamic internal tissues and organs. Furthermore, although hemostatic hydrogels prepared from mussel-inspired chemistry showed good adhesive properties, employing costly dopamine and DOPA to prepare these hydrogels as well as possible neurological effects of dopamine can limit their large-scale production and commercialization. To tackle the aforementioned challenges, plant-derived polyphenol compounds including TA possessing catechol/pyrogallol groups can be utilized as a low-cost and safe alternative for dopamine to impart adhesion properties to hydrogels that are promptly scalable. However, it should be noted that to drive polymer-TA hydrogel formation, external stimuli or additives are required since TA's multiple noncovalent interactions can lead to coacervation.

- Bacterial infections at the wound site are a common problem that can impair wound healing. Development of hemostatic hydrogels with efficient antibacterial properties is therefore urgently needed. However, most engineered hydrogels reported in literature, lack antibacterial effect. One promising strategy to endow hemostatic hydrogels with antibacterial effect can be embedding antibacterial drugs or metallic nanoparticles into hydrogel networks. Incorporating materials with the ability to deliver antibacterial elements (e.g., copper, zinc, etc.) into hydrogels which also have acceleratory effect on wound healing as well as growth factors, is an interesting approach to impart efficient wound healing effect to hydrogels.
- Prior to initiating animal studies, the performance of hemostatic hydrogels in vitro needs to be comprehensively evaluated. The most relevant tests that need to be performed on hydrogels to evaluate their hemostatic capabilities include clotting time assay, thrombus formation, and platelet adhesion tests. Moreover, polymeric hydrogels used for hemostatic applications are required to withstand the pressure of the bleeding while adhering to the tissues to seal the injured site. Thus, bursting pressure tests are required to be carried out to assess the capacity of hydrogels to seal the wounds when exposed to substantial pressures from biological fluids (blood). In addition to biocompatibility tests, the hemolytic properties of the hydrogels that show potential to rupture RBCs need to be evaluated. Biodegradability is one of the important characteristics of an ideal hemostatic hydrogel. However, some of the studies described here did not assess the degradation profile of the hydrogels and it is not clear how the materials would be cleared from the injection site. In this context, in vitro and in vivo studies are extremely necessary to evaluate the hydrogel biodegradability.
- It is noticeable that preclinical animal studies are critical and should be conducted to ascertain the effectiveness and safety of hemostatic materials proposed for stanching bleeding injuries during surgery and in civilian and battlefield settings. Nevertheless, the hemostatic functions of some of the polymeric hydrogel systems discussed in this review paper have been only evaluated in vitro, and their hemostatic capability in vivo therefore remains an open question. Hence, more dedicated research is required to validate the findings in vivo using suitable animal models.
- As highlighted in this article, rats and rabbits are commonly used animal models to study the in vivo hemostatic efficacies of the investigated hydrogels. However, larger animals such as the pig can be more promising models to assess the hemostatic effects of polymeric hydrogel systems owing to their physiological and anatomical similarities to humans, thereby more precisely reflecting the hemostatic effectiveness in more realistic situations.^[165]
- It is also important to point out that it has become challenging to compare the various technologies and materials developed by different groups given the large heterogeneity in the animal models used, including type of species, type of injury, measurement of hemostatic criteria, etc. Standardized animal models and measurement criteria need to be established.
- Current approved hemostats were not compared in many of these studies. Future studies are needed to focus on direct comparison of the newly developed hydrogel platforms with currently approved products to establish the possible superiority of their performance in vivo.
- Another significant challenge that needs to be highlighted is related to the occurrence of diffuse hemorrhage (external and internal) from polytrauma (following, for example, a car crash, a blast injury, etc.) where there is no specific accessible site to impart bleeding control. Since all hydrogel systems, including injectable and shear thinning ones, require a specific location access to be deployed in the body, these may not be sufficient for diffuse polytrauma and noncompressible hemorrhage scenarios.

Ultimately, polymeric hydrogel systems with multiple functionalities are swiftly emerging as a versatile technology platform for hemostatic application. Proving the potential of these life-saving technologies through a significant number of preclinical studies is expected to revolutionize bleeding control options in emergency, surgical practice, civilian, and military settings worldwide and would improve the quality of treatment for patients suffering from uncontrolled bleeding and impaired wound healing.

Acknowledgements

This work was supported by University of Malaya through grant no. GPF030A-2018 and Ministry of Higher Education of Malaysia, FRGS grant no. FP076-2018A. N.M. acknowledges financial support from FunGlass project (Alexander Dubcek University of Trencin, Slovakia).

Conflict of Interest

The authors declare no conflict of interest.

Keywords

adhesives, hemostasis, hemostats, injectable hydrogels, wound healing

Received: May 28, 2020

Revised: August 9, 2020

Published online:

- [1] D. R. Spahn, B. Bouillon, V. Cerny, J. Duranteau, D. Filipescu, B. J. Hunt, R. Komadina, M. Maegele, G. Nardi, L. Riddez, C.-M. Samama, J.-L. Vincent, R. Rossaint, *Crit. Care* **2019**, 23, 98.
- [2] N. Curry, S. Hopewell, C. Dorée, C. Hyde, K. Brohi, S. Stanworth, *Crit. Care* **2011**, 15, R92.
- [3] A. M. Behrens, M. J. Sikorski, P. Kofinas, *J. Biomed. Mater. Res., Part A* **2014**, 102, 4182.
- [4] C. Gajjar, M. McCord, M. King, *Biotextiles as Medical Implants: 19. Hemostatic Wound Dressings*, Elsevier Inc., New York **2013**.
- [5] P. M. Mannucci, M. Levi, *N. Engl. J. Med.* **2007**, 356, 2301.
- [6] a) M. A. Schreiber, D. J. Neveleff, *AORN J.* **2011**, 94, S1; b) J. McCarthy, in *Assisting in Surgery: Patient-Centered Care*, (Eds: J. C. Rothrock, P. C. Seifert, CCI, Denver, CO **2009**.
- [7] M. Marietta, L. Facchini, P. Pedrazzi, S. Busani, G. Torelli, *Transplant. Proc.* **2006**, 38, 812.
- [8] a) H. Clark, *The History of Hemostasis*, Paul B. Hoeber, New York **1929**; b) D. M. Harmening, *Clinical Hematology and Fundamentals of Hemostasis*, FA Davis Company, Philadelphia, PA, USA **2009**.
- [9] D. A. Hickman, C. L. Pawlowski, U. D. Sekhon, J. Marks, A. S. Gupta, *Adv. Mater.* **2018**, 30, 1700859.
- [10] S. Pourshahrestani, E. Zeimaran, I. Djordjevic, N. A. Kadri, M. R. Towler, *Mater. Sci. Eng., C* **2016**, 58, 1255.
- [11] a) C. Schuhmacher, J. Pratschke, S. Weiss, S. Schneeberger, A. L. Mihaljevic, R. Schirren, M. Winkler, N. Emmanouilidis, *Med. Devices* **2015**, 8, 167; b) L. S. Nissen, J. Hunter, H. D. Schröder, K. Rütz, P. Bollen, *J. Surg. Surgical Res.* **2017**, 3, 038; c) K. M. Lewis, C. E. Kuntze, H. Gulle, *Med. Devices* **2016**, 9, 1.
- [12] G. R. Mueller, T. J. Pineda, H. X. Xie, J. S. Teach, A. D. Barofsky, J. R. Schmid, K. W. Gregory, *J. Trauma Acute Care Surg.* **2012**, 73, S134.
- [13] a) M. K. Klein, N. D. Tshilis, T. A. Pritts, M. R. Kibbe, *J. Surg. Res.* **2020**, 248, 182; b) M. Duggan, A. Rago, U. Sharma, G. Zugates, J. Freyman, R. Busold, J. Caulkins, Q. Pham, Y. Chang, A. Mejjaddam, *J. Trauma Acute Care Surg.* **2013**, 74, 1462; c) M. P. Peev, A. Rago, J. O. Hwabejire, M. J. Duggan, J. Beagle, J. Marini, G. Zugates, R. Busold, T. Freyman, G. S. Velmahos, *J. Trauma Acute Care Surg.* **2014**, 76, 619; d) A. P. Rago, A. Larentzakis, J. Marini, A. Picard, M. J. Duggan, R. Busold, M. Helmick, G. Zugates, J. Beagle, U. Sharma, *J. Trauma Acute Care Surg.* **2015**, 78, 324.
- [14] a) W. D. Spotnitz, *Am Surg.* **2012**, 78, 1305; b) W. D. Spotnitz, *Int. Scholarly Res. Not.* **2014**, 2014.
- [15] M. A. Traver, D. G. Assimos, *Rev. Urol.* **2006**, 8, 104.
- [16] W. D. Spotnitz, S. Burks, *Clin. Appl. Thromb./Hemostasis* **2010**, 16, 497.
- [17] H. Seyednejad, M. Imani, T. Jamieson, A. Seifalian, *Br. J. Surg.* **2008**, 95, 1197.
- [18] a) R. Watrowski, C. Jaeger, J. Forster, *In Vivo* **2017**, 31, 251; b) H. E. Achneck, B. Sileshi, R. M. Jamiolkowski, D. M. Albala, M. L. Shapiro, J. H. Lawson, *Ann. Surg.* **2010**, 251, 217.
- [19] O. Chiara, S. Cimbanassi, G. Bellanova, M. Chiarugi, A. Mingoli, G. Olivero, S. Ribaldi, G. Tugnoli, S. Basilicò, F. J. B. s. Bindi, *BMC Surg.* **2018**, 18, 68.
- [20] a) W. D. Spotnitz, S. Burks, *Transfusion* **2008**, 48, 1502; b) M. Mishra, *Concise Encyclopedia of Biomedical Polymers and Polymeric Biomaterials*, CRC Press, Boca Raton, FL **2017**.
- [21] a) D. G. Cerdá, A. M. Ballester, A. Aliena-Valero, A. Carabén-Redaño, J. M. Lloris, *Surg. Today* **2015**, 45, 939; b) S. C. Woodward, J. B. Herrmann, J. L. Cameron, G. Brandes, E. J. Pulaski, F. Leonard, *Ann. Surg.* **1965**, 162, 113; c) E. Cho, J. S. Lee, K. Webb, *Acta Biomater.* **2012**, 8, 2223.
- [22] Y. Li, T. Xu, Z. Tu, W. Dai, Y. Xue, C. Tang, W. Gao, C. Mao, B. Lei, C. Lin, *Theranostics* **2020**, 10, 4929.
- [23] Q. V. Nguyen, J. H. Park, D. S. Lee, *Eur. Polym. J.* **2015**, 72, 602.
- [24] M. Liu, X. Zeng, C. Ma, H. Yi, Z. Ali, X. Mou, S. Li, Y. Deng, N. He, *Bone Res.* **2017**, 5, 1.
- [25] a) S. Van Vlierberghe, P. Dubruel, E. Schacht, *Biomacromolecules* **2011**, 12, 1387; b) E. M. Ahmed, *J. Adv. Res.* **2015**, 6, 105; c) Y. Li, J. Rodrigues, H. Tomas, *Chem. Soc. Rev.* **2012**, 41, 2193; d) E. Caló, V. V. Khutoryanskiy, *Eur. Polym. J.* **2015**, 65, 252; e) M. Guvendiren, H. D. Lu, J. A. Burdick, *Soft Matter* **2012**, 8, 260.
- [26] a) L. Yu, J. Ding, *Chem. Soc. Rev.* **2008**, 37, 1473; b) J. H. Lee, *Biomater. Res.* **2018**, 22, 27.
- [27] M. Patenaude, N. M. Smeets, T. Hoare, *Macromol. Rapid Commun.* **2014**, 35, 598.
- [28] G. Lokhande, J. K. Carrow, T. Thakur, J. R. Xavier, M. Parani, K. J. Bayless, A. K. Gaharwar, *Acta Biomater.* **2018**, 70, 35.
- [29] a) J. Li, A. Celiz, J. Yang, Q. Yang, I. Wamala, W. Whyte, B. Seo, N. Vasilyev, J. Vlassak, Z. Suo, *Science* **2017**, 357, 378; b) C. Ghobril, M. Grinstaff, *Chem. Soc. Rev.* **2015**, 44, 1820; c) N. Annabi, K. Yue, A. Tamayol, A. Khademhosseini, *Eur. J. Pharm. Biopharm.* **2015**, 95, 27; d) A. Duarte, J. Coelho, J. Bordado, M. Cidade, M. Gil, *Prog. Polym. Sci.* **2012**, 37, 1031.
- [30] W. Huang, Y. Wang, Y. Chen, Y. Zhao, Q. Zhang, X. Zheng, L. Chen, L. Zhang, *Adv. Healthcare Mater.* **2016**, 5, 2813.
- [31] W. Zhu, Y. J. Chuah, D.-A. Wang, *Acta Biomater.* **2018**, 74, 1.
- [32] a) N. Artzi, T. Shazly, C. Crespo, A. B. Ramos, H. K. Chenault, E. R. Edelman, *Macromol. Biosci.* **2009**, 9, 754; b) Y. Lee, H. J. Chung, S. Yeo, C.-H. Ahn, H. Lee, P. B. Messersmith, T. G. Park, *Soft Matter* **2010**, 6, 977; c) V. Krishnados, A. Melillo, B. Kanjilal, T. Hannah, E. Ellis, A. Kapetanakis, J. Hazelton, J. San Roman, A. Masoumi, J. Leijten, *ACS Appl. Mater. Interfaces* **2019**, 11, 38373.
- [33] a) Y. Tu, N. Chen, C. Li, H. Liu, R. Zhu, S. Chen, Q. Xiao, S. Ramakrishna, L. He, *Acta Biomater.* **2019**, 90, 1; b) A. Sivashanmugam, R. A. Kumar, M. V. Priya, S. V. Nair, R. Jayakumar, *Eur. Polym. J.* **2015**, 72, 543; c) W. Hu, Z. Wang, Y. Xiao, S. Zhang, J. Wang, *Biomater. Sci.* **2019**, 7, 843.
- [34] B. P. Nuytens, T. Thijs, H. Deckmyn, K. Broos, *Thromb. Res.* **2011**, 127, S26.
- [35] a) K. Broos, H. B. Feys, S. F. De Meyer, K. Vanhoorelbeke, H. Deckmyn, *Blood Rev.* **2011**, 25, 155; b) J. F. Fullard, *Curr. Pharm. Des.* **2004**, 10, 1567.
- [36] a) L. W. Chan, X. Wang, H. Wei, L. D. Pozzo, N. J. White, S. H. Pun, *Sci. Transl. Med.* **2015**, 7, 277ra29; b) I. N. Chernysh, C. Nagaswami, P. K. Purohit, J. W. Weisel, *Sci. Rep.* **2012**, 2, 879.
- [37] M. Hoffman, D. M. Monroe III, *Thromb. Haemost.* **2001**, 85, 958.
- [38] M. Hoffman, *J. Thromb. Thrombolysis* **2003**, 16, 17.
- [39] a) I. George Broughton, J. E. Janis, C. E. Attinger, *Plast. Reconstr. Surg.* **2006**, 117, 12S; b) S. Das, A. B. Baker, *Front. Bioeng. Biotechnol.* **2016**, 4, 82.
- [40] A. C. d. O. Gonzalez, T. F. Costa, Z. d. A. Andrade, A. R. A. P. Medrado, *An. Bras. Dermatol.* **2016**, 91, 614.
- [41] H. L. Orsted, D. Keast, L. Forest-Lalande, M. F. Megie, *Wound Care Can.* **2011**, 9, 4.
- [42] J. S. Boateng, K. H. Matthews, H. N. Stevens, G. M. Eccleston, *J. Pharm. Sci.* **2008**, 97, 2892.
- [43] J. L. Monaco, W. T. Lawrence, *Clin. Plast. Surg.* **2003**, 30, 1.
- [44] a) M. C. Echave, L. S. Burgo, J. L. Pedraz, G. Orive, *Curr. Pharm. Des.* **2017**, 23, 3567; b) S. Afewerki, A. Sheikhi, S. Kannan, S. Ahdian, A. Khademhosseini, *Bioeng. Transl. Med.* **2019**, 4, 96; c) S. Kuttappan, D. Mathew, M. B. Nair, *Int. J. Biol. Macromol.* **2016**, 93, 1390; d) B.

- J. Klotz, D. Gawlitza, A. J. Rosenberg, J. Malda, F. P. Melchels, *Trends Biotechnol.* **2016**, *34*, 394; e) S. S. Silva, J. F. Mano, R. L. Reis, *Crit. Rev. Biotechnol.* **2010**, *30*, 200; f) S. Huang, X. Fu, *J. Controlled Release* **2010**, *142*, 149.
- [45] a) F. di Lena, *J. Mater. Chem. B* **2014**, *2*, 3567; b) J. T. Correll, E. Wise, *Proc. Soc. Exp. Biol. Med.* **1945**, *58*, 233; c) Y. Tomizawa, *Artif. Organs* **2005**, *8*, 137.
- [46] a) C. S. Kitchens, B. A. Konkle, C. M. Kessler, *Consultative Hemostasis and Thrombosis: Expert Consult-Online and Print*, Elsevier Health Sciences, Philadelphia, PA **2013**; b) A. Roger, S. L. Bachman, A. A. Wheeler, K. N. Bartow, J. S. Scott, *Surg. Annu.* **2007**, *142*, S39.
- [47] a) M. Mohiti-Asli, E. Lobo, *Wound Healing Biomaterials*, Elsevier, Amsterdam **2016**; b) Q. Xing, K. Yates, C. Vogt, Z. Qian, M. C. Frost, F. J. S. r. Zhao, *Sci. Rep.* **2015**, *4*, 4706.
- [48] a) S. E. Baker, A. M. Sawvel, N. Zheng, G. D. Stucky, *Chem. Mater.* **2007**, *19*, 4390; b) A. K. Gaharwar, S. M. Mihaila, A. Swami, A. Patel, S. Sant, R. L. Reis, A. P. Marques, M. E. Gomes, A. Khademhosseini, *Adv. Mater.* **2013**, *25*, 3329.
- [49] a) B. Ruzicka, E. Zaccarelli, *Soft Matter* **2011**, *7*, 1268; b) N. Bitinis, M. Hernández, R. Verdejo, J. M. Kenny, M. Lopez-Manchado, *Adv. Mater.* **2011**, *23*, 5229; c) R. Waters, S. Pacelli, R. Maloney, I. Medhi, R. P. Ahmed, A. Paul, *Nanoscale* **2016**, *8*, 7371; d) D. Chimene, D. L. Alge, A. K. Gaharwar, *Adv. Mater.* **2015**, *27*, 7261; e) M. Parani, G. Lokhande, A. Singh, A. K. Gaharwar, *ACS Appl. Mater. Interfaces* **2016**, *8*, 10049; f) A. K. Gaharwar, V. Kishore, C. Rivera, W. Bullock, C. J. Wu, O. Akkus, G. Schmidt, *Macromol. Biosci.* **2012**, *12*, 779; g) S. Afewerki, L. S. Magalhães, A. D. Silva, T. D. Stocco, E. C. Silva Filho, F. R. Marciano, A. O. Lobo, *Adv. Healthcare Mater.* **2019**, 1900158.
- [50] D. W. Thompson, J. T. Butterworth, *J. Colloid Interface Sci.* **1992**, *151*, 236.
- [51] A. K. Gaharwar, R. K. Avery, A. Assmann, A. Paul, G. H. McKinley, A. Khademhosseini, B. D. Olsen, *ACS Nano* **2014**, *8*, 9833.
- [52] A. Zaupa, A. T. Neffe, B. F. Pierce, U. Nöchel, A. Lendlein, *Biomacromolecules* **2011**, *12*, 75.
- [53] A. M. Smith, J. A. Callow, *Biological Adhesives*, Springer, Berlin, Germany **2006**.
- [54] M. Rahimnejad, W. Zhong, *RSC Adv.* **2017**, *7*, 47380.
- [55] D. S. Hwang, H. Zeng, Q. Lu, J. Israelachvili, J. H. Waite, *Soft Matter* **2012**, *8*, 5640.
- [56] a) W.-Y. Quan, Z. Hu, H.-Z. Liu, Q.-Q. Ouyang, D.-Y. Zhang, S.-D. Li, P.-W. Li, Z.-M. Yang, *Molecules* **2019**, *24*, 2586; b) S. K. Madhurakkat Perikamana, J. Lee, Y. B. Lee, Y. M. Shin, E. J. Lee, A. G. Mikos, H. Shin, *Biomacromolecules* **2015**, *16*, 2541; c) H. Lee, N. F. Scherer, P. B. Messersmith, *Proc. Natl. Acad. Sci. USA* **2006**, *103*, 12999.
- [57] Y. C. Choi, J. S. Choi, Y. J. Jung, Y. W. Cho, *J. Mater. Chem. B* **2014**, *2*, 201.
- [58] a) A. Eckly, B. Hechler, M. Freund, M. Zerr, J. P. Cazenave, F. Lanza, P. Mangin, C. Gachet, *J. Thromb. Haemost.* **2011**, *9*, 779; b) T. Saldeen, D. Li, J. L. Mehta, *J. Am. Coll. Cardiol.* **1999**, *34*, 1208; c) E. Scarcello, D. Lison, *J. Funct. Biomater.* **2020**, *11*, 2.
- [59] N. Rajabi, M. Kharaziha, R. Emadi, A. Zarrabi, H. Mokhtari, S. Salehi, *J. Colloid Interface Sci.* **2020**, *564*, 155.
- [60] A. Assmann, A. Vegh, M. Ghasemi-Rad, S. Bagherifard, G. Cheng, E. S. Sani, G. U. Ruiz-Esparza, I. Noshadi, A. D. Lassaletta, S. Gangadharan, *Biomaterials* **2017**, *140*, 115.
- [61] Y. Hong, F. Zhou, Y. Hua, X. Zhang, C. Ni, D. Pan, Y. Zhang, D. Jiang, L. Yang, Q. Lin, *Nat. Commun.* **2019**, *10*, 1.
- [62] a) J. K. Blusztajn, *Science* **1998**, *281*, 794; b) B. Yue, E. Pattison, W. L. Roberts, A. L. Rockwood, O. Danne, C. Lueders, M. Möckel, *Clin. Chem.* **2008**, *54*, 590.
- [63] J.-W. Luo, C. Liu, J.-H. Wu, L.-X. Lin, H.-M. Fan, D.-H. Zhao, Y.-Q. Zhuang, Y.-L. Sun, *Mater. Sci. Eng., C* **2019**, *98*, 628.
- [64] a) M. Park, B.-S. Kim, H. K. Shin, S.-J. Park, H.-Y. Kim, *Mater. Sci. Eng., C* **2013**, *33*, 5051; b) S. Kokot, *Encyclopedia of Materials: Science and Technology*, Elsevier, Oxford **2001**.
- [65] a) G. Thakur, F. C. Rodrigues, K. Singh, *Cutting-Edge Enabling Technologies for Regenerative Medicine*, Springer, Singapore **2018**; b) A. Shavandi, T. H. Silva, A. A. Bekhit, A. E.-D. A. Bekhit, *Biomater. Sci.* **2017**, *5*, 1699.
- [66] a) J. McLellan, S. G. Thornhill, S. Shelton, M. Kumar, *Keratin as a Protein Biopolymer*, Springer International Publishing, Cham **2019**; b) S. Xu, L. Sang, Y. Zhang, X. Wang, X. Li, *Mater. Sci. Eng., C* **2013**, *33*, 648; c) C. J. Kowalczewski, S. Tombyln, D. C. Wasnick, M. R. Hughes, M. D. Ellenburg, M. F. Callahan, T. L. Smith, M. E. Van Dyke, L. R. Burnett, J. M. Saul, *Biomaterials* **2014**, *35*, 3220; d) S. A. Shah, M. Sohail, M. U. Minhas, S. Khan, M. de Matas, V. Sikstone, Z. Hussain, M. Abbasi, M. Kousar, *Int. J. Biol. Macromol.* **2019**, *139*, 975.
- [67] a) M. B. Rahmany, R. R. Hantgan, M. Van Dyke, *Biomaterials* **2013**, *34*, 2492; b) D. Wang, W. Li, Y. Wang, H. Yin, Y. Ding, J. Ji, B. Wang, S. Hao, *Colloids Surf. B* **2019**, *182*, 110367.
- [68] T. Aboushwareb, D. Eberli, C. Ward, C. Broda, J. Holcomb, A. Atala, M. Van Dyke, *J. Biomed. Mater. Res. B* **2009**, *90*, 45.
- [69] W. Li, F. Gao, J. Kan, J. Deng, B. Wang, S. Hao, *Colloids Surf. B* **2019**, *175*, 436.
- [70] S. Dhall, J. P. Silva, Y. Liu, M. Hrynyk, M. Garcia, A. Chan, J. Lyubovitsky, R. J. Neufeld, M. Martins-Green, *Clin. Sci.* **2015**, *129*, 1115.
- [71] Z. Sun, X. Chen, X. Ma, X. Cui, Z. Yi, X. Li, *J. Mater. Chem. B* **2018**, *6*, 6133.
- [72] Z. Sun, Z. Yi, H. Zhang, X. Ma, W. Su, X. Sun, X. Li, *Carbohydr. Polym.* **2017**, *175*, 159.
- [73] Y. He, Q. Qu, T. Luo, Y. Gong, Z. Hou, J. Deng, Y. Xu, B. Wang, S. Hao, *ACS Biomater. Sci. Eng.* **2019**, *5*, 1113.
- [74] a) D. Ma, Y. Wang, W. Dai, *Mater. Sci. Eng., C* **2018**, *89*, 456; b) M. A. Tomeh, R. Hadianamrei, X. Zhao, *Pharmaceutics* **2019**, *11*, 494.
- [75] C. Lei, H. Zhu, J. Li, X. Feng, J. Chen, *J. Biomater. Sci., Polym. Ed.* **2016**, *27*, 403.
- [76] M. T. Sultan, O. J. Lee, S. H. Kim, H. W. Ju, C. H. Park, *Novel Biomaterials for Regenerative Medicine*, Springer, Singapore **2018**.
- [77] a) M. A. Serban, B. Panilaitis, D. L. Kaplan, *J. Biomed. Mater. Res., Part A* **2011**, *98A*, 567; b) T. Yucel, N. Kojic, G. G. Leisk, T. J. Lo, D. L. Kaplan, *J. Struct. Biol.* **2010**, *170*, 406.
- [78] a) J. Guo, W. Sun, J. P. Kim, X. Lu, Q. Li, M. Lin, O. Mrowczynski, E. B. Rizk, J. Cheng, G. Qian, *Acta Biomater.* **2018**, *72*, 35; b) H. Fan, J. Wang, Q. Zhang, Z. Jin, *ACS Omega* **2017**, *2*, 6668.
- [79] a) M. Auriemma, A. Piscitelli, R. Pasquino, P. Cerruti, M. Malinconico, N. Grizzuti, *Eur. Polym. J.* **2015**, *63*, 123; b) D. P. Makris, G. Boskou, N. K. Andrikopoulos, *J. Food Compos. Anal.* **2007**, *20*, 125.
- [80] a) C. Wang, H. Zhou, H. Niu, X. Ma, Y. Yuan, H. Hong, C. Liu, *Biomater. Sci.* **2018**, *6*, 3318; b) N. Li, X. Yang, W. Liu, G. Xi, M. Wang, B. Liang, Z. Ma, Y. Feng, H. Chen, C. Shi, *Macromol. Biosci.* **2018**, *18*, 1800209.
- [81] J. Shin, J. S. Lee, C. Lee, H. J. Park, K. Yang, Y. Jin, J. H. Ryu, K. S. Hong, S. H. Moon, H. M. Chung, *Adv. Funct. Mater.* **2015**, *25*, 3814.
- [82] S. Bai, X. Zhang, P. Cai, X. Huang, Y. Huang, R. Liu, M. Zhang, J. Song, X. Chen, H. Yang, *Nanoscale Horiz.* **2019**, *4*, 1333.
- [83] a) R. Cheung, T. Ng, J. Wong, W. Chan, *Mar. Drugs* **2015**, *13*, 5156; b) M. Liu, Y. Shen, P. Ao, L. Dai, Z. Liu, C. Zhou, *RSC Adv.* **2014**, *4*, 23540; c) S.-Y. Ong, J. Wu, S. M. Moochhala, M.-H. Tan, J. Lu, *Biomaterials* **2008**, *29*, 4323; d) A. Martins, S. Facchi, H. Follmann, A. Pereira, A. Rubira, E. Muniz, *Int. J. Mol. Sci.* **2014**, *15*, 20800.
- [84] T.-C. Chou, E. Fu, C.-J. Wu, J.-H. Yeh, *Biochem. Biophys. Res. Commun.* **2003**, *302*, 480.
- [85] a) Y. Okamoto, R. Yano, K. Miyatake, I. Tomohiro, Y. Shigemasa, S. Minami, *Carbohydr. Polym.* **2003**, *53*, 337; b) J. Yang, F. Tian, Z. Wang, Q. Wang, Y. J. Zeng, S. Q. Chen, *J. Biomed. Mater. Res. B* **2008**, *84B*, 131; c) S. B. Rao, C. P. Sharma, *J. Biomed. Mater. Res.* **1997**, *34*, 21.
- [86] a) V. Balan, L. Verestiuc, *Eur. Polym. J.* **2014**, *53*, 171; b) C. C. E. Helms, M. Marvel, W. Zhao, M. Stahle, R. Vest, G. Kato, J. Lee, G. Christ, M. Gladwin, R. Hantgan, *J. Thromb. Haemost.* **2013**, *11*, 2148.

- [87] R. Jayakumar, M. Prabakaran, S. Nair, H. Tamura, *Biotechnol. Adv.* **2010**, *28*, 142.
- [88] a) G. Peluso, O. Petillo, M. Ranieri, M. Santin, L. Ambrosic, D. Calabró, B. Avallone, G. Balsamo, *Biomaterials* **1994**, *15*, 1215; b) H. Ueno, T. Mori, T. Fujinaga, *Adv. Drug Del. Rev.* **2001**, *52*, 105; c) K. Kojima, Y. Okamoto, K. Kojima, K. Miyatake, H. Fujise, Y. Shigemasa, S. Minami, *J. Vet. Med. Sci.* **2004**, *66*, 1595.
- [89] T. Takei, H. Nakahara, H. Ijima, K. Kawakami, *Acta Biomater.* **2012**, *8*, 686.
- [90] a) H. Liu, C. Wang, C. Li, Y. Qin, Z. Wang, F. Yang, Z. Li, J. Wang, *RSC Adv.* **2018**, *8*, 7533; b) I.-Y. Kim, S.-J. Seo, H.-S. Moon, M.-K. Yoo, I.-Y. Park, B.-C. Kim, C.-S. Cho, *Biotechnol. Adv.* **2008**, *26*, 1; c) A. D. Sezer, F. Hatipoglu, E. Cevher, Z. Oğurtan, A. L. Bas, J. Akbuğa, *AAPS PharmSciTech* **2007**, *8*, E94.
- [91] a) S. Pourshahrestani, E. Zeimaran, N. A. Kadri, N. Gargiulo, H. M. Jindal, S. V. Naveen, S. D. Sekaran, T. Kamarul, M. R. Towler, *ACS Appl. Mater. Interfaces* **2017**, *9*, 31381; b) Z. Hu, D.-Y. Zhang, S.-T. Lu, P.-W. Li, S.-D. Li, *Mar. Drugs* **2018**, *16*, 273.
- [92] N. S. Muthiah Pillai, K. Eswar, S. Amirthalingam, U. Mony, P. Kerala Varma, R. Jayakumar, *ACS Appl. Biol. Mater.* **2019**, *2*, 865.
- [93] M. N. Sundaram, S. Amirthalingam, U. Mony, P. K. Varma, R. Jayakumar, *Int. J. Biol. Macromol.* **2019**, *129*, 936.
- [94] H. Geng, Q. Dai, H. Sun, L. Zhuang, A. Song, F. Caruso, J. Hao, J. Cui, *ACS Appl. Biol. Mater.* **2020**, *3*, 1258.
- [95] S. Khunmanee, Y. Jeong, H. Park, *J. Tissue Eng.* **2017**, *8*, 2041731417726464.
- [96] X. Zhao, H. Wu, B. Guo, R. Dong, Y. Qiu, P. X. Ma, *Biomaterials* **2017**, *122*, 34.
- [97] J. Qu, X. Zhao, Y. Liang, T. Zhang, P. X. Ma, B. Guo, *Biomaterials* **2018**, *183*, 185.
- [98] J. Hoque, R. G. Prakash, K. Paramanandham, B. R. Shome, J. Haldar, *Mol. Pharm.* **2017**, *14*, 1218.
- [99] J. Desbrieres, C. Martinez, M. Rinaudo, *Int. J. Biol. Macromol.* **1996**, *19*, 21.
- [100] a) M. B. Dowling, R. Kumar, M. A. Keibler, J. R. Hess, G. V. Bochichio, S. R. Raghavan, *Biomaterials* **2011**, *32*, 3351; b) D.-T. Vo, C.-K. Lee, *Carbohydr. Polym.* **2017**, *164*, 109.
- [101] X. Du, Y. Liu, X. Wang, H. Yan, L. Wang, L. Qu, D. Kong, M. Qiao, L. Wang, *Mater. Sci. Eng.* **2019**, *104*, 109930.
- [102] J. Liu, J. Li, F. Yu, Y.-x. Zhao, X.-m. Mo, J.-f. Pan, *Int. J. Biol. Macromol.* **2020**, *147*, 653.
- [103] D. P. Nair, M. Podgórski, S. Chatani, T. Gong, W. Xi, C. R. Fenoli, C. N. Bowman, *Chem. Mater.* **2014**, *26*, 724.
- [104] J. H. Ryu, Y. Lee, W. H. Kong, T. G. Kim, T. G. Park, H. Lee, *Biomacromolecules* **2011**, *12*, 2653.
- [105] Y. Zhang, Y. Thomas, E. Kim, G. F. Payne, *J. Phys. Chem. B* **2012**, *116*, 1579.
- [106] Q. Q. Wang, M. Kong, Y. An, Y. Liu, J. J. Li, X. Zhou, C. Feng, J. Li, S. Y. Jiang, X. J. Cheng, *J. Mater. Sci.* **2013**, *48*, 5614.
- [107] S. Hu, S. Bi, D. Yan, Z. Zhou, G. Sun, X. Cheng, X. Chen, *Carbohydr. Polym.* **2018**, *184*, 154.
- [108] X. Zhang, G.-h. Sun, M.-p. Tian, Y.-n. Wang, C.-c. Qu, X.-j. Cheng, C. Feng, X.-g. Chen, *Int. J. Biol. Macromol.* **2019**, *138*, 321.
- [109] W. Nie, X. Yuan, J. Zhao, Y. Zhou, H. Bao, *Carbohydr. Polym.* **2013**, *96*, 342.
- [110] X. Du, Y. Liu, H. Yan, M. Rafique, S. Li, X. Shan, L. Wu, M. Qiao, D. Kong, L. Wang, *Biomacromolecules* **2020**, *21*, 1243.
- [111] a) K. M. Park, K. S. Ko, Y. K. Joung, H. Shin, K. D. Park, *J. Mater. Chem.* **2011**, *21*, 13180; b) K. M. Park, Y. M. Shin, Y. K. Joung, H. Shin, K. D. Park, *Biomacromolecules* **2010**, *11*, 706; c) N. Q. Tran, Y. K. Joung, E. Lih, K. D. Park, *Biomacromolecules* **2011**, *12*, 2872.
- [112] E. Lih, J. S. Lee, K. M. Park, K. D. Park, *Acta Biomater.* **2012**, *8*, 3261.
- [113] a) F. J. Pavinatto, A. Pavinatto, L. Caseli, D. S. dos Santos, T. M. Nobre, M. E. Zaniquelli, O. N. Oliveira, *Biomacromolecules* **2007**, *8*, 1633; b) I. Fiebrig, S. Harding, S. Davis, *Colloid and Polymer Science*, Springer, Berlin **1994**.
- [114] a) K. Yue, G. Trujillo-de Santiago, M. M. Alvarez, A. Tamayol, N. Annabi, A. Khademhosseini, *Biomaterials* **2015**, *73*, 254; b) L. Wang, B. Li, F. Xu, Y. Li, Z. Xu, D. Wei, Y. Feng, Y. Wang, D. Jia, Y. Zhou, *Biomaterials* **2017**, *145*, 192; c) B. Li, L. Wang, F. Xu, X. Gang, U. Demirci, D. Wei, Y. Li, Y. Feng, D. Jia, Y. Zhou, *Acta Biomater.* **2015**, *22*, 59.
- [115] L. Wang, X. Zhang, K. Yang, Y. V. Fu, T. Xu, S. Li, D. Zhang, L. N. Wang, C. S. Lee, *Adv. Funct. Mater.* **2019**, *3*, 1904156.
- [116] a) M. Kong, X. G. Chen, K. Xing, H. J. Park, *Int. J. Food Microbiol.* **2010**, *144*, 51; b) Y. Liu, K. Ai, L. Lu, *Chem. Rev.* **2014**, *114*, 5057; c) M. E. Lyng, P. Schattling, B. Städler, *Nanomedicine* **2015**, *10*, 2725.
- [117] L. J. Eggermont, Z. J. Rogers, T. Colombani, A. Memic, S. A. Bencherif, *Trends Biotechnol.* **2020**, *38*, 418.
- [118] X. Zhao, B. Guo, H. Wu, Y. Liang, P. X. Ma, *Nat. Commun.* **2018**, *9*, 2784.
- [119] S. Hou, Y. Liu, F. Feng, J. Zhou, X. Feng, Y. Fan, *Adv. Healthcare Mater.* **2020**, *9*, 1901041.
- [120] K. L. Goa, P. Benfield, *Drugs* **1994**, *47*, 536.
- [121] M. N. Collins, C. Birkinshaw, *Carbohydr. Polym.* **2013**, *92*, 1262.
- [122] a) Z. Hussain, H. E. Thu, H. Katas, S. N. A. Bukhari, *Polym. Rev.* **2017**, *57*, 594; b) M. Galeano, F. Polito, A. Bitto, N. Irrera, G. M. Campo, A. Avenoso, M. Calò, P. L. Cascio, L. Minutoli, M. Barone, *Biochim. Biophys. Acta* **2011**, *1812*, 752.
- [123] M. Sakoda, M. Kaneko, S. Ohta, P. Qi, S. Ichimura, Y. Yatomi, T. Ito, *Biomacromolecules* **2018**, *19*, 3280.
- [124] F. Müller, N. J. Mutch, W. A. Schenk, S. A. Smith, L. Esterl, H. M. Spronk, S. Schmidbauer, W. A. Gahl, J. H. Morrissey, T. Renné, *Cell* **2009**, *139*, 1143.
- [125] Y. Liang, X. Zhao, T. Hu, B. Chen, Z. Yin, P. X. Ma, B. Guo, *Small* **2019**, *15*, 1900046.
- [126] D. Duerschmied, C. Bode, *Hämostaseologie* **2009**, *29*, 356.
- [127] S. An, E. J. Jeon, J. Jeon, S.-W. Cho, *Mater. Horiz.* **2019**, *6*, 1169.
- [128] S. Hong, Y. S. Na, S. Choi, I. T. Song, W. Y. Kim, H. Lee, *Adv. Funct. Mater.* **2012**, *22*, 4711.
- [129] J. Yang, M. A. C. Stuart, M. Kamperman, *Chem. Soc. Rev.* **2014**, *43*, 8271.
- [130] M. Morra, C. Cassinelli, *J. Biomater. Sci., Polym. Ed.* **1999**, *10*, 1107.
- [131] S. W. Whiteheart, *Blood* **2011**, *118*, 1190.
- [132] a) K. Y. Lee, D. J. Mooney, *Chem. Rev.* **2001**, *101*, 1869; b) T. Boonthekul, H.-J. Kong, D. J. Mooney, *Biomaterials* **2005**, *26*, 2455; c) K. Y. Lee, D. J. Mooney, *Prog. Polym. Sci.* **2012**, *37*, 106.
- [133] a) S. Blair, P. Jarvis, M. Salmon, C. McCollum, *Br. J. Surg.* **1990**, *77*, 568; b) H. Hattori, Y. Amano, Y. Nogami, B. Takase, M. Ishihara, *Ann. Biomed. Eng.* **2010**, *38*, 3724.
- [134] B. Aderibigbe, B. Buyana, *Pharmaceutics* **2018**, *10*, 42.
- [135] C. K. Song, M.-K. Kim, J. Lee, E. Davaa, R. Baskaran, S.-G. Yang, *Maromol. Res.* **2019**, *27*, 119.
- [136] a) X. Li, Y. Weng, X. Kong, B. Zhang, M. Li, K. Diao, Z. Zhang, X. Wang, H. Chen, *J. Mater. Sci. Mater. Med.* **2012**, *23*, 2857; b) X. Xu, Y. Weng, L. Xu, H. Chen, *Int. J. Biol. Macromol.* **2013**, *60*, 272.
- [137] J. Cao, L. Xiao, X. Shi, *RSC Adv.* **2019**, *9*, 36858.
- [138] a) M. P. Rode, A. B. Batti Angulski, F. A. Gomes, M. M. da Silva, T. d. S. Jeremias, R. G. de Carvalho, D. G. Lucif Vieira, L. F. C. Oliveira, L. Fernandes Maia, A. G. Trentin, *J. Biomater. Appl.* **2018**, *33*, 422; b) J. Liu, X. Zhan, J. Wan, Y. Wang, C. Wang, *Carbohydr. Polym.* **2015**, *121*, 27.
- [139] a) S. M. Mihaila, A. K. Gaharwar, R. L. Reis, A. P. Marques, M. E. Gomes, A. Khademhosseini, *Adv. Healthcare Mater.* **2013**, *2*, 895; b) S. N. Bhattacharyya, B. Manna, P. Ashbaugh, R. Coutinho, B. Kaufman, *Inflammation* **1997**, *21*, 133.
- [140] A. Thakur, M. K. Jaiswal, C. W. Peak, J. K. Carrow, J. Gentry, A. Dolatshahi-Pirouz, A. K. Gaharwar, *Nanoscale* **2016**, *8*, 12362.

- [141] K. Naito, K. Fujikawa, *J. Biol. Chem.* **1991**, 266, 7353.
- [142] H. Tan, K. G. Marra, *Materials* **2010**, 3, 1746.
- [143] a) A. A. D'souza, R. Shegokar, *Expert Opin. Drug Delivery* **2016**, 13, 1257; b) J. Zhu, *Biomaterials* **2010**, 31, 4639.
- [144] a) N. A. Peppas, K. B. Keys, M. Torres-Lugo, A. M. Lowman, *J. Controlled Release* **1999**, 62, 81; b) C.-C. Lin, K. S. Anseth, *Pharm. Res.* **2009**, 26, 631.
- [145] A. N. Azadani, P. B. Matthews, L. Ge, Y. Shen, C.-S. Jhun, T. S. Guy, E. E. Tseng, *Ann. Thorac. Surg.* **2009**, 87, 1154.
- [146] Y. Bu, L. Zhang, J. Liu, L. Zhang, T. Li, H. Shen, X. Wang, F. Yang, P. Tang, D. Wu, *ACS Appl. Mater. Interfaces* **2016**, 8, 12674.
- [147] a) M. Zhu, W. Liu, H. Liu, Y. Liao, J. Wei, X. Zhou, D. Xing, *ACS Appl. Mater. Interfaces* **2015**, 7, 12873; b) G. Qi, L. Li, F. Yu, H. Wang, *ACS Appl. Mater. Interfaces* **2013**, 5, 10874.
- [148] a) I. Strehin, Z. Nahas, K. Arora, T. Nguyen, J. Elisseeff, *Biomaterials* **2010**, 31, 2788; b) Q. Lu, E. Danner, J. H. Waite, J. N. Israelachvili, H. Zeng, D. S. Hwang, *J. R. Soc. Interface* **2013**, 10, 20120759.
- [149] Y. Bu, L. Zhang, G. Sun, F. Sun, J. Liu, F. Yang, P. Tang, D. Wu, *Adv. Mater.* **2019**, 31, 1901580.
- [150] M. Mehdizadeh, H. Weng, D. Gyawali, L. Tang, J. Yang, *Biomaterials* **2012**, 33, 7972.
- [151] Z. Zhang, X. Wang, Y. Wang, J. Hao, *Biomacromolecules* **2018**, 19, 980.
- [152] P. H. T. Uhlherr, J. Guo, C. Tiu, X.-M. Zhang, J.-Q. Zhou, T.-N. Fang, *J. Non-Newton. Fluid Mech.* **2005**, 125, 101.
- [153] a) Y. Zhang, B. Yang, X. Zhang, L. Xu, L. Tao, S. Li, Y. Wei, *Chem. Commun.* **2012**, 48, 9305; b) L. Dong, S. Xia, H. Chen, J. Chen, J. Zhang, *Biomaterials* **2009**, 30, 4416.
- [154] R. Wang, B. Zhou, W. Liu, X.-h. Feng, S. Li, D.-f. Yu, J.-c. Chang, B. Chi, H. Xu, *J. Biomater. Appl.* **2015**, 29, 1167.
- [155] H. Gao, S.-Z. Luo, *RSC Adv.* **2016**, 6, 58521.
- [156] N. Nakajima, H. Sugai, S. Tsutsumi, S. H. Hyon, *Key Eng. Mater.* **2007**, 342–343, 713.
- [157] Y. M. Kim, C. H. Kim, M. R. Park, S. C. Song, *Bull. Korean Chem. Soc.* **2016**, 37, 372.
- [158] H. Kubota, T. Matsunobu, K. Uotani, H. Takebe, A. Satoh, T. Tanaka, M. Taniguchi, *Biosci. Biotechnol. Biochem.* **1993**, 57, 1212.
- [159] W. Chen, R. Wang, T. Xu, X. Ma, Z. Yao, B. Chi, H. Xu, *J. Mater. Chem. B* **2017**, 5, 5668.
- [160] a) S. Hong, D. Pirovich, A. Kilcoyne, C. H. Huang, H. Lee, R. Weissleder, *Adv. Mater.* **2016**, 28, 8675; b) L. Li, W. Smitthipong, H. Zeng, *Polym. Chem.* **2015**, 6, 353.
- [161] X. Han, G. Meng, Q. Wang, L. Cui, H. Wang, J. Wu, Z. Liu, X. Guo, *J. Biomater. Appl.* **2019**, 33, 915.
- [162] a) N. Chang, Y. Li, M. Zhou, J. Gao, Y. Hou, M. Jiang, G. Bai, *Biomed. Pharmacother.* **2017**, 87, 698; b) X. Yang, J. Cui, A. Ding, *Sichuan Tradit. Chin. Med.* **2006**, 24, 17.
- [163] C. Cui, C. Fan, Y. Wu, M. Xiao, T. Wu, D. Zhang, X. Chen, B. Liu, Z. Xu, B. Qu, *Adv. Mater.* **2019**, 31, 1905761.
- [164] X. Fan, S. Wang, Y. Fang, P. Li, W. Zhou, Z. Wang, M. Chen, H. Liu, *Mater. Sci. Eng., C* **2020**, 109, 110649.
- [165] M. Swindle, A. Makin, A. Herron, F. Clubb Jr, K. Frazier, *Vet. Pathol.* **2012**, 49, 344.



Sara Pourshahrestani received her M.Sc. degree in organic chemistry from the University of Isfahan (Iran) and obtained her Ph.D. degree in biomaterials and tissue engineering from the University of Malaya (Malaysia). She is currently a postdoctoral fellow at the Department of Biomedical Engineering, University of Malaya. Her current research areas cover biomaterials for hemostasis, wound healing, and tissue engineering applications.



Aldo R. Boccaccini is a professor of biomaterials and Head of the Institute of Biomaterials at University of Erlangen-Nuremberg, Germany. He is also a visiting professor at Imperial College London. His research activities are in the broad area of glasses, ceramics, and composites for biomedical applications with focus on tissue engineering scaffolds. He is a Fellow of the Institute of Materials, Minerals and Mining (UK), American Ceramic Society, Society of Glass Technology and European Ceramic Society. Boccaccini serves in the Executive Committee of the Federation of European Materials Societies and in the Council of the European Society for Biomaterials.